

# Formation and properties of whey protein fibrils

Ardy Kroes-Nijboer

**Thesis committee****Thesis supervisor**

Prof. dr. E. van der Linden

Professor of Food Physics, Wageningen University

**Thesis co-supervisor**

Dr. P. Venema

Assistant professor, Food Physics Group, Wageningen University

**Other members**

Prof. dr. P. Dejmek

Lund University, Sweden

Prof. dr. M.A. Cohen Stuart

Wageningen University

Prof. dr. J.C.M. van Hest

Radboud University Nijmegen

Prof. dr. R. Mezzenga

ETH-Zürich, Switzerland

This research was conducted under the auspices of the Graduate School of VLAG

# Formation and properties of whey protein fibrils

Ardy Kroes-Nijboer

## **Thesis**

submitted in fulfilment of the requirements for the degree of doctor

at Wageningen University

by the authority of the Rector Magnificus

Prof. dr. M.J. Kropff,

in the presence of the

Thesis Committee appointed by the Academic Board

to be defended in public

on Friday 14 October 2011

at 4 p.m. in the Aula.

Ardy Kroes-Nijboer

Formation and properties of whey protein fibrils

176 pages.

PhD Thesis, Wageningen University, Wageningen, NL (2011)

With references, with summaries in Dutch and English

ISBN 978-94-6173-024-4

# Contents

## *Chapter 1*

Introduction	7
--------------	---

## *Chapter 2*

The critical aggregation concentration of $\beta$ -lg based fibril formation	17
------------------------------------------------------------------------------	----

## *Chapter 3*

The influence of protein hydrolysis on the growth kinetics of $\beta$ -lg fibrils	35
-----------------------------------------------------------------------------------	----

## *Chapter 4*

Thioflavin T fluorescence assay for $\beta$ -lg fibrils hindered by DAPH	65
--------------------------------------------------------------------------	----

## *Chapter 5*

Fracture of protein fibrils as induced by elongational flow	87
-------------------------------------------------------------	----

## *Chapter 6*

The behaviour of fibril-peptide mixtures at varying pH	109
--------------------------------------------------------	-----

## *Chapter 7*

General Discussion	133
--------------------	-----

Summary	159
---------	-----

Samenvatting	163
--------------	-----

Dankwoord	167
-----------	-----

Curriculum Vitae	172
------------------	-----

Publications	173
--------------	-----

Training activities	175
---------------------	-----



# *Chapter 1*

## **Introduction**

## Protein fibrils

Proteins are, besides carbohydrates and fat, one of the main sources of our diet. Proteins are essential for the human body, but also fulfil an important role in the texturing of foods. This role of proteins as texturizer in food products can be expanded when structures of different morphologies can be formed with different functionalities. These structures with different morphologies can be created by treating proteins using various conditions. Depending on these conditions, such as temperature, ionic strength, pH and protein concentration, different structures can be formed ranging from random aggregates to fibrils.<sup>1</sup> Fibrils are long linear assemblies that typically have a width in the order of a few nanometers, whereas their length is several micrometers long (Figure 1). They can be formed by heating, for example, a solution of the protein  $\beta$ -lactoglobulin ( $\beta$ -lg) at low pH and at low ionic strength. The high aspect ratio makes them interesting as structurant in foods that are functional at relatively low concentrations, for example, as thickening or gelling agent. Increasing our knowledge on the formation and the properties of fibrils will also pave the road towards their practical application in i.e. foods.

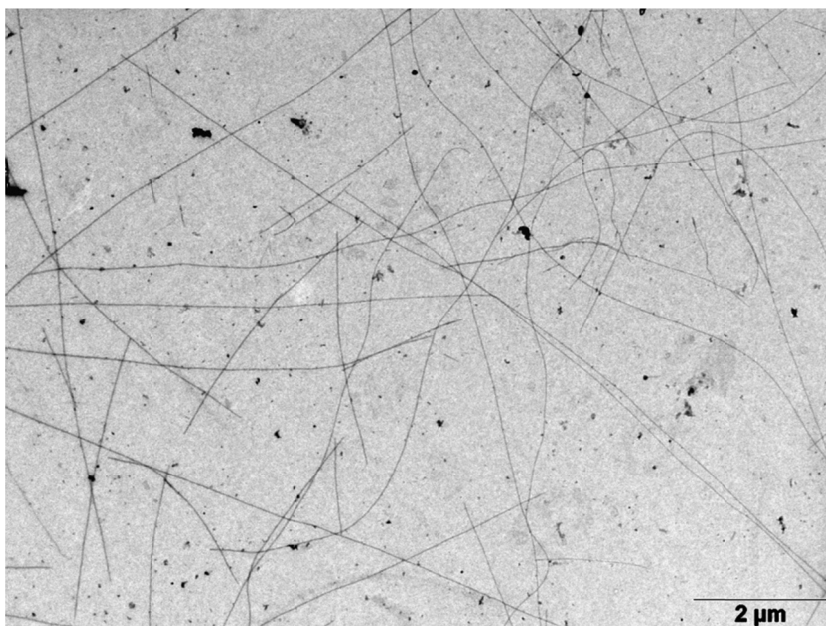


Figure 1. Protein fibrils derived from  $\beta$ -lg.

## Formation and properties of whey protein fibrils

Several food proteins have shown the ability to form fibrils, like egg white proteins<sup>2-5</sup>, soy proteins<sup>6</sup> and whey proteins<sup>7-23</sup>. Whey proteins used to be a waste product from cheese production. However, whey proteins are nowadays important proteins for the food industry, because of their nutritional value and functional properties.<sup>24</sup> In contrast to the random aggregates that are formed when whey protein isolate (WPI) is heated at pH values close to the iso-electric point, fibrils are formed when WPI is heated at low pH and low ionic strength.<sup>9, 10, 16, 23, 25, 26</sup>  $\beta$ -Lactoglobulin, which represents about 60% of the proteins in WPI was found to be the only fibril forming protein when WPI is heated at pH 2 and 80°C.<sup>10</sup>  $\beta$ -Lactoglobulin is a globular protein and has a molar mass of 18 400 g mol<sup>-1</sup> and a radius of about 2 nm.<sup>9</sup> At pH 2 the  $\beta$ -lg is highly charged, which was conjectured to hinder the formation of random aggregated and therefore induces the formation of long linear aggregates, i.e. fibrils.<sup>1-9, 20, 27</sup> However, recently it was shown by Akkermans et al, that peptides, and not the intact monomers, are the building blocks of the fibrils derived from  $\beta$ -lg that was heated at 80°C and pH 2.<sup>8</sup> This gives a different picture, since now the protein has to be hydrolyzed first, before the fibril formation can take place.

The fibrils derived from  $\beta$ -lg typically have a length between 1 and 10  $\mu$ m and a thickness of about 4 nm.<sup>13, 16, 21, 23, 28</sup> They are semi-flexible and have a persistence length of about 1.6  $\mu$ m.<sup>29</sup> Recent research showed that depending on the conditions multistranded fibrils can be formed with a thickness up to 180 nm and a persistence length depending on the number of strands composing the fibrils.<sup>30-32</sup> The dimensions of the fibrils are important for the applications of the fibrils. Since the fibrils are too thin to scatter visible light, the gels that are formed when  $\beta$ -lg is heated at low pH are transparent.<sup>13, 16, 17, 27</sup> Using the fibrils in a cold-gelation process, protein gels can be produced at weight fractions smaller than 0.07 wt %.<sup>33</sup> It was found that the viscosity of WPI solutions is increased upon addition of fibrils, showing the functionality of the fibrils as thickeners. Next to their application as

thickening or gelling agent, the fibrils can also be used in the production of microcapsules.<sup>34-36</sup> Layers of fibrils are deposited on oil droplets in oil-in-water emulsions to form capsules. The fibrils increase the strength of the capsules<sup>35</sup> and the length distribution of the fibrils are expected to influence the coverage and thereby the permeability of the capsules.

## Aim and outline of this thesis

Although the ability to form fibrils seems to be a generic property of proteins,<sup>37, 38</sup> and the fibril formation has been investigated in different directions, the fibril formation is still not completely understood. What is the physical mechanism behind the fibril formation? What are the energies involved in the fibril formation? It was shown that the hydrolysis of  $\beta$ -lactoglobulin is needed before fibrils can form, but what is the influence of hydrolysis on the kinetics of fibril formation?

Next to the more fundamental questions about the formation of the fibrils, additional questions on the properties of the fibrils and the ability to tune these properties arise. Is the tensile strength of the fibrils high enough to be mechanically stable against treatments like stirring, mixing or homogenization? Is there a way to tune the length distribution of the fibrils? How do the fibrils behave in products that have a different pH than the pH at which they are produced? Addressing these questions is key for the successful application of the fibrils in food products.

The aim of this thesis was to unravel the fibril formation process of  $\beta$ -lactoglobulin, to analyze some of the properties of the fibrils and to investigate possible routes to influence these properties. In Figure 2 a schematic outline of this thesis is given. In the first part of this thesis (*Chapter 2 to 3*) the process of fibril formation of  $\beta$ -lg at pH 2 is analyzed. In *Chapter 2* the focus is on the thermodynamic aspects of the selfassembly of the peptides into fibrils, where in *Chapter 3* the focus is on the kinetics of the fibril formation.

In the second part of this thesis the properties of the fibrils are investigated (*Chapter 4 to 6*). In *Chapter 4* the possible disaggregation of the fibrils by 4,5-dianilinophthalimide (DAPH) is investigated, a bioactive compound that was found to be able to disaggregate protein fibrils involved in neurodegenerative diseases.<sup>39</sup> *Chapter 5* describes a method where elongational flow is used to influence the length distribution of the fibrils. Using this method an estimate for the tensile strength of the fibrils could be derived. In *Chapter 6* the stability of the fibril solutions against pH changes is investigated, thereby focussing on the aggregation of the different fractions that are present in the solutions around pH 5. Finally, *Chapter 7* provides a general discussion on how the results of the previous chapters contribute to the field of fibril formation and their properties.

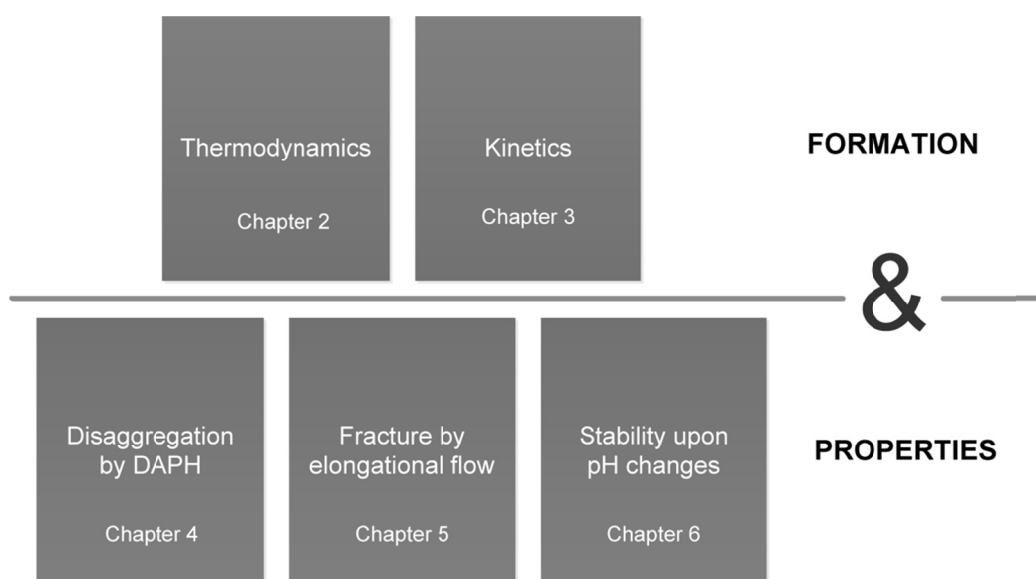


Figure 2. Schematic representation of the outline of this thesis.

## References

1. Doi, E., Gels and gelling of globular proteins. *Trends in Food Science & Technology* **1993**, 4, (1), 1-5.
2. Arnaudov, L. N.; de Vries, R., Thermally Induced Fibrillar Aggregation of Hen Egg White Lysozyme. *Biophysical Journal* **2005**, 88, (1), 515-526.
3. Krebs, M. R. H.; Wilkins, D. K.; Chung, E. W.; Pitkeathly, M. C.; Chamberlain, A. K.; Zurdo, J.; Robinson, C. V.; Dobson, C. M., Formation and seeding of amyloid fibrils from wild-type hen lysozyme and a peptide fragment from the [beta]-domain. *Journal of Molecular Biology* **2000**, 300, (3), 541-549.
4. Veerman, C.; de Schiffart, G.; Sagis, L. M. C.; van der Linden, E., Irreversible self-assembly of ovalbumin into fibrils and the resulting network rheology. *International Journal of Biological Macromolecules* **2003**, 33, 121-127.
5. Weijers, M.; Velde, v. d. F.; Stijnman, A.; Pijpekamp, A.; Visschers, R. W., Structure and rheological properties of acid-induced egg white protein gels. *Food Hydrocolloids* **2005**, 1-14.
6. Akkermans, C.; Van der Goot, A. J.; Venema, P.; Gruppen, H.; Vereijken, J. M.; Van der Linden, E.; Boom, R. M., Micrometer-Sized Fibrillar Protein Aggregates from Soy Glycinin and Soy Protein Isolate. *Journal of agricultural and food chemistry* **2007**, 55, (24), 9877-9882.
7. Akkermans, C.; van der Goot, A. J.; Venema, P.; van der Linden, E.; Boom, R. M., Formation of fibrillar whey protein aggregates: Influence of heat and shear treatment, and resulting rheology. *Food Hydrocolloids* **2008**, 22, (7), 1315-1325.
8. Akkermans, C.; Venema, P.; van der Goot, A. J.; Gruppen, H.; Bakx, E. J.; Boom, R. M.; van der Linden, E., Peptides are Building Blocks of Heat-Induced Fibrillar Protein Aggregates of  $\beta$ -Lactoglobulin Formed at pH 2. *Biomacromolecules* **2008**, 9, (5), 1474-1479.

9. Aymard, P.; Nicolai, T.; Durand, D., Static and Dynamic Scattering of *beta*-Lactoglobulin Aggregates Formed after Heat-Induced Denaturation at pH 2. *Macromolecules* **1999**, *32*, 2542-2552.
10. Bolder, S. G. S. G.; Hendrickx, H. H.; Sagis, L. M. L. M. C.; van der Linden, E. E., Fibril assemblies in aqueous whey protein mixtures. *Journal of agricultural and food chemistry* **2006**, *54*, (12), 4229-34.
11. Durand, D.; Christophe Gimel, J.; Nicolai, T., Aggregation, gelation and phase separation of heat denatured globular proteins. *Physica A: Statistical Mechanics and its Applications* **2002**, *304*, (1-2), 253-265.
12. Gimel, J. C.; Durand, D.; Nicolai, T., Structure and distribution of aggregates formed after heat-induced denaturation of globular proteins. *Macromolecules* **1994**, *27*, (2), 583-589.
13. Gosal, W. S.; Clark, A. H.; Pudney, P. D. A.; Ross-Murphy, S. B., Novel amyloid fibrillar networks derived from a globular protein: B-lactoglobulin. *Langmuir* **2002**, *18*, 7174-7181.
14. Gosal, W. S.; Ross-Murphy, S. B., Globular protein gelation. *Current opinion in colloid & interface science* **2000**, *5*, 188-194.
15. Ikeda, S.; Morris, V. J., Fine-Stranded and Particulate Aggregates of Heat-Denatured Whey Proteins Visualized by Atomic Force Microscopy. *Biomacromolecules* **2002**, *3*, (2), 382-389.
16. Kavanagh, G. M.; Clark, A. H.; Ross-Murphy, S. B., Heat-induced gelation of globular proteins: part 3. Molecular studies on low pH beta-lactoglobulin gels. *International Journal of Biological Macromolecules* **2000**, *28*, 41-50.
17. Langton, M.; Hermansson, A.-M., Fine-stranded and particulate gels of  $\beta$ -lactoglobulin and whey protein at varying pH. *Food Hydrocolloids* **1992**, *5*, 523-539.
18. Le Bon, C.; Nicolai, T.; Durand, D., Growth and structure of aggregates of heat-denatured beta-Lactoglobulin. *International Journal of Food Science and Technology* **1999**, *34*, 451-465.

19. Lefèvre, T.; Subirade, M., Molecular differences in the formation and structure of fine-stranded and particulate beta-lactoglobulin gels. *Biopolymers* **2000**, 54, (7), 578-586.
20. Renard, D.; Lefebvre, J.; Griffin, M. C. A.; Griffin, W. G., Effects of pH and salt environment on the association of beta-lactoglobulin revealed by intrinsic fluorescence studies. *International Journal of Biological Macromolecules* **1998**, 22, 41-49.
21. Rogers, S. S.; Venema, P.; Sagis, L. M. C.; van der Linden, E.; Donald, A. M., Measuring length distribution of a fibril system: A flow birefringence technique applied to amyloid fibrils. *Macromolecules* **2005**, 38, 2948-2958.
22. Schokker, E. P., Heat-induced aggregation of beta-lactoglobulin AB at pH 2.5 as influenced by ionic strength and protein concentration. *International dairy journal* **2000**, 10, (4), 233.
23. Veerman, C. C.; Ruis, H. H.; Sagis, L. M. L. M. C.; van der Linden, E. E., Effect of electrostatic interactions on the percolation concentration of fibrillar beta-lactoglobulin gels. *Biomacromolecules* **2002**, 3, (4), 869.
24. Smithers, G. W., Whey and whey proteins--From '[gutter-to-gold]'. *International Dairy Journal* **2008**, 18, (7), 695-704.
25. Bromley, E. H. C.; Krebs, M. R. H.; Donald, A. M., Aggregation across the length-scales in beta-lactoglobulin. *Faraday Discussions* **2005**, 128, 13-27.
26. Gosal, W. S.; Clark, A. H.; Ross-Murphy, S. B., Fibrillar beta-lactoglobulin gels: Part 1. Fibril formation and structure. *Biomacromolecules* **2004**, 5, (6), 2408-2419.
27. Clark, A. H.; Kavanagh, G. M.; Ross-Murphy, S. B., Globular protein gelation - theory and experiment. *Food Hydrocolloids* **2001**, 15, 383-400.
28. Arnoudov, L. N.; Vries, d. R.; Ippel, H.; Mierlo, v. C. P. M., Multiple steps during the formation of beta-lactoglobulin fibrils. *Biomacromolecules* **2003**, 4, 1614-1622.
29. Sagis, L. M. C.; Veerman, C.; van der Linden, E., Mesoscopic Properties of Semiflexible Amyloid Fibrils. *Langmuir* **2004**, 20, 924-927.

30. Adamcik, J.; Jung, J.-M.; Flakowski, J.; De Los Rios, P.; Dietler, G.; Mezzenga, R., Understanding amyloid aggregation by statistical analysis of atomic force microscopy images. *Nat Nano* **2010**, 5, (6), 423-428.
31. Bolisetty, S.; Adamcik, J.; Mezzenga, R., Snapshots of fibrillation and aggregation kinetics in multistranded amyloid [small beta]-lactoglobulin fibrils. *Soft Matter* **2011**, 7, (2), 493-499.
32. Lara, C. c.; Adamcik, J.; Jordens, S.; Mezzenga, R., General Self-Assembly Mechanism Converting Hydrolyzed Globular Proteins Into Giant Multistranded Amyloid Ribbons. *Biomacromolecules* **2011**, 12, (5), 1868-1875.
33. Veerman, C., Gels at Extremely Low Weight Fractions Formed by Irreversible Self-Assembly of Proteins. *Macromolecular bioscience* **2003**, 3, (5), 243.
34. Humblet-Hua, N.-P.; Sagis, L. M. C.; Scheltens, G.; Yi, L.; van der Linden, E. In *Encapsulation systems based on proteins, polysaccharides, and protein-polysaccharide complexes*, 5th International Symposium on Food Rheology and Structure, Zurich, Switzerland, 2009; Fischer, P.; Pollard, M.; Windhab, E. J., Eds. Zurich, Switzerland, 2009; pp 180-183.
35. Sagis, L. M. C.; de Ruiter, R.; Miranda, F. J. R.; de Ruiter, J.; Schroen, K.; van Aelst, A. C.; Kieft, H.; Boom, R.; van der Linden, E., Polymer Microcapsules with a Fiber-Reinforced Nanocomposite Shell. *Langmuir* **2008**, 24, (5), 1608-1612.
36. Humblet-Hua, K. N. P.; Scheltens, G.; van der Linden, E.; Sagis, L. M. C., Encapsulation systems based on ovalbumin fibrils and high methoxyl pectin. *Food Hydrocolloids* **2011**, 25, (3), 307-314.
37. Chiti, F.; Dobson, C. M., Protein Misfolding, Functional Amyloid, and Human Disease. *Annual Review of Biochemistry* **2006**, 75, 333-366.
38. Dobson, C. M., Protein folding and misfolding. *Nature* **2003**, 426, (6968), 884.
39. Blanchard, B. J.; Chen, A.; Rozeboom, L. M.; Stafford, K. A.; Weigele, P.; Ingram, V. M., Efficient reversal of Alzheimers's disease fibril formation and elimination of neurotoxicity by a small molecule. *PNAS* **2004**, 101, 14326-14332.

Chapter 2 is published as: Kroes-Nijboer, A., Bouman, J., Venema, P., van der Linden, E. (2009) The critical aggregation concentration of  $\beta$ -lg based fibril formation. *Food Biophysics* (4) 59–63.

## *Chapter 2*

### **The critical aggregation concentration of $\beta$ -lg based fibril formation**

## Abstract

The critical aggregation concentration (CAC) for fibril formation of  $\beta$ -lactoglobulin ( $\beta$ -lg) at pH 2 was determined at 343, 353, 358, 363 and 383 K using a Thioflavin T assay and was approximately 0.16 wt %. The accuracy of the CAC was increased by measuring the conversion into fibrils at different stirring speeds. The corresponding binding energy per mol, as determined from the CAC was 13 RT ( $\sim 40$  kJ mol<sup>-1</sup>) for the measured temperature range. The fact that the CAC was independent of temperature within the experimental error, indicates that the fibril formation of  $\beta$ -lg at pH 2 and the measured temperature range is an entropy-driven process.

## Introduction

Amyloid fibrils are linear protein aggregates that are typically micrometers long, but only a few nanometers thick. They can be formed from various food proteins like egg white proteins<sup>1-5</sup>, soy proteins<sup>6</sup> and whey proteins<sup>7-25</sup>. The fibrils can for example be used as structurants and thickeners to give food products a specific texture. However, fibrillar protein aggregation is not only studied because of its potential use in food products, but the formation of fibrils is also related with amyloid diseases, where the amyloid fibrils occur in proteinaceous deposits called plaques.<sup>26</sup> Although the amyloid fibrils have been studied in different research areas, there is a common interest in knowledge about the formation and molecular structure of the fibrils. The formation of amyloid fibrils is suggested to be a generic form of aggregation.<sup>26,27</sup> The amyloid fibrils are characterized by a cross- $\beta$  structure,<sup>28,29</sup> where the  $\beta$ -sheets are arranged parallel to the long axis of the fibril, with their constituent  $\beta$ -strands perpendicular to this axis.<sup>30,31</sup> Another property of the amyloid fibrils is that they have the ability to bind to amyloid specific dyes like Congo Red<sup>32</sup> and Thioflavin T (ThT).<sup>33</sup>

We are interested in the formation of fibrils of  $\beta$ -lactoglobulin ( $\beta$ -lg), a globular protein that has a molar mass of 18 400 g mol<sup>-1</sup>, and a radius of about 2 nm.<sup>11</sup>  $\beta$ -Lg has been extensively studied because it is readily available in large quantities and of its importance to the food industry.<sup>34</sup> Fibrils are formed when  $\beta$ -lg is heated at low pH, far from the iso-electric point of the protein.<sup>11,14,20,24,34,35</sup> Despite extensive studies on fibril formation and the fact that it is known how to produce the  $\beta$ -lg fibrils, the fibril formation process is still not completely understood. For instance the critical aggregation concentration (CAC), which is an important parameter that can be used to estimate binding energies involved in the fibril formation, is still under discussion. Having reliable values for the CAC will lead to a better understanding of the fibril formation process. Values for the CAC of fibril formation of  $\beta$ -lg at pH 2 that are reported in literature, show a large disparity. Arnaudov et al.<sup>21</sup> defined the critical

concentration as the concentration were the conversion of protein into fibrils was too low to be determined with NMR spectroscopy, in this case 2.5 wt % was reported. However, in their AFM pictures fibrils were observed in solutions with protein concentrations of 1 wt %  $\beta$ -lg.<sup>21</sup> Rogers et al.<sup>23</sup> found fibril formation in equivalent  $\beta$ -lg solutions with concentrations as low as 0.5 wt %. In whey protein isolate (WPI) solutions, where 65% of the protein is  $\beta$ -lg, fibrils were formed at concentrations of 0.5 wt % WPI. [24] This corresponds to a  $\beta$ -lg concentration of about 0.33 wt %. In short, in literature the values for the CAC of fibril formation of  $\beta$ -lg at pH 2 range from protein concentrations as low as 0.33 wt % up to concentrations of 2.5 wt %.

In the present study an alternative route is used to determine the CAC for fibril formation of  $\beta$ -lg at pH 2 and elevated temperatures i.e., by using the assumption that flow will influence the kinetics of fibril formation but not the thermodynamics. To obtain CAC values for the fibril formation the conversion of protein into fibrils as a function of total protein concentration (0.2 wt % - 2 wt %) was measured. This was done using a ThT assay, which is widely used to determine the presence of amyloid fibrils and to examine the kinetics of fibril formation.<sup>33,34,36-39</sup> To increase the accuracy of the determination of the CAC, fibrils were produced under different stirring conditions (at rest, stirred at 290 rpm and at 1200 rpm). The fibril formation starts with reversible aggregation and upon longer heating the binding between the building blocks of the fibrils becomes irreversible.<sup>21,25</sup> Therefore the CAC at the start of the aggregation process is treated as a thermodynamic equilibrium and the thermodynamic principles of self-assembly<sup>40</sup> were used to estimate the corresponding binding energy. The temperature dependence of the CAC was used to estimate the enthalpy and entropy contribution to the fibril formation.

## Materials and Methods

### *Sample preparation*

$\beta$ -Lg was obtained from Sigma (product no. L0130, lot. no. 095K7006). A stock solution (about 9 wt %) was made by dissolving the protein powder in HCl solution of pH 2. The pH of the protein solution was adjusted to pH 2 with 6M HCl solution. Subsequently, this stock solution was filtered through a protein filter (FD 30/0.45  $\mu$ m Ca-S from Schleicher & Schuell) to remove any traces of undissolved protein. The protein concentration of the stock solution was determined using an UV spectrophotometer (Cary 50 Bio, Varian) and a calibration curve of known  $\beta$ -lg concentrations at a wavelength of 278 nm. The stock solution was diluted to protein concentrations of 2 wt %, 1 wt %, 0.5 wt % and 0.2 wt % with HCl solution of pH 2.

#### *Heating and stirring*

$\beta$ -Lg solutions of the various protein concentrations were heated in small glass vials (20 ml) in a metal stirring and heating plate for 24 hours at 343, 353, 358, 363 and 383 K. The protein solutions were stirred during heating at 2 different stirring rates, corresponding to 290 and 1200 rpm. At 353 K a series of protein solutions was also heated at rest. All samples were heated in duplicates. The samples at 383 K were heated in glass vials (10 ml) with a crimp cap (with septum of silicone/PTFE 3mm) to allow pressures above atmospheric pressure.

#### *Thioflavin T fluorescence*

The ThT fluorescence assay was used to measure the conversion of protein into fibrils after heating the protein solutions. A ThT stock solution (3.0 mM) was made by dissolving 7.9 mg ThT in 8 ml phosphate buffer (10 mM phosphate, 150 mM NaCl at pH 7.0). This stock solution was filtered through a 0.2  $\mu$ m filter (Schleicher & Schuell). The stock solution was diluted 50 times in a phosphate buffer (10 mM phosphate, 150 mM NaCl at pH 7.0) before use.

After heating the protein solutions, aliquots of the fibril samples (48  $\mu$ l) were mixed with 4 ml ThT solution and allowed to bind to the ThT for 1 minute. The fluorescence of the samples was measured using a fluorescence spectrophotometer (Perkin Elmer

LS 50 B). The excitation wavelength was set on 460 nm (slit width 4.0 nm) and the emission spectrum was recorded between 470 and 500 nm (slit width 2.5 nm) at a scanning speed of 200 nm/min. The fluorescence intensity was determined at 482 nm. The fluorescence intensity of the ThT solution was subtracted as a background. The errors in fluorescence were typically < 3%.

## Results and Discussion

### *CAC and stirring*

The fibril formation of  $\beta$ -lg at pH 2 was strongly dependent on the heating temperature, as can be seen in Figure 1. The optimal temperature for this fibril formation process, i.e. the temperature where the conversion was maximal, was close to 353 K. A similar optimum was found for 0.5 wt %  $\beta$ -lg under stirred conditions by Rogers et al.<sup>41</sup>

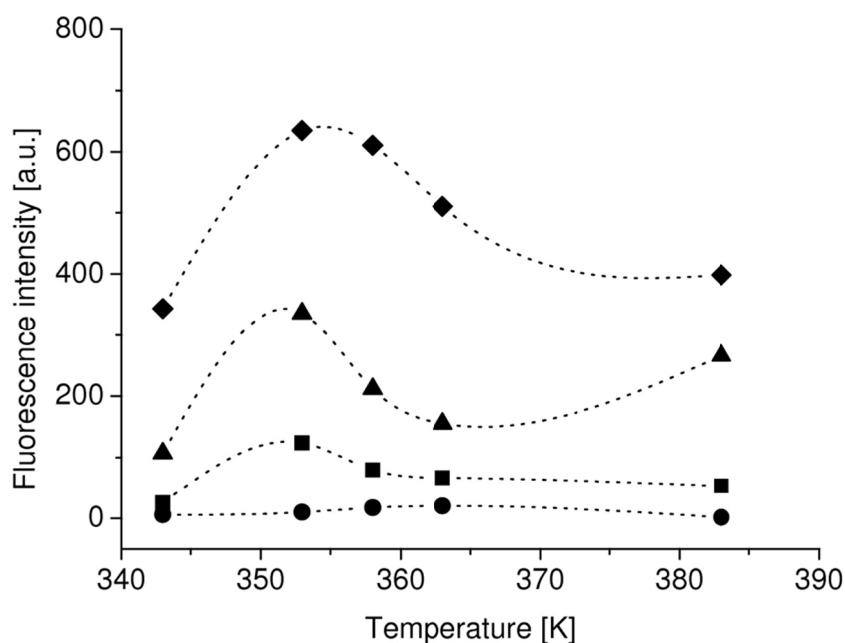


Figure 1. Maximal conversion of protein into fibrils as a function of temperature for various  $\beta$ -lg concentrations. Samples were stirred during heating at 290 rpm. ● 0.2 wt %, ■ 0.5 wt %, ▲ 1 wt %, ◆ 2 wt %.

To determine the CAC for fibril formation at 353 K, the conversion of protein into fibrils was measured as a function of the total protein concentration using a ThT assay. From this the CAC was determined by extrapolating the conversion data to zero conversion. Figure 2 shows that the conversion of protein into fibrils is linearly related to the total protein concentration, with a slope depending on the stirring rate. The influence of flow on the conversion was also reported by other researchers.<sup>25,42,43</sup> Figure 2 shows that the 3 lines have a common intersection point at 0.16 wt %, showing that the CAC for fibril formation is not dependent on the stirring rate. Reversely, the CAC can be determined accurately if one uses different flow conditions. Indeed, the kinetics is changed by the flow (i.e. slope of the lines in Figure 2), the thermodynamics (intersection point of the lines in Figure 2) is not.

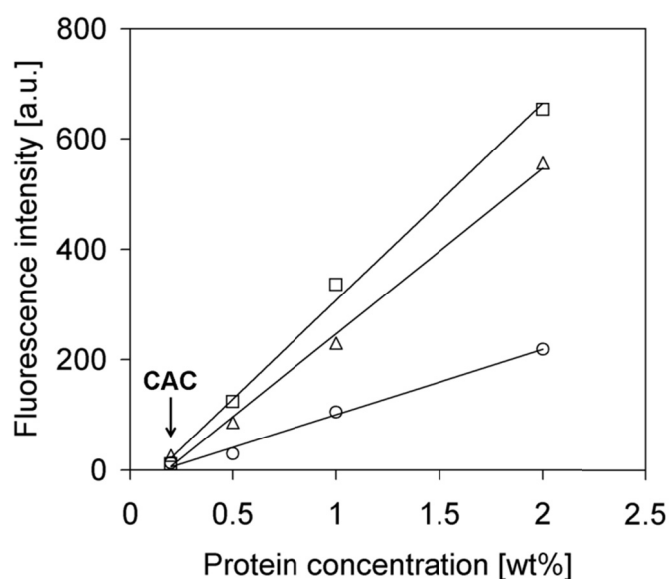


Figure 2. The protein concentration versus the conversion into fibrils of  $\beta$ -Ig solutions (pH 2) heated for 24 hours at 353 K. The solutions were stirred at 290 rpm ( $\square$ ) during heating, stirred at 1200 rpm ( $\Delta$ ) during heating or heated in rest ( $\circ$ ).

*Binding energy*

The thermodynamics of self-assembly was used to estimate the binding energy, i.e. the decrease in the Gibbs free energy when a fibril is extended by one mol of building blocks.<sup>40</sup> For determining the CAC we do not have to use thermodynamic equilibrium properties. However, at the concentration just below the CAC, thermodynamic equilibrium exists and the principles of self-assembly are still valid. The relation between the molar fraction of fibrillar (i.e. linear) aggregates consisting of  $N$  building blocks,  $x_N$ , and the binding energy,  $a$ , is given by<sup>40</sup>

$$x_N = N[x_1 \cdot e^a]^N \quad [1]$$

with  $a$  expressed in units of  $RT$  and where  $x_1$  is the molar fraction of the building blocks. From Equation [1] it follows that for large  $N$  and for  $x_1$  becoming larger than  $e^{-a}$  the right hand term becomes much larger than unity, invalidating the requirement that  $x_N$  should be smaller than 1. This implies that  $x_{1,CAC} \approx e^{-a}$  is a natural limit of the molar fraction of building blocks and denotes the CAC. Above this concentration aggregates will be formed. The relation between the CAC and  $a$  can thus be written as

$$x_{1,CAC} \approx e^{-a} \quad [2].$$

At the optimal temperature for fibril formation (353 K) the CAC, as determined from Figure 1 at a protein concentration of 0.16 wt % ( $x_{1,CAC} = 1.6 \times 10^{-6}$ ), leads to a binding energy of 13.4  $RT$  (39.1  $\text{kJ mol}^{-1}$ ). Since the fibril formation of  $\beta$ -lg is a complex process where several mechanisms are involved, one should keep in mind that the determined binding energy is the binding energy when the fibrils are extended by one mol of building blocks. After this initial binding subsequently intermolecular  $\beta$ -sheet formation will take place<sup>14,15</sup> which will make the binding stronger and

irreversible, unless a strong chaotropic agent like guanidinium chloride is added.<sup>21,25,44</sup>

#### *Temperature dependence of the CAC*

To see the effect of temperature on the CAC and binding energy of the fibril formation, the same experiments were also performed at 343 K, 358 K, 363 K and 383 K. For these temperatures the maximal conversion of protein into fibrils as a function of the total protein concentration are shown in Figure 3A-D. In order to measure the CAC we need to determine the protein concentration where the fluorescence signal becomes zero (the CAC). This was done by extrapolating the conversion data to zero conversion. A priori the functional form of the conversion relative to protein concentration is unknown. However, based on the results at 353K we have assumed a linear relation between the total protein concentration and the conversion of protein into fibrils at all temperatures. All linear fits gave a  $R^2 > 0.94$ .

The CAC's and corresponding binding energies for all temperatures are shown in Table 1. All the calculated binding energies in Table 1 have a value of about 13 RT (about 40 kJ mol<sup>-1</sup>), where the binding energy has a shallow maximum at the temperature where the fibril formation is maximal, 353 K.

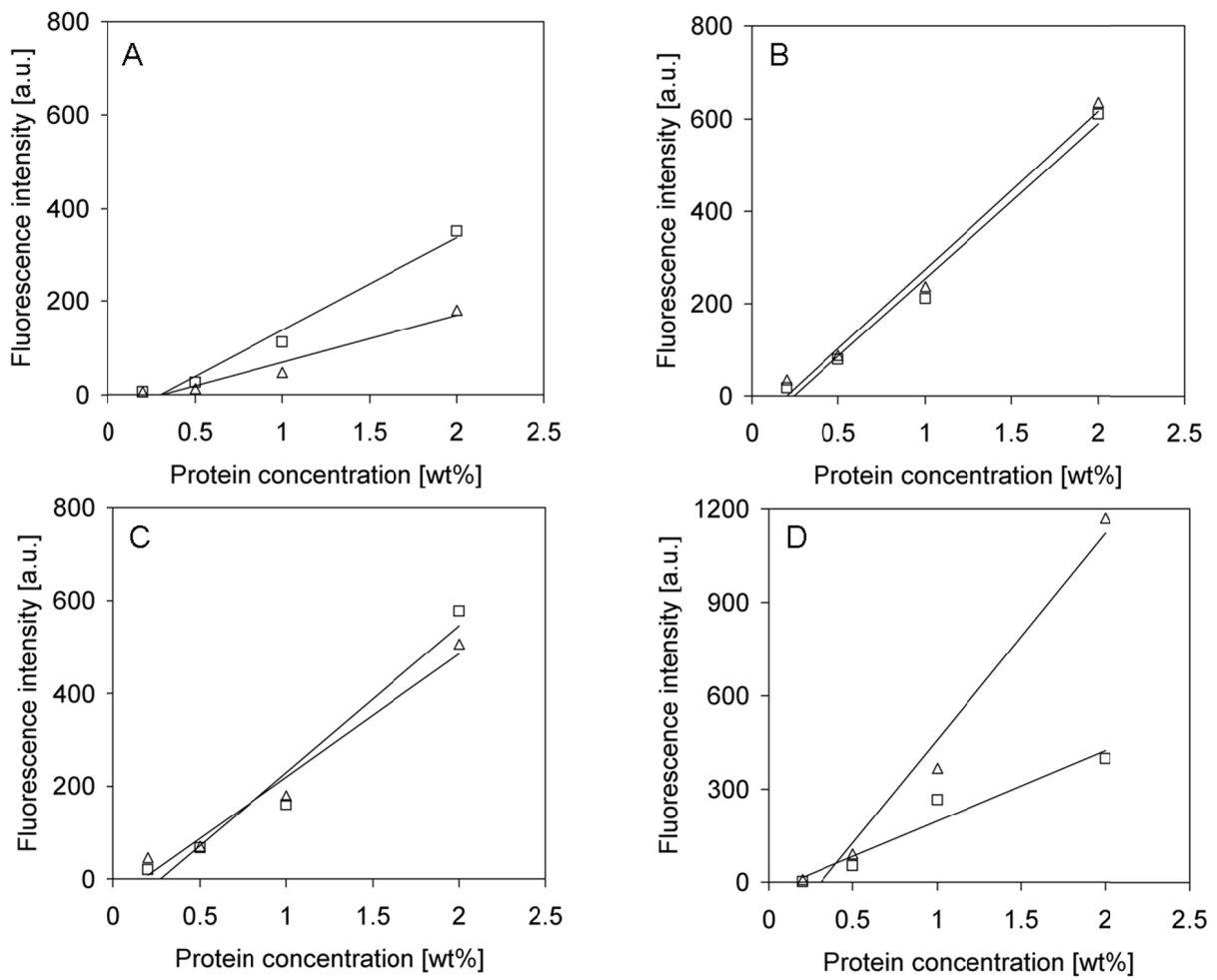


Figure 3. The protein concentration versus the conversion into fibrils of  $\beta$ -Ig solutions (pH 2) heated at 343 K (A), 358 K (B), 363 K (C) and 383 K (D). The solutions were stirred at 290 rpm (□) or stirred at 1200 rpm (△) during heating.

Table 1. The CAC and corresponding binding energy ( $\alpha$ ) at various temperatures.

Temperature [K]	CAC [wt %]	$X_{1,CAC}$ [mol fraction]	$\alpha$ [RT]	$\alpha$ [kJ mol <sup>-1</sup> ]
343	0.33	3.2E-06	12.6	36.1
353	0.16	1.6E-06	13.4	39.1
358	0.23	2.3E-06	13.0	38.7
363	0.24	2.4E-06	12.9	39.1
383	0.25	2.5E-06	12.9	41.1

### Enthalpy and Entropy

Using de Van 't Hoff equation and the temperature dependence of the CAC, the entropy and enthalpy of aggregate formation can be determined (see for example Yu et al.<sup>45</sup>). For this the following equations were used:

$$\Delta G^0 = RT \ln x_{1,CAC} \quad [3]$$

$$\Delta H^0 = -RT^2 \left[ \frac{\partial \ln x_{1,CAC}}{\partial T} \right] \quad [4]$$

$$\Delta G^0 = \Delta H^0 - T\Delta S^0 \quad [5]$$

where  $\Delta G^0$  and  $\Delta H^0$  are standard molar Gibbs free energy and molar enthalpy of aggregate formation and  $x_{1,CAC}$  is the molar fraction of the CAC. With  $\Delta G^0$  and  $\Delta H^0$ , the molar entropy of aggregate formation,  $\Delta S^0$  can be obtained. However, the values for the  $x_{1,CAC}$  of fibril formation of  $\beta$ -lg at pH 2 do not depend on the temperature (see Table 1) within the experimental error. This means that  $\Delta H^0$  is close to zero and as a result we find that  $\Delta S^0 \cong -\frac{\Delta G^0}{T}$ . Since  $\Delta G^0$  is in the order of -40 kJ mol<sup>-1</sup> (see

Table 1) the change in entropy is positive, making the fibril formation an entropy-driven process.

## Conclusion

The relations between the protein concentration and the conversion into fibrils were extrapolated to obtain the CAC for fibril formation of  $\beta$ -lg at pH 2 and elevated temperatures. The fibril formation took place under different stirring speeds and although the kinetics of the fibril formation was influenced by the stirring speed, the CAC was not. This was used to increase the accuracy at which the CAC was determined. The corresponding binding energy was 13 RT ( $\sim 40$  kJ mol<sup>-1</sup>) for all measured temperatures. This temperature independence indicates that the growth of fibrils obtained from  $\beta$ -lg is an entropy-driven process.

## References

1. Krebs, M. R. H.; Wilkins, D. K.; Chung, E. W.; Pitkeathly, M. C.; Chamberlain, A. K.; Zurdo, J.; Robinson, C. V.; Dobson, C. M., Formation and seeding of amyloid fibrils from wild-type hen lysozyme and a peptide fragment from the [beta]-domain. *Journal of Molecular Biology* **2000**, 300, (3), 541-549.
2. Veerman, C.; de Schiffart, G.; Sagis, L. M. C.; van der Linden, E., Irreversible self-assembly of ovalbumin into fibrils and the resulting network rheology. *Int. J. Biol. Macromol.* **2003**, 33, (1-3), 121-127.
3. Arnaudov, L. N.; de Vries, R., Thermally Induced Fibrillar Aggregation of Hen Egg White Lysozyme. *Biophysical Journal* **2005**, 88, (1), 515-526.
4. Weijers, M.; Sagis, L. M. C.; Veerman, C.; Sperber, B.; van der Linden, E., Rheology and structure of ovalbumin gels at low pH and low ionic strength. *Food Hydrocolloids* **2002**, 16, (3), 269-276.

5. Veerman, C.; Sagis, L. M. C.; Heck, J.; van der Linden, E., Mesostructure of fibrillar bovine serum albumin gels. *International Journal of Biological Macromolecules* **2003**, *31*, 139-146.
6. Akkermans, C.; Van der Goot, A. J.; Venema, P.; Gruppen, H.; Vereijken, J. M.; Van der Linden, E.; Boom, R. M., Micrometer-Sized Fibrillar Protein Aggregates from Soy Glycinin and Soy Protein Isolate. *Journal of agricultural and food chemistry* **2007**, *55*, (24), 9877-9882.
7. Langton, M.; Hermansson, A.-M., Fine-stranded and particulate gels of  $\beta$ -lactoglobulin and whey protein at varying pH. *Food Hydrocolloids* **1992**, *5*, 523-539.
8. Gimel, J. C.; Durand, D.; Nicolai, T., Structure and distribution of aggregates formed after heat-induced denaturation of globular proteins. *Macromolecules* **1994**, *27*, (2), 583-589.
9. Aymard, P.; Durand, D.; Nicolai, T., A Comparison of the Structure of  $\beta$ -Lactoglobulin Aggregates Formed at pH7 and pH2. *Int. J. Pol. Anal. Char.* **1996**, *2*(2), 115 - 119.
10. Renard, D.; Lefebvre, J.; Griffin, M. C. A.; Griffin, W. G., Effects of pH and salt environment on the association of beta-lactoglobulin revealed by intrinsic fluorescence studies. *International Journal of Biological Macromolecules* **1998**, *22*, 41-49.
11. Aymard, P.; Nicolai, T.; Durand, D., Static and Dynamic Scattering of  $\beta$ -Lactoglobulin Aggregates Formed after Heat-Induced Denaturation at pH 2. *Macromolecules* **1999**, *32*, 2542-2552.
12. Le Bon, C.; Nicolai, T.; Durand, D., Growth and structure of aggregates of heat-denatured beta-Lactoglobulin. *International Journal of Food Science and Technology* **1999**, *34*, 451-465.
13. Gosal, W. S.; Ross-Murphy, S. B., Globular protein gelation. *Current opinion in colloid & interface science* **2000**, *5*, 188-194.
14. Kavanagh, G. M.; Clark, A. H.; Ross-Murphy, S. B., Heat-induced gelation of globular proteins: part 3. Molecular studies on low pH beta-lactoglobulin gels. *International Journal of Biological Macromolecules* **2000**, *28*, 41-50.

15. Lefèvre, T.; Subirade, M., Molecular differences in the formation and structure of fine-stranded and particulate beta-lactoglobulin gels. *Biopolymers* **2000**, 54, (7), 578-586.
16. Schokker, E. P., Heat-induced aggregation of beta-lactoglobulin AB at pH 2.5 as influenced by ionic strength and protein concentration. *International dairy journal* **2000**, 10, (4), 233.
17. Durand, D.; Christophe Gimel, J.; Nicolai, T., Aggregation, gelation and phase separation of heat denatured globular proteins. *Physica A: Statistical Mechanics and its Applications* **2002**, 304, (1-2), 253-265.
18. Ikeda, S.; Morris, V. J., Fine-Stranded and Particulate Aggregates of Heat-Denatured Whey Proteins Visualized by Atomic Force Microscopy. *Biomacromolecules* **2002**, 3, (2), 382-389.
19. Gosal, W. S.; Clark, A. H.; Pudney, P. D. A.; Ross-Murphy, S. B., Novel amyloid fibrillar networks derived from a globular protein: B-lactoglobulin. *Langmuir* **2002**, 18, 7174-7181.
20. Veerman, C.; Ruis, H.; Sagis, L. M. C.; van der Linden, E., Effect of electrostatic interactions on the percolation concentration of fibrillar beta-lactoglobulin gels. *Biomacromolecules* **2002**, 3, (4), 869.
21. Arnoudov, L. N.; Vries, d. R.; Ippel, H.; Mierlo, v. C. P. M., Multiple steps during the formation of beta-lactoglobulin fibrils. *Biomacromolecules* **2003**, 4, 1614-1622.
22. Veerman, C.; Sagis, L.M.C.; van der Linden, E., Gels at Extremely Low Weight Fractions Formed by Irreversible Self-Assembly of Proteins. *Macromolecular bioscience* **2003**, 3, (5), 243.
23. Rogers, S. S.; Venema, P.; Sagis, L. M. C.; van der Linden, E.; Donald, A. M., Measuring length distribution of a fibril system: A flow birefringence technique applied to amyloid fibrils. *Macromolecules* **2005**, 38, 2948-2958.

24. Bolder, S. G. S. G.; Hendrickx, H. H.; Sagis, L. M. L. M. C.; van der Linden, E. E., Fibril assemblies in aqueous whey protein mixtures. *Journal of agricultural and food chemistry* **2006**, 54, (12), 4229-34.
25. Akkermans, C.; Venema, P.; van der Goot, A.; Boom, R.; van der Linden, E., Enzyme-Induced Formation of  $\beta$ -Lactoglobulin Fibrils by AspN Endoproteinase. *Food Biophysics* **2008**, 3, (4), 390-394.
26. Chiti, F.; Dobson, C.M., Protein Misfolding, Functional Amyloid, and Human Disease. *Annu. Rev. Biochem.* **2006**, 75, 333-366.
27. Dobson, C.M., Protein folding and misfolding. *Nature* **2003**, 426(6968), 884.
28. Glenner, G. G., Amyloid deposits and amyloidosis - the beta-fibrilloses 1. *N. Engl. J. Med.* **1980**, 302, 1383-1292.
29. Glenner, G. G., Amyloid deposits and amyloidosis - the beta-fibrilloses 1. *N. Engl. J. Med.* **1980**, 302, 1333-1343.
30. Serpell, L.C.; Sunde, M.; Blake, C.C.F., The molecular basis of amyloidosis. *Cell. Mol. Life Sci.* **1997**, 53, 871-887.
31. Nelson, R.; Sawaya, M. R.; Balbirnie, M.; Madsen, A. O.; Riek, C.; Grothe, R.; Eisenberg, D., Structure of the cross-beta spine of amyloid-like fibrils. *Nature* **2005**, 435, 773-778.
32. Glenner, G. G.; Page, D. L.; Eanes, E. D., The relation of the properties of congo red-stained amyloid fibrils to the  $\beta$ -conformation. *J. Histochem. Cytochem.* **1972**, 20(10), 821-826.
33. Naiki, H. H., Fluorometric determination of amyloid fibrils in vitro using fluorescent dye, thioflavine T. *Analytical biochemistry* **1989**, 177, (2), 244.
34. Bromley, E. H. C.; Krebs, M. R. H.; Donald, A. M., Aggregation across the length-scales in beta-lactoglobulin. *Faraday Discussions* **2005**, 128, 13-27.
35. Gosal, W. S.; Clark, A. H.; Ross-Murphy, S. B., Fibrillar beta-lactoglobulin gels: Part 1. Fibril formation and structure. *Biomacromolecules* **2004**, 5, (6), 2408-2419.

36. LeVine, H., Quantification of  $\beta$ -sheet amyloid fibril structures with Thioflavin T In *Methods in Enzymology: Amyloids, Prions and other Protein Aggregates*, Wetzel, R., Ed. Academic Press: London, 1999; Vol. 309, pp 285-305.
37. Naiki, H.; Gejyo, F., [20] Kinetic analysis of amyloid fibril formation. *Methods in Enzymology* **1999**, 309, 305-318.
38. Nielsen, L. L.; Khurana, R. R.; Coats, A. A.; Frokjaer, S. S.; Brange, J. J.; Vyas, S. S.; Uversky, V. V. N.; Fink, A. A. L., Effect of environmental factors on the kinetics of insulin fibril formation: elucidation of the molecular mechanism. *Biochemistry* **2001**, 40, (20), 6036-46.
39. Groenning, M.; Olsen, L.; van de Weert, M.; Flink, J. M.; Frokjaer, S.; Jørgensen, F. S., Study on the binding of Thioflavin T to beta-sheet-rich and non-beta-sheet cavities. *Journal of structural biology* **2007**, 158, 358-369.
40. Israelachvili, J., Chapter 16: Thermodynamic principles of self-assembly, in *Intermolecular & Surface Forces*, **1992**, (Academic Press, California, USA), 341-365.
41. Rogers, S. S., Some physical properties of amyloid fibrils, *PhD Thesis*, Cambridge University, UK, **2005**.
42. Hill, E. K.; Krebs, B.; Goodall, D. G.; Howlett, G. J.; Dunstan, D. E., Shear Flow Induces Amyloid Fibril Formation. *Biomacromolecules* **2006**, 7, (1), 10-13.
43. Bolder, S. G.; Sagis, L. M. C.; Venema, P.; van der Linden, E., Effect of Stirring and Seeding on Whey Protein Fibril Formation. *Journal of agricultural and food chemistry* **2007**, 55, (14), 5661-5669.
44. Meersman, F.; Dobson, C. M., Probing the pressure-temperature stability of amyloid fibrils provides new insights into their molecular properties. *Biochimica et Biophysica Acta (BBA) - Proteins & Proteomics* **2006**, 1764, (3), 452-460.
45. Yu, J-A.; Oh, S-H.; Park, Y-R.; Kim, J-S., Enthalpy-Entropy Compensation in Aggregation of Poly(styrene-co-sodium methacrylate) Ionomers in Aqueous Solution. *Macromolecular Symposium*, **2007**, 249-250, 445-449.



Chapter 3 is published as: Kroes-Nijboer, A., Venema, P., Bouman, J., van der Linden, E. (2011) The influence of protein hydrolysis on the growth kinetics of  $\beta$ -lg fibrils. *Langmuir* 27 (10), 5753–5761.

## *Chapter 3*

### **The influence of protein hydrolysis on the growth kinetics of $\beta$ -lg fibrils**

## Abstract

Recently it was found that protein hydrolysis is an important step in the formation of  $\beta$ -lactoglobulin fibrils at pH 2 and elevated temperatures. The objective of the present study was to further investigate the influence of hydrolysis on the kinetics of fibril formation. Both the hydrolysis of  $\beta$ -lactoglobulin and the growth of the fibrils were followed as a function of time and temperature, using SDS polyacrylamide gel electrophoresis and a Thioflavin T fluorescence assay. As an essential extension to existing models, the quantification of the effect of the hydrolysis on the fibrillar growth was established by a simple polymerization model including a hydrolysis step.

## Introduction

$\beta$ -Lactoglobulin ( $\beta$ -lg) fibrils are linear aggregates that arise when  $\beta$ -lg is heated at pH 2.<sup>1, 2</sup>  $\beta$ -Lg is a globular whey protein that is readily available in large quantities and an important protein for the food industry. The fibrils derived from  $\beta$ -lg have a high aspect ratio, which makes them interesting for the application in food products, for example as thickening or gelling agents. They can also be used in the production of microcapsules to give them more strength.<sup>3, 4</sup> To be able to tune the properties of the fibrils derived from  $\beta$ -lg, it is important to have knowledge about the kinetics of the fibril formation and the factors that are influencing this. Fibrils derived from  $\beta$ -lg share certain properties with amyloid fibrils<sup>5</sup>, which are being studied very intensively.<sup>6-14</sup> Not only the typical amyloid characteristics are present in the fibrils derived from  $\beta$ -lg, also the growth curves have the commonly measured sigmoidal shape. The amyloid fibril formation typically starts with a lag phase in which there is no significant measurable growth. The lag phase is followed by a polymerization or growth phase in which the fibril concentration increases very rapidly and eventually, the growth of the fibrils levels off. However, an essential difference with the commonly studied amyloigenic peptides is that in the fibril formation of  $\beta$ -lg, the hydrolysis of  $\beta$ -lg is an essential step. The fact that hydrolysis is playing a role in the fibril formation of  $\beta$ -lg was already mentioned by Bolder et al.<sup>15</sup> They showed that for fibrils derived from  $\beta$ -lg the fibril growth curves already level off when only 5 to 40 % of the total protein is converted into fibrils, depending on the protein concentration.<sup>15, 16</sup> Bolder et al. suggested that this low conversion was caused by the lack of active monomers available for fibril formation, due to the hydrolysis of the  $\beta$ -lg which takes place during the prolonged heating at pH 2.<sup>15</sup> However, recent research showed that the hydrolysis has a different role in the fibril formation.<sup>17-19</sup> Akkermans et al. found that the building blocks of the fibrils derived from  $\beta$ -lg are not the intact monomers, but small peptides derived from  $\beta$ -lg by hydrolysis.<sup>18</sup> They showed that not all the peptides that are formed during hydrolysis of the  $\beta$ -lg are

converted into fibrils, which also explains the conversion levels that are substantial lower than 100%. To identify which peptides are present and which peptides are absent in the fibrils they determined the molecular masses of the peptides using mass spectrometry. These results were compared with all theoretically possible peptides that could result from cleavage before or after the aspartic acid residues in  $\beta$ -lg, which are the most sensitive bonds for hydrolysis at pH 2 and high temperature. Their results show that the more hydrophobic peptides with a low charge and a high capacity to form  $\beta$ -sheets are included in the fibrils.<sup>18</sup> For more details about the sequences of the peptides involved we refer to the paper of Akkermans et al.<sup>18</sup> For fibrils derived from hen egg-white lysozyme (HEWL) it was already shown that peptides are the building blocks of the fibrils.<sup>17, 19</sup> Frare et al. showed that amyloid fibrils obtained from HEWL after incubation at pH 2 and 65°C consist of peptide fragments derived from the partial acid hydrolysis of Asp-X peptide bonds.<sup>19</sup> Mishra et al. verified that HEWL hydrolysis into peptides when it is heated for 10 days at pH 1.6 and 65°C. Besides, they show that the addition of intact full length HEWL was even slowing down the fibril formation.<sup>17</sup> The finding that peptides are the building blocks of the fibrils, shows the importance of the hydrolysis in the fibril formation process of  $\beta$ -lg at pH 2. Peptides have to be produced before the fibrillar assembly can start. This finding is also supported by a study of Akkermans et al. in which it is shown that fibrils could also be formed after enzymatic hydrolysis of the  $\beta$ -lg by the enzyme AspN endoproteinase.<sup>20</sup> This enzyme cleaves the peptide bonds N-terminal to aspartic acid residues,<sup>21</sup> the same peptide bonds that are preferably cleaved during acid hydrolysis at pH 2.<sup>18</sup> From these observations the question arises how the hydrolysis kinetics influences the growth kinetics of the fibrils obtained from  $\beta$ -lg. In the past several models were proposed to describe the growth kinetics of the fibril formation of  $\beta$ -lg at pH 2. For example, Bromley et al. used a simple nucleation and growth model to fit their kinetic growth data.<sup>5</sup> A more extensive model for the fibril formation of  $\beta$ -lg at pH 2 was derived by Arnaudov and de Vries which involves a nucleation step and a simple addition reaction for the growth of the fibrils.<sup>22</sup> The

model also includes a side reaction leading to the irreversible denaturation and inactivation of a part of the protein molecules.<sup>22</sup> Recently, Loveday et al.<sup>23</sup> could fit their fibril growth data well using the general protein aggregation model given by Morris et al.<sup>24</sup> Morris et al. attributed mechanistic meaning to the parameters used in the model, but since the fibril formation of  $\beta$ -lg at pH 2 requires an extra step, namely the hydrolysis of  $\beta$ -lg, in the case of Loveday et al. the parameters have no mechanistic meaning.<sup>23</sup> Despite the fact that models exist that describe the kinetic growth of  $\beta$ -lg at pH 2, none of these models take into account the hydrolysis of  $\beta$ -lg. Therefore the objective of the present study was to investigate the role of hydrolysis on the growth kinetics of fibril formation. For this we consider the fibril formation as a two-step process. In the first step the proteins are hydrolyzed and in the second step some of the peptides produced by hydrolysis self-assemble into fibrils. The first step, the hydrolysis of  $\beta$ -lg at various temperatures and pH 2, was followed by SDS polyacrylamide gel electrophoresis (SDS-PAGE). Simultaneously the growth of the fibrils at these temperatures was followed using a Thioflavin T (ThT) fluorescence assay. The experimental data show that the hydrolysis rate is an important factor influencing the fibril formation. To quantify the effect of hydrolysis on the fibrillar growth a simple polymerization model including a hydrolysis step is forwarded in this research.

## Materials & Methods

### *Sample preparation*

$\beta$ -Lg was obtained from Sigma (product no. L0130, lot. no. 095K7006). A stock solution (about 9 wt %) was made by dissolving the protein powder in HCl solution of pH 2. The pH of the protein solution was adjusted to pH 2 with 6M HCl solution. Subsequently, this stock solution was filtered through a protein filter (FD 30/0.45  $\mu$ m Ca-S from Schleicher & Schuell) to remove any traces of undissolved protein. The protein concentration of the stock solution was determined using a UV

spectrophotometer (Cary 50 Bio, Varian) and a calibration curve of known  $\beta$ -lg concentrations at a wavelength of 278 nm. The stock solution was diluted to protein concentrations of 2, 1, 0.5, 0.2 wt % with HCl solution of pH 2.

#### *Fibril formation*

$\beta$ -Lg solutions of 1 wt % were heated in small glass vials (20 ml) in an isolated metal stirring and heating plate for several hours at 353, 358, 363, 373, 378 and 383 K. At 353 K and 363 K also  $\beta$ -lg solutions of 0.2, 0.5 and 2.0 wt % were heated. To reduce the lag phase in the fibril formation, the protein solutions were mildly stirred during heating using a magnetic stirring bar. A thermocouple was used to measure the temperature in a vial that contains paraffin oil. To follow the process, aliquots of the fibril forming solution were taken, cooled down on ice-water and subsequently analyzed using a ThT fluorescence assay within half an hour. Besides, the aliquots of the fibril forming solution were analyzed with SDS-PAGE. The samples of 373, 378 and 383 K were heated in glass vials (10 ml) with a crimp cap (with septum of silicone/PTFE 3mm) to allow elevated pressures. Since subsequent sampling is not possible from vial with crimp caps, samples were taken from different vials at different times. At 373, 378 and 383K the samples were only heated up to 5 hours, because the total conversion of protein into fibrils is reached earlier at these higher temperatures.

#### *Thioflavin T fluorescence assay*

The ThT fluorescence assay was used to measure the conversion of protein into fibrils during heating of the protein solutions. A ThT stock solution (3.0 mM) was made by dissolving 7.9 mg ThT in 8 ml phosphate buffer (10 mM phosphate, 150 mM NaCl at pH 7.0). This stock solution was filtered through a 0.2  $\mu$ m filter (Schleicher & Schuell). The stock solution was diluted 50x in a phosphate buffer (10 mM phosphate, 150 mM NaCl at pH 7.0) before use.

Aliquots of the fibril samples (48  $\mu$ l) were mixed with 4 ml ThT solution and allowed to bind to the ThT for 1 minute. The fluorescence of the samples was measured using a fluorescence spectrophotometer (Perkin Elmer LS 50 B). The excitation wavelength was set on 460 nm (slit width 4.0 nm) and the emission spectrum was recorded between 470 and 500 nm (slit width 2.5 nm) at a scanning speed of 200 nm/min. The fluorescence intensity peak was determined at 482 nm. The fluorescence intensity of the ThT solution was subtracted as a background. Samples were measured in duplicates.

#### *Gel Electrophoresis (SDS-PAGE)*

SDS -PAGE was performed using a XCell *SureLock*<sup>TM</sup> Mini-Cell (Invitrogen Corporation, Carlsbad, California 92008, USA). Samples were run on NuPAGE<sup>®</sup> Novex 4-12% Bis-Tris gels with NuPAGE<sup>®</sup> MES SDS running buffer (Invitrogen Corporation) under non-reducing conditions. The gels were stained with SimplyBlue<sup>TM</sup> SafeStain (Invitrogen Corporation). The intensities of the  $\beta$ -Ig bands were quantified using a Bio-Rad Imaging Densitometer (Model GS-710).

## Results & Discussion

#### *Hydrolysis as a function of time and temperature*

Since we were interested in the role of hydrolysis in the fibril formation, the hydrolysis of  $\beta$ -Ig was followed during the fibril formation process. Upon hydrolysis the  $\beta$ -Ig monomers were broken down into peptides. This break-down of the full monomer at various temperatures was followed by SDS-PAGE (see Figure 1).

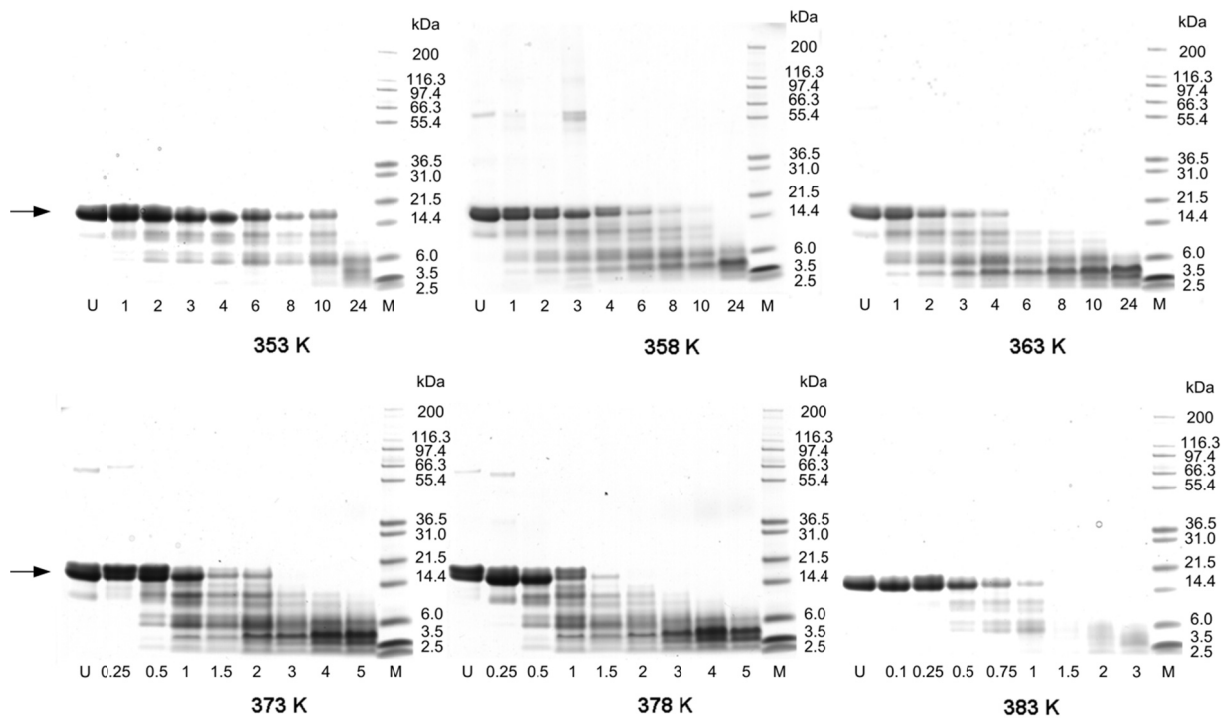


Figure 1. SDS-PAGE for 1 wt %  $\beta$ -lactoglobulin heated at pH 2 and 353 K, 358 K, 363 K, 373 K, 378 K and 383 K. The horizontal numbers represent hours of heating. (U) is the unheated sample, (M) is the marker. The arrow on the left depict the  $\beta$ -lg bands (18.4 kDa).

The band of the  $\beta$ -lg monomer (18.4 kDa) disappears upon heating because the  $\beta$ -lg is hydrolyzed into small peptides at these temperatures and low pH. This hydrolysis process is essential for the fibril formation, since peptides are the building blocks of the fibrils.<sup>18</sup> At the same time, new bands are appearing at the smaller molecular weights, which are the peptides that are not built into the fibrils. Due to hydrolysis the density of these bands is increasing during the fibril formation. However, for the analysis of the hydrolysis we are therefore taking the rate in which the intact  $\beta$ -lg molecule is disappearing (so not the smaller peptides that are produced) as a measure for the rate of hydrolysis. The densities of the  $\beta$ -lg bands were quantified using a densitometer and from these band densities the rate of hydrolysis of  $\beta$ -lg at pH 2 was determined (Figure 2). To avoid differences in staining from gel to gel,

band densities of  $\beta$ -lg were normalized relative to the band density of the unheated samples. The hydrolysis kinetics were fit to a single-exponential rate equation:

$$I_t = I_0 \cdot e^{-k_h \cdot t} \quad [1]$$

where  $I_t$  is the density of the  $\beta$ -lg band at time  $t$ ,  $I_0$  is the initial density of the unheated  $\beta$ -lg,  $k_h$  is the hydrolysis rate constant, and  $t$  is time in minutes.

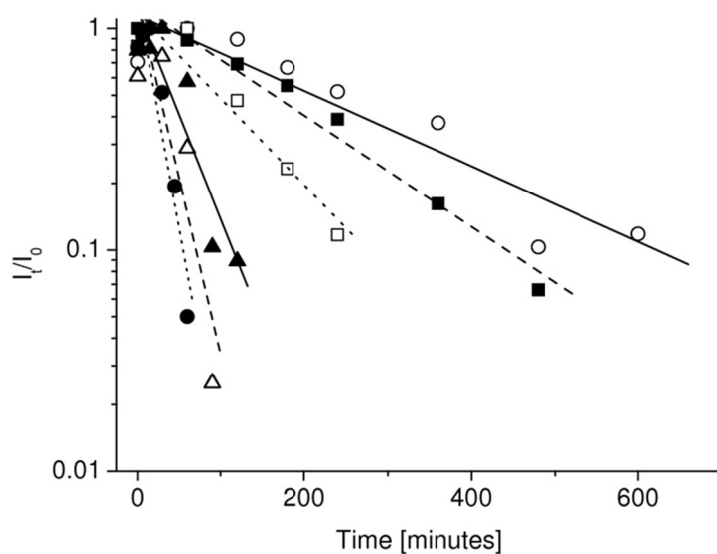


Figure 2. The normalized  $\beta$ -lg band densities as a function of time at various temperatures: 353 K ( $\circ$ ), 358 K ( $\blacksquare$ ), 363 K ( $\square$ ), 373 K ( $\blacktriangle$ ), 378 K ( $\triangle$ ) and 383 K ( $\bullet$ ). The lines represent the fit to a single-exponential rate equation, with correlation coefficients of about 0.88.

Figure 2 shows that the hydrolysis can be described by a first order-reaction. The rate of the hydrolysis of the  $\beta$ -lg is clearly dependent on the temperature. At 353 K it takes more than 10 hours for the  $\beta$ -lg band to disappear, whereas at 383 K the  $\beta$ -lg band has already disappeared after 90 minutes of heating (Figure 1). This temperature dependence of the hydrolysis can be described by the Arrhenius equation:

$$k_h = k_0 \cdot e^{-\frac{E_a}{RT}} \quad [2]$$

where  $k_h$  is the hydrolysis rate constant,  $E_a$  is the activation energy,  $R$  is the gas constant and  $k_0$  a pre-exponential factor. From Figure 3 the activation energy  $E_a$  was determined to be 97 kJ mol<sup>-1</sup> (corresponding to about 39 kT) with  $k_0 = 8.5 \times 10^{11}$  min<sup>-1</sup>.

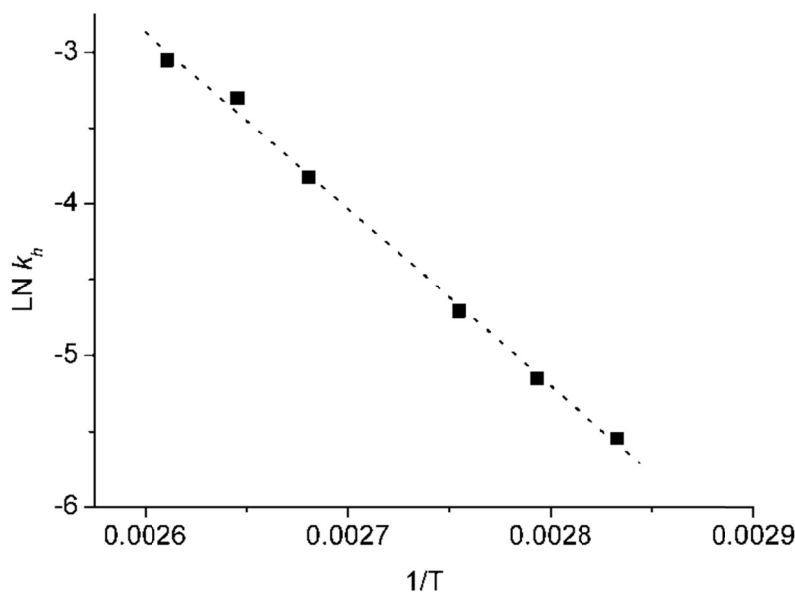


Figure 3. Determination of the  $-E_A/R$  (slope) of the hydrolysis. The slope is -11661, which gives a  $E_a$  of 97 kJ mol<sup>-1</sup> (correlation coefficient of 0.9968).

#### *Fibril formation as a function of time and temperature*

The fibril formation of  $\beta$ -lg was followed in time at the various temperatures using a ThT fluorescence assay (Figure 4). At all measured temperatures the growth curves show the common sigmoidal shape. However, no obvious lag phase is visible for the growth curves, in contrast to what has been found for  $\beta$ -lg solutions heated under quiescent conditions at pH 2. This reduction or even absence of the lag phase was found before<sup>25, 26</sup> and indicates that when flow is applied the fibril formation is not delayed by nucleation. In order to facilitate the analysis of the influence of

temperature on the fibril formation, we change to dimensionless parameters in the next paragraph. The important role of hydrolysis on the growth kinetics of the fibrils is shown by combining the gel data (Figure 1) and the growth curves (Figure 4). Figure 4 shows that the growth of the fibrils is narrowly following the hydrolysis and that as soon as the  $\beta$ -lg band has disappeared ( $\beta$ -lg has been hydrolyzed) the growth curves are leveling off. The results support the view that the formation of peptides by hydrolysis precedes their incorporation into the fibrils, still not rejecting the possibility of further hydrolysis of the peptides when already incorporated in the fibril by the so-called “fibril shaving process”.<sup>17</sup>

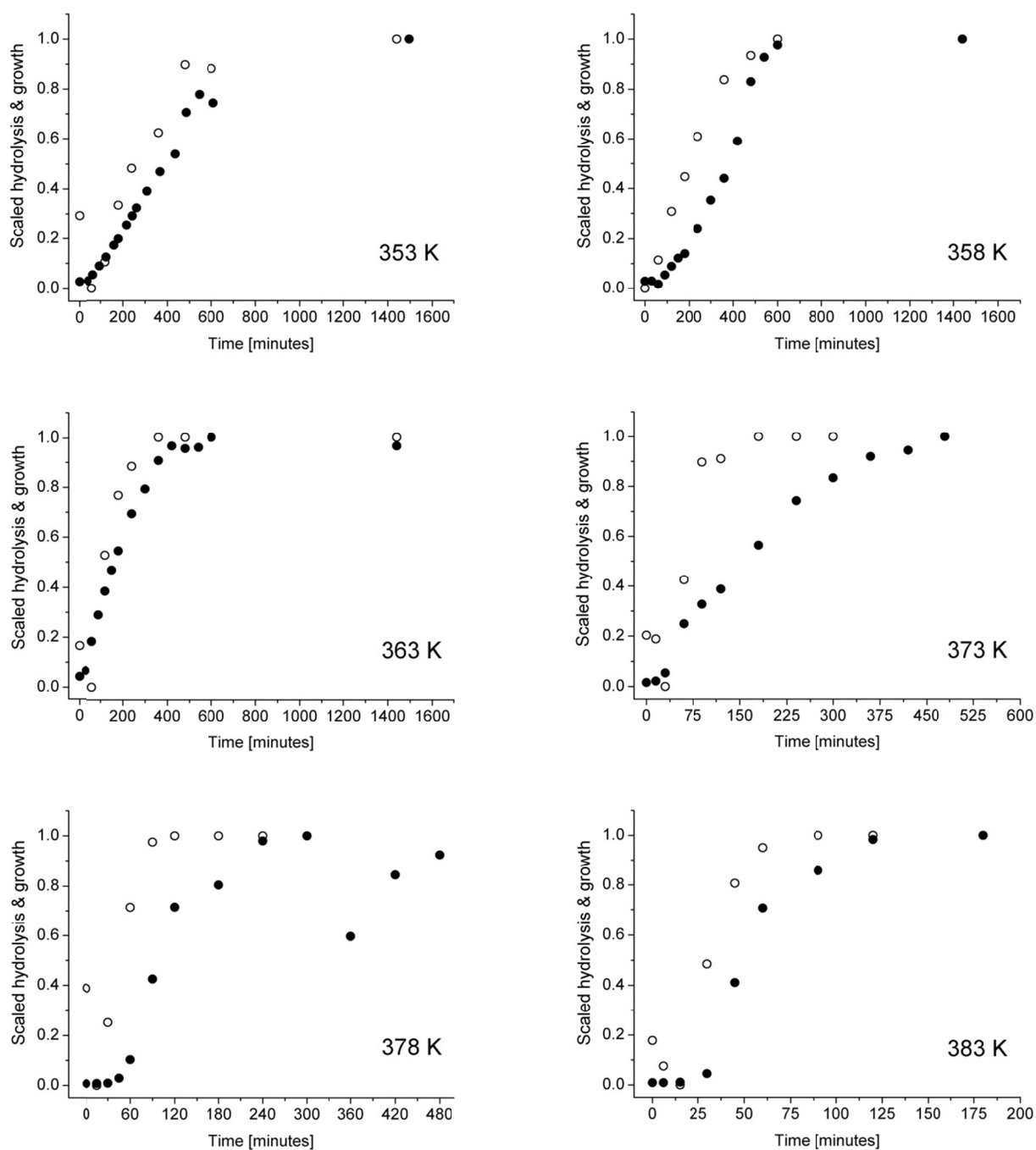


Figure 4. Hydrolysis ( $\circ$ ) and fibril growth curve ( $\bullet$ ) of a  $\beta$ -lactoglobulin solution (1 wt %) measured as a function of time. Solutions were heated at different temperatures (353K, 358K, 363K, 373K, 378K, 383K) and pH 2. Note that the graphs at different temperatures are plotted at different time scales to clearly show both the full hydrolysis and fibril growth curves for each temperature.

Theory

In an attempt to model the kinetics of aggregation of the fibrils, while keeping the number of fitting parameters to a minimum, the simplest possible aggregation model was considered. The hydrolysis, however, was still taken explicitly into account. In this model the fibril formation is modeled as a two-step process: (1) the hydrolysis of the  $\beta$ -lg monomers into peptides of which only a part will function as building blocks for the fibrils, (2) the subsequent irreversible self-assembly of these building blocks into fibrils (Figure 5).

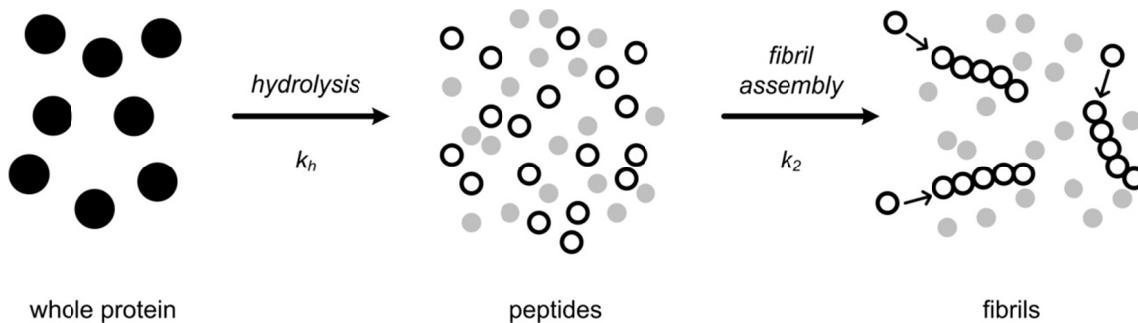


Figure 5. Schematic representation of the fibril formation of  $\beta$ -lg at pH 2. The first step is the hydrolysis of the monomers into peptides (of which only a part will function as building blocks) with rate constant  $k_h$  and the second step is the subsequent irreversible self-assembly of these building blocks into fibrils with rate constant  $k_2$ .

We will assume that fibrils  $M_i$ , with polymerization number  $i \geq 2$ , and peptides that serve as building blocks  $M_1$ , can join together in the reaction:



Here we omit the possible reaction between different fibrils. Since we are measuring the total length concentration and not the length distribution this is expected to be a

reasonable approximation. Since we stir the solutions during fibril formation, we find much shorter lags time than those are normally found under quiescent conditions. We therefore assume that the fibril formation is not delayed by a nucleation event. The break-up of the fibrils is not considered in this model, which is in a good approximation valid as was found by Akkermans.<sup>27</sup>

As a result we may write the following set of differential equations for the growth of the fibrils:

$$\frac{dc_i(t)}{dt} = k_2 \cdot (c_{i-1}(t)c_1(t) - c_i(t)c_1(t)) \quad \text{for } i \geq 2 \quad [4]$$

where  $c_i$  is the concentration of fibrils consisting of  $i$  building blocks at time  $t$ ,  $k_2$  is a reaction constant for the building block addition and  $c_1$  is the concentration of available building blocks independent of fibril length. The first term on the right hand side represents the increase in fibril concentration of length  $i$  while the second term on the right hand side represents the decrease in fibrils concentration of length  $i$ . The total concentration of building blocks  $M$  that are incorporated in the fibrils at time  $t$  is given by:

$$M(t) = \sum_{i \geq 2} ic_i(t) \quad [5]$$

The concentration of building blocks that are available to self-assemble into fibrils at time  $t$  is given by:

$$c_1(t) = C_0 \cdot (1 - e^{-k_h t}) - \sum_{i \geq 2} ic_i(t) \quad [6]$$

where  $c_1$  is the concentration of available building blocks at time  $t$ ,  $k_h$  the hydrolysis constant and  $C_0$  the concentration of building blocks that are eventually available

after complete hydrolysis. The first term in Equation 6 on the right hand side represents the concentration of building blocks available at time  $t$  if the building blocks would not have been incorporated into the fibrils at all. The last term in Equation 6 corrects for this and represents the concentration of building blocks that has been incorporated into the fibrils at time  $t$ . The difference is the concentration  $c_1$  of building blocks still available at time  $t$ . Here we made the simplifying Ansatz that all peptides that finally get incorporated in the fibrils follow the same kinetics. We assume that  $C_0$  is directly proportional, but not identical, to the protein concentration  $C_p$ . The boundary conditions are given by:

$$c_i(t=0) = 0 \quad \text{for } \forall i \quad [7]$$

For further analysis it is convenient to make these equations dimensionless by defining:

$$n_i(t') = \frac{c_i(t)}{C_0} \quad t' = k_2 C_0 t \quad \lambda = \frac{k_h}{k_2 C_0} \quad N(t') = \frac{M(t')}{C_0} \quad [8]$$

Leading to:

$$\frac{dn_i(t')}{dt'} = (n_{i-1}(t')n_1(t') - n_i(t')n_1(t')) \quad \text{for } i \geq 2 \quad [9]$$

$$N = \sum_{i \geq 2} i n_i(t') \quad [10]$$

$$n_1(t') = (1 - e^{-\lambda t'}) - \sum_{i \geq 2} i n_i(t') \quad [11]$$

$$n_i(t'=0) = 0 \quad \text{for } \forall i \quad [12]$$

In the above model the hydrolysis step acts as a source term driving the fibrillar assembly.

*Comparing theory with experiment*

In order to compare the theoretical predictions from the model with the experimental results we consider the growth curves, as determined by the ThT assay. By normalizing the growth curves as determined by this assay by their final plateau value, we can directly compare these curves to  $N$  as a function of time as defined by Equation 10. Equations 9-12 represent a set of coupled autonomic non-linear equations for which no obvious analytical solution exists and therefore a numerical analysis was performed. Having already determined the hydrolysis constant  $k_h$  we have reduced our parameter space to only one parameter, i.e.  $k_2C_0$ , that can be determined by fitting the numerical solution of Equations 9-12 to the experimental growth curves. Note that the parameter  $k_2C_0$  appears as a scaling parameter for time  $t$  as well as for the hydrolysis constant  $k_h$ . First, the parameter  $k_2C_0$  was determined as a function of temperature at a fixed concentration  $C_0$  (Figure 6 and Table 1, 1 wt % total protein). From these fits it is found that  $k_2C_0$  and therefore parameter  $k_2$  is independent of temperature to a good approximation in the temperature range that was used. At first sight this might be surprising, however, one has to realize that the self-assembly of building blocks into fibrils consists of two steps; (1) first building blocks and fibrils must come in close proximity by diffusion and (2) after that a reaction between them must take place. When the rate at which building blocks and fibrils come in close proximity by diffusion is much smaller than the reaction rate between the building blocks and the fibrils, the diffusion is the rate-limiting step. In this case the self-assembly will be diffusion controlled, explaining this behaviour of  $k_2$ . This in contrast to the hydrolysis step, which is a first order chemical reaction that is strongly dependent on temperature. Only at temperatures above 378 K and therefore at elevated pressures,  $k_2C_0$  seems to increase.

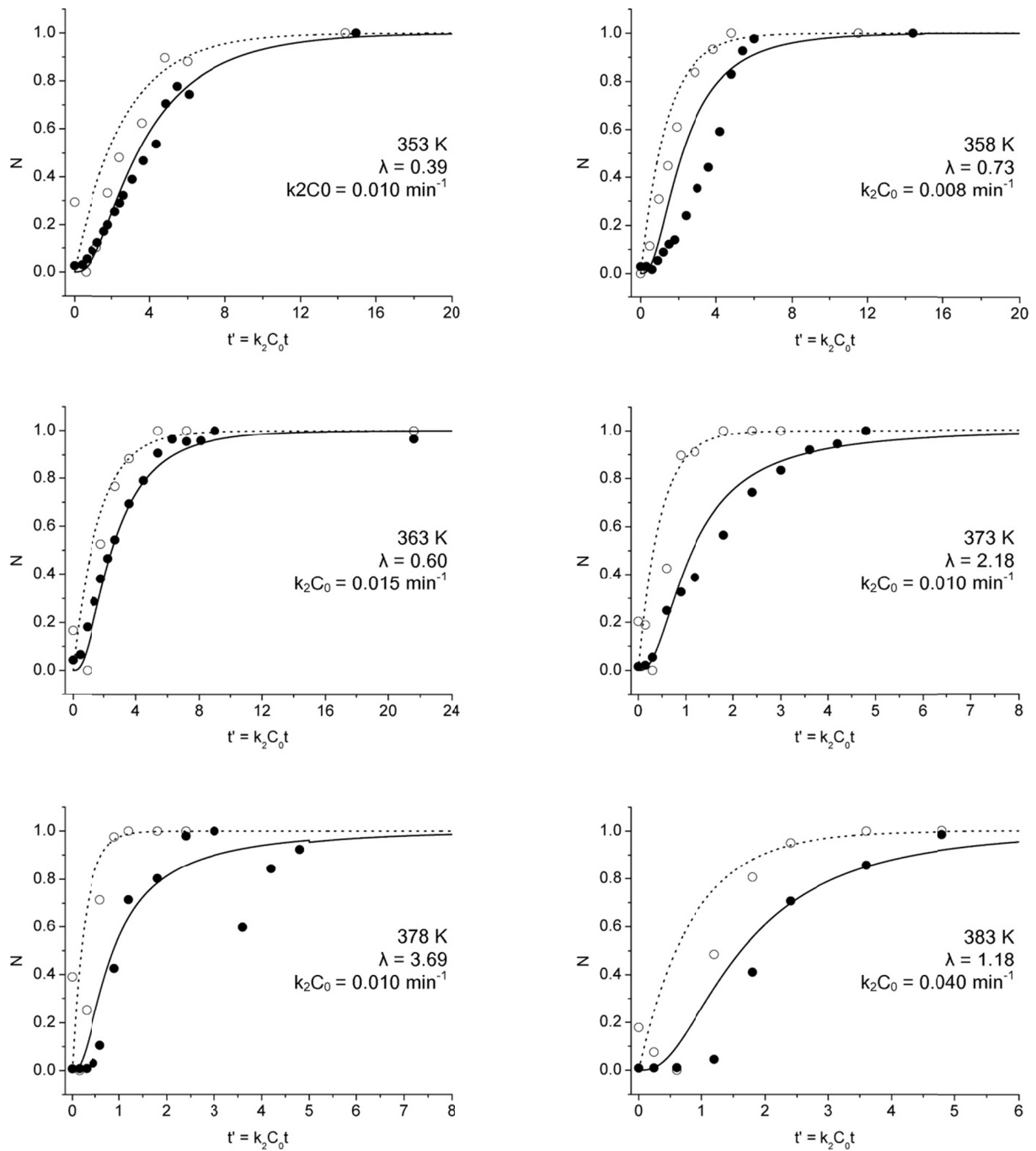


Figure 6. Growth curves of the fibril assembly process at various temperatures and a protein concentration  $C_p$  of 1 wt %, where the total (scaled) number of building blocks incorporated in the fibrils  $N$  is plotted against (scaled) time  $t'$ . Filled circles represent the experimental growth data, open circles represent the hydrolysis of  $\beta$ -lg, solid lines represent the fibril growth in the model and the dotted lines represent the hydrolysis in the model.

Table 1. Parameters used to model the hydrolysis of  $\beta$ -lg and fibril formation at various temperatures and a concentration  $C_p$  of 1 wt %, with hydrolysis rate constant  $k_h$ , scaling parameter  $k_2C_0$  including the rate of incorporation of the building blocks into the fibrils and the concentration of building blocks available after complete hydrolysis, and  $\lambda$  showing the relation between  $k_h$  and  $k_2C_0$ .

T [K]	$C_p$ [wt%]	$k_h$ [min <sup>-1</sup> ]	$k_2C_0$ [min <sup>-1</sup> ]	$\lambda$
353	1	0.0039	0.010	0.390
358	1	0.0058	0.008	0.725
363	1	0.0090	0.015	0.6
373	1	0.0218	0.010	2.18
378	1	0.0369	0.010	3.69
383	1	0.0473	0.040	1.18

After having determined the parameter  $k_2C_0$  for every temperature at a fixed concentration, we could use this information for a critical test of the model and predict the growth curves for other concentrations  $C_0$ . By changing concentration  $C_0$  and keeping the temperature range fixed we could directly compare the theoretical predictions, this time *without any* adjustable parameters (Figure 7, 8 and Table 2) since in this case  $k_2C_0$  is known. Given the simplicity of our model we find reasonable fits for the growth curves. Especially considering the various temperatures that are included in this research and the wide range of  $k_2C_0$  that is explored. Only at low concentrations (Figure 8) the model is deviating from our fibril growth data. At these low concentrations the nucleation, which we did not include into our model, might start to play a role.

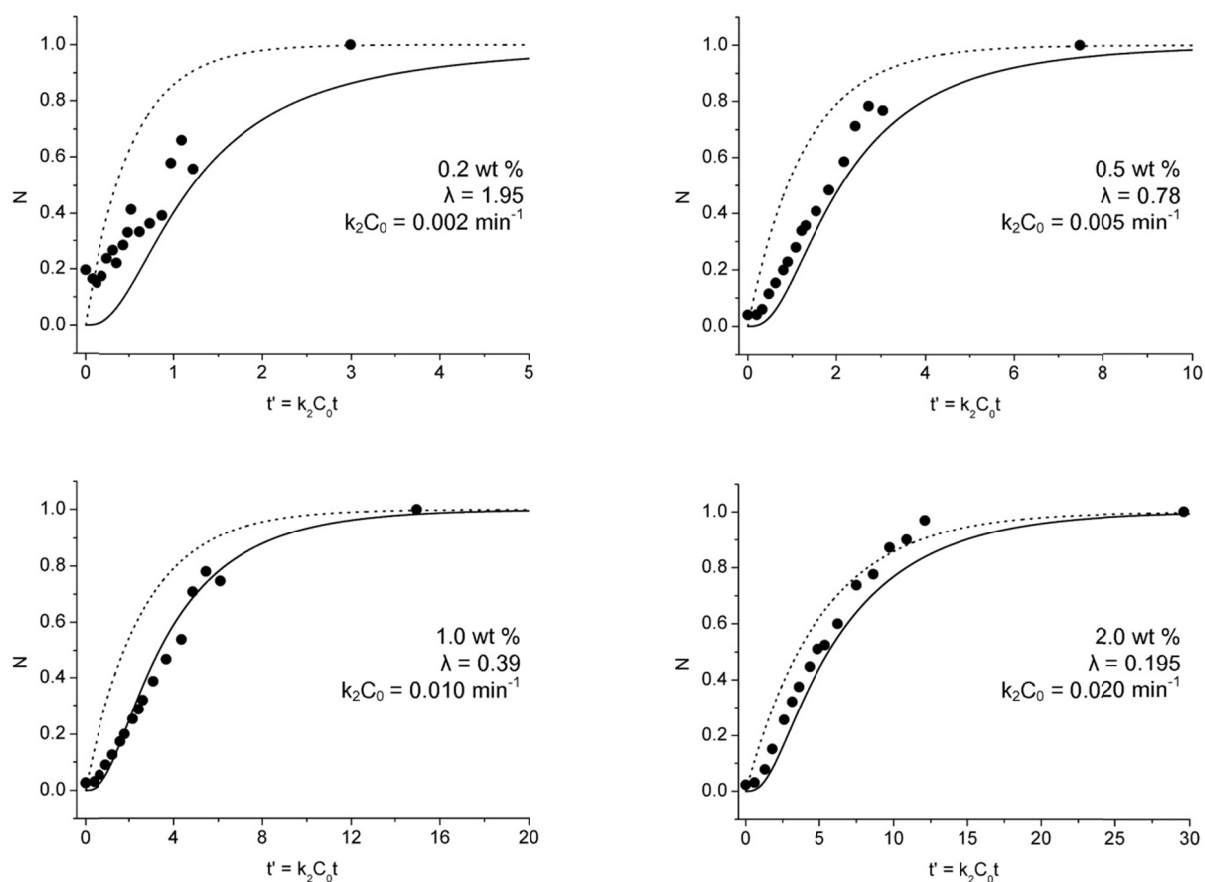


Figure 7. Growth curves of the fibril assembly process at 353 K and protein concentrations  $C_p$  of 0.2, 0.5, 1 and 2 wt %, where the total (scaled) number of building blocks incorporated in the fibrils  $N$  is plotted against (scaled) time  $t'$ . Black dots represent the experimental data, solid lines represent the model and the dotted lines represent the hydrolysis in the model.

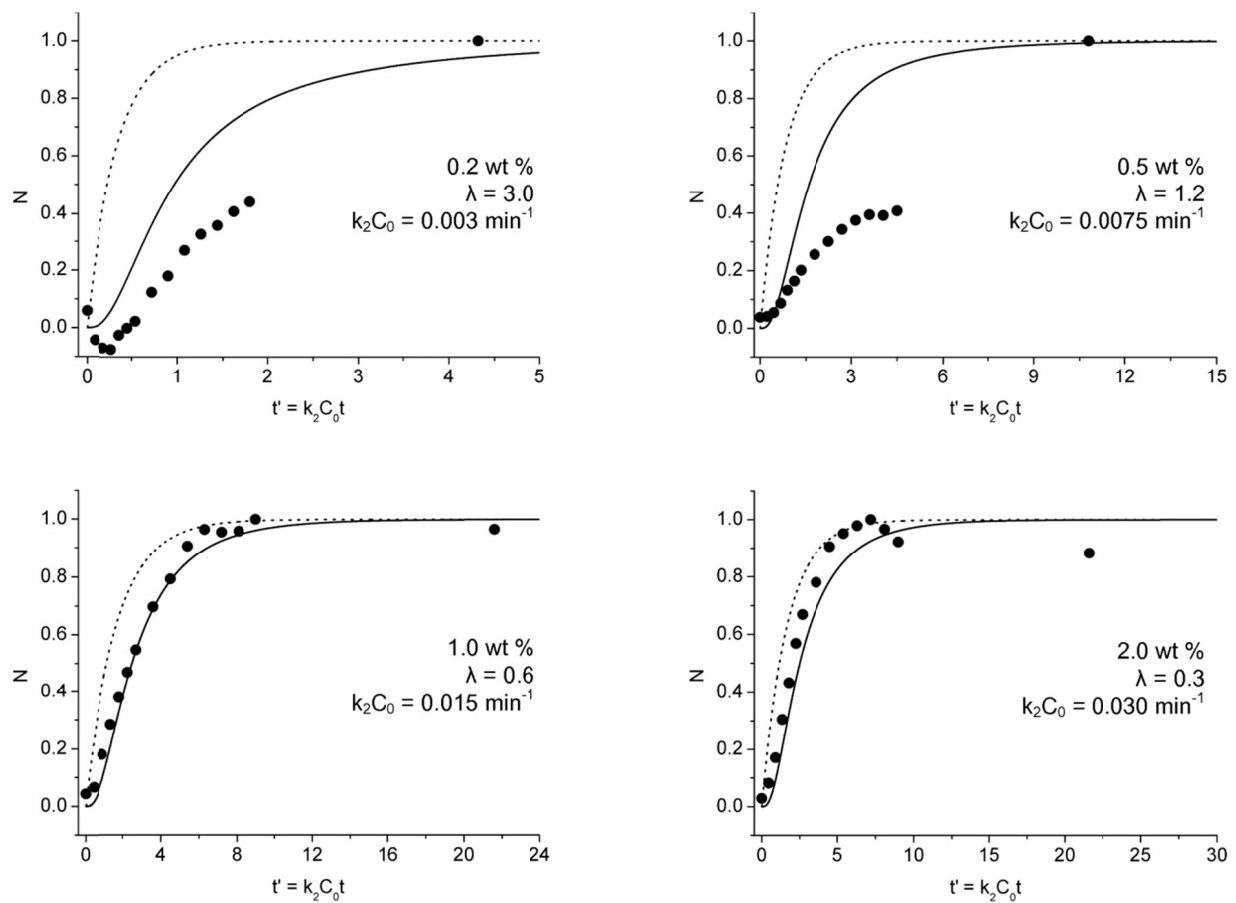


Figure 8. Growth curves of the fibril assembly process at 363 K and protein concentrations  $C_p$  of 0.2, 0.5, 1 and 2 wt %, where the total (scaled) number of building blocks incorporated in the fibrils  $N$  is plotted against (scaled) time  $t'$ . Black dots represent the experimental data, solid lines represent the model and the dotted lines represent the hydrolysis in the model.

Table 2. Parameters used to model the hydrolysis of  $\beta$ -lg and fibril formation at 353 K and 363 K and concentrations  $C_p$  of 0.2, 0.5, 1 and 2 wt %, with hydrolysis rate constant  $k_h$ , scaling parameter  $k_2C_0$  including the rate of incorporation of the building blocks into the fibrils and the concentration of building blocks available after complete hydrolysis, and  $\lambda$  showing the relation between  $k_h$  and  $k_2C_0$

T [K]	$C_p$ [wt%]	$k_h$ [min <sup>-1</sup> ]	$k_2C_0$ [min <sup>-1</sup> ]	$\lambda$
353	0.2	0.0039	0.002	1.95
353	0.5	0.0039	0.005	0.78
353	1.0	0.0039	0.010	0.39
353	2.0	0.0039	0.020	0.195
363	0.2	0.0090	0.003	3
363	0.5	0.0090	0.0075	1.2
363	1.0	0.0090	0.015	0.6
363	2.0	0.0090	0.030	0.3

The behaviour of  $\lambda = \frac{k_h}{k_2C_0}$  as a function of temperature and concentration gives us important information on the mechanism of fibril formation. When  $\lambda > 1$ , and therefore  $k_h > k_2C_0$ , the incorporation of the building blocks into the fibrils is the rate limiting step for fibrillar growth. When  $\lambda < 1$ , and therefore  $k_2C_0 > k_h$ , the hydrolysis is the rate limiting step for fibrillar growth. As a function of concentration we find a crossover in the mechanism of fibrillar growth. At concentrations  $C_0$  that are low enough to make  $\lambda > 1$ , the incorporation of the building blocks into the fibrils is the rate limiting step. At concentrations  $C_0$  that are high enough to make  $\lambda < 1$ , this situation inverts and the hydrolysis becomes the rate limiting step. This crossover concentration shifts towards higher concentrations with increasing temperature. From Equations 9-12 it can be shown that the normalized total length concentration

$N$  of the fibrils at short times (  $t' \ll 1$  or  $t \ll (k_2 C_0^{-1})$  ) to leading order is given by (see Appendix I):

$$N(t') \sim \frac{2}{3} \lambda^2 t'^3 \quad \text{valid for } t' \ll 1 \quad [13]$$

This means that the initial fibrillar growth is controlled by  $\lambda = \frac{k_h}{k_2 C_0}$ , something also reflected in the experimental growth curve (Figure 9). This result supports our assumption that in our study nucleation does not play a prominent role in the fibril formation of  $\beta$ -lg. Only at very low concentrations the model is deviating from the measured growth data. At these low concentrations nucleation might start to play a role.

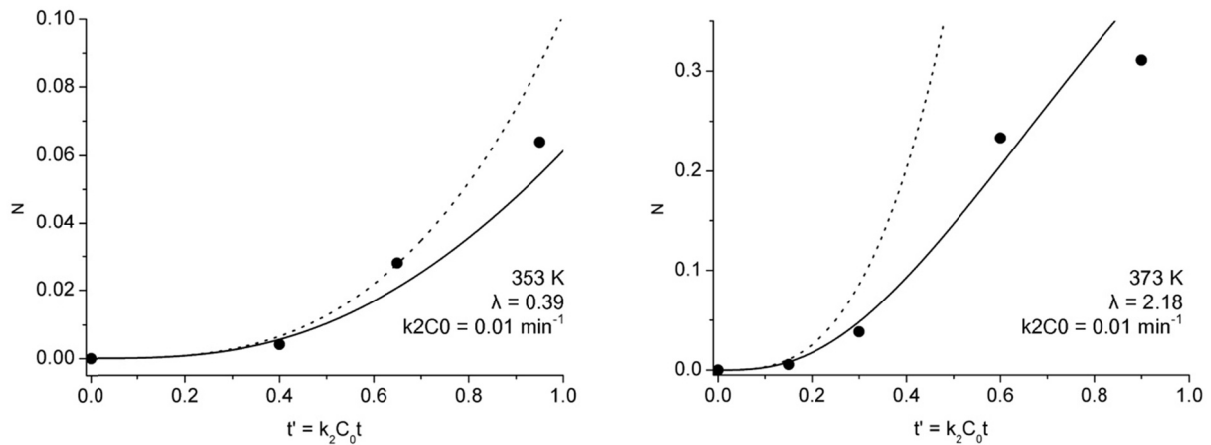


Figure 9. Initial part of the growth curves of the fibril assembly process at 353 and 373 K and a protein concentration  $C_p$  of 1 wt %, where the total (scaled) number of building blocks incorporated in the fibrils  $N$  is plotted against (scaled) time  $t'$ . Black dots represent the experimental data, solid lines represent the model and the dotted lines represent  $N(t') = \frac{2}{3} \lambda^2 t'^3$ .

## Conclusions

Both the hydrolysis of  $\beta$ -lactoglobulin and the growth of the fibrils were followed as a function of time and temperature, using SDS polyacrylamide gel electrophoresis and a Thioflavin T fluorescence assay. A simple polymerization model, including a hydrolysis step was found to model the kinetics of fibril formation satisfactorily. As a function of protein concentration a crossover in the mechanism of fibril formation is found. At concentrations that are low enough to make  $\lambda > 1$ , the incorporation of peptides into the fibrils is rate limiting for the fibrillar growth, while at concentrations that are high enough to make  $\lambda < 1$ , the hydrolysis becomes rate limiting. This crossover concentration shifts towards higher concentrations with increasing temperature. In addition, the results support the view that the formation of peptides by hydrolysis precedes their incorporation into the fibrils.

## References

1. Aymard, P.; Nicolai, T.; Durand, D., Static and Dynamic Scattering of *beta*-Lactoglobulin Aggregates Formed after Heat-Induced Denaturation at pH 2. *Macromolecules* **1999**, *32*, 2542-2552.
2. Kavanagh, G. M.; Clark, A. H.; Ross-Murphy, S. B., Heat-induced gelation of globular proteins: part 3. Molecular studies on low pH *beta*-lactoglobulin gels. *International Journal of Biological Macromolecules* **2000**, *28*, 41-50.
3. Humblet-Hua, K. N. P.; Scheltens, G.; van der Linden, E. Sagis, L. M. C., Encapsulation systems based on ovalbumin fibrils and high methoxyl pectin. *Food Hydrocolloids*, **2011**, *25*, (4), 569-576.
4. Sagis, L. M. C.; de Ruiter, R.; Miranda, F. J. R.; de Ruiter, J.; Schroen, K.; van Aelst, A. C.; Kieft, H.; Boom, R.; van der Linden, E., Polymer Microcapsules with a Fiber-Reinforced Nanocomposite Shell. *Langmuir* **2008**, *24*, (5), 1608-1612.
5. Bromley, E. H. C.; Krebs, M. R. H.; Donald, A. M., Aggregation across the length-scales in *beta*-lactoglobulin. *Faraday Discussions* **2005**, *128*, 13-27.

6. Booth, D. R.; Sunde, M.; Bellotti, V.; Robinson, C. V.; Hutchinson, W. L.; Fraser, P. E.; Hawkins, P. N.; Dobson, C. M.; Radford, S. E.; Blake, C. C.; Pepys, M. B., Instability, unfolding and aggregation of human lysozyme variants underlying amyloid fibrillogenesis. *Nature* **1997**, 385, (6619), 787-93.
7. Chiti, F., Designing conditions for in vitro formation of amyloid protofilaments and fibrils. *Proceedings of the National Academy of Sciences of the United States of America* **1999**, 96, (7), 3590.
8. Kelly, J. W., Mechanisms of amyloidogenesis. *Nature structural biology* **2000**, 7, (10), 824-6.
9. Koo, E. H., Amyloid diseases: Abnormal protein aggregation in neurodegeneration. *Proceedings of the National Academy of Sciences of the United States of America* **1999**, 96, (18), 9989.
10. Nelson, R.; Sawaya, M. R.; Balbirnie, M.; Madsen, A. Ø.; Riek, C.; Grothe, R.; Eisenberg, D., Structure of the cross-beta spine of amyloid-like fibrils. *Nature* **2005**, 435, (7043), 773-8.
11. Serpell, L. C., Alzheimer's amyloid fibrils: structure and assembly. *Biochimica et biophysica acta* **2000**, 1502, (1), 16-30.
12. Sipe, J. D.; Cohen, A. S., Review: History of the Amyloid Fibril. *Journal of Structural Biology* **2000**, 130, (2-3), 88-98.
13. Smith, J. F.; Knowles, T. P. J.; Dobson, C. M.; Macphee, C. E.; Welland, M. E., Characterization of the nanoscale properties of individual amyloid fibrils. *Proceedings of the National Academy of Sciences of the United States of America* **2006**, 103, (43), 15806-11.
14. Knowles, T. P. J.; Waudby, C. A.; Devlin, G. L.; Cohen, S. I. A.; Aguzzi, A.; Vendruscolo, M.; Terentjev, E. M.; Welland, M. E.; Dobson, C. M., An Analytical Solution to the Kinetics of Breakable Filament Assembly. *Science* **2009**, 326, (5959), 1533-1537.

15. Bolder, S. G.; Sagis, L. M. C.; Venema, P.; van der Linden, E., Effect of Stirring and Seeding on Whey Protein Fibril Formation. *Journal of agricultural and food chemistry* **2007**, 55, (14), 5661-5669.
16. Veerman, C. C.; Ruis, H. H.; Sagis, L. M. L. M. C.; van der Linden, E. E., Effect of electrostatic interactions on the percolation concentration of fibrillar beta-lactoglobulin gels. *Biomacromolecules* **2002**, 3, (4), 869.
17. Mishra, R.; Sorgjerd, K.; Nystrom, S.; Nordigarden, A.; Yu, Y.-C.; Hammarstrom, P., Lysozyme Amyloidogenesis Is Accelerated by Specific Nicking and Fragmentation but Decelerated by Intact Protein Binding and Conversion. *Journal of Molecular Biology* **2007**, 366, 1029-1044.
18. Akkermans, C., Peptides are Building Blocks of Heat-Induced Fibrillar Protein Aggregates of  $\beta$ -Lactoglobulin Formed at pH 2. *Biomacromolecules* **2008**, 9, (5), 1474.
19. Frare, E.; Polverino De Laureto, P.; Zurdo, J.; Dobson, C. M.; Fontana, A., A highly amyloidogenic region of hen lysozyme. *Journal of molecular biology* **2004**, 340, (5), 1153-65.
20. Akkermans, C.; Venema, P.; van der Goot, A.; Boom, R.; van der Linden, E., Enzyme-Induced Formation of  $\beta$ -Lactoglobulin Fibrils by AspN Endoproteinase. *Food Biophysics* **2008**, 3, (4), 390-394.
21. Grimwood, B. G.; Plummer, T. H.; Tarentino, A. L., Purification and Characterization of a Neutral Zinc Endopeptidase Secreted by *Flavobacterium meningosepticum*. *Archives of Biochemistry and Biophysics* **1994**, 311, (1), 127-132.
22. Arnaudov, L. N.; Renko de, V., Theoretical modeling of the kinetics of fibrillar aggregation of bovine beta-lactoglobulin at pH 2. *The Journal of Chemical Physics* **2007**, 126, (14), 145106.
23. Loveday, S. M.; Wang, X. L.; Rao, M. A.; Anema, S. G.; Creamer, L. K.; Singh, H., Tuning the properties of [beta]-lactoglobulin nanofibrils with pH, NaCl and CaCl<sub>2</sub>. *International dairy journal* **2010**, 20, (9), 571-579.
24. Morris, A. M.; Watzky, M. A.; Agar, J. N.; Finke, R. G., Fitting Neurological Protein Aggregation Kinetic Data via a 2-Step, Minimal/"Ockham's Razor" Model:

The Finke–Watzky Mechanism of Nucleation Followed by Autocatalytic Surface Growth†. *Biochemistry* **2008**, *47*, (8), 2413-2427.

25. Akkermans, C.; Venema, P.; Rogers, S.; van der Goot, A.; Boom, R.; van der Linden, E., Shear Pulses Nucleate Fibril Aggregation. *Food Biophysics* **2006**, *1*, (3), 144-150.

26. Hill, E. K.; Krebs, B.; Goodall, D. G.; Howlett, G. J.; Dunstan, D. E., Shear Flow Induces Amyloid Fibril Formation. *Biomacromolecules* **2006**, *7*, (1), 10-13.

27. Akkermans, C.; van der Goot, A. J.; Venema, P.; van der Linden, E.; Boom, R. M., Formation of fibrillar whey protein aggregates: Influence of heat and shear treatment, and resulting rheology. *Food Hydrocolloids* **2008**, *22*, (7), 1315-1325.

## Appendix I

In order to derive Equation 13 we define a set of equations to derive the different moments of the fibril distribution:

$$P = \sum_{i \geq 2} n_i(t') \quad [\text{A.1}]$$

and

$$N = \sum_{i \geq 2} i n_i(t') \quad [\text{A.2}]$$

Starting from

$$\frac{dn_i(t')}{dt'} = (n_{i-1}(t')n_1(t') - n_i(t')n_1(t')) \quad \text{for } i \geq 2 \quad [\text{A.3}]$$

we write

$$\frac{d \sum_{i \geq 2} n_i(t')}{dt'} = n_1(t') \left( \sum_{i \geq 2} n_{i-1}(t') - \sum_{i \geq 2} n_i(t') \right) \quad [\text{A.4}]$$

and use

$$\sum_{i \geq 2} n_{i-1}(t') = n_1(t') + \sum_{i \geq 2} n_i(t') \quad [\text{A.5}]$$

to find

$$\frac{dP(t')}{dt'} = n_1^2(t') \quad [\text{A.6}]$$

Starting again from [A.3] we can write

$$\frac{d \sum_{i \geq 2} i n_i(t')}{dt'} = n_1(t') \left( \sum_{i \geq 2} i n_{i-1}(t') - \sum_{i \geq 2} i n_i(t') \right) \quad [\text{A.7}]$$

and use

$$\sum_{i \geq 2} i n_{i-1}(t') = \sum_{i \geq 2} (i-1) n_{i-1}(t') + n_{i-1}(t') \quad [\text{A.8}]$$

which can also be written as

$$\sum_{i \geq 2} i n_{i-1}(t') = \sum_{i \geq 2} i n_i(t') + n_1(t') + \sum_{i \geq 2} n_{i-1}(t') \quad [\text{A.9}]$$

Using (A.5) we find

$$\sum_{i \geq 2} i n_{i-1}(t') = \sum_{i \geq 2} i n_i(t') + n_1(t') + \sum_{i \geq 2} n_i(t') + n_1(t') \quad [\text{A.10}]$$

leading to

$$\frac{dN(t')}{dt'} = n_1(t')(2n_1(t') + P(t')) \quad [\text{A.11}]$$

For  $t' \ll 1$

$$n_1(t') = (1 - e^{-\lambda t'}) - \sum_{i \geq 2} i n_i(t') \quad [\text{A.12}]$$

reduces to

$$n_1(t') = \lambda t' \quad [\text{A.13}]$$

Substitution of (A.13) in (A.6) leads to

$$P(t') = \frac{1}{3} \lambda^2 t'^3 \quad [\text{A.14}]$$

Substitution of (A.14) in (A.11) leads to a leading behaviour for  $t' \ll 1$ :

$$N(t') = \frac{2}{3} \lambda^2 t'^3 \quad [\text{A.15}]$$



Chapter 4 is published as: Kroes-Nijboer, A., Lubbersen, Y. S., Venema, P., van der Linden, E (2009) Thioflavin T fluorescence assay for  $\beta$ -lg fibrils hindered by DAPH. *Journal of Structural Biology* (165) 140-145.

## *Chapter 4*

### **Thioflavin T fluorescence assay for $\beta$ -lg fibrils hindered by DAPH**

## Abstract

The molecule 4,5-dianilinophthalimide was recently found to be an efficient compound in disaggregating amyloid fibrils involved in the Alzheimer's disease. In this study we have investigated whether the compound 4,5-dianilinophthalimide was able to disaggregate fibrils derived from  $\beta$ -lactoglobulin. In addition to a Thioflavin T fluorescence assay, flow-induced birefringence was used as an independent technique to measure the total length concentration of the fibrils. An additional advantage of the latter technique is that not only the total length concentration, but also the length distribution of the fibrils can be measured. The results from flow-induced birefringence showed that the total amount of fibrils and also the length distribution of the fibrils was not influenced by the addition of 4,5-dianilinophthalimide, even though this was suggested by the results of the Thioflavin T assay. The results of flow-induced birefringence were confirmed by rheological measurements and transmission electron microscopy. Our findings show that the use of a Thioflavin T assay in order to probe the possible disaggregating effect of certain compounds can give misleading results.

## Introduction

Fibrillar, amyloid protein aggregates can be derived from many different proteins like  $\beta$ -lactoglobulin ( $\beta$ -lg). These fibrils are characterized by a cross  $\beta$ -conformation<sup>1, 2</sup> where the  $\beta$ -sheets are arranged parallel to the fibril axis with their constituent  $\beta$ -strands perpendicular to the fibril axis.<sup>3, 4</sup> A second characteristic of these amyloid fibrils is that they are typically micrometers in length with a width of only a few nanometers.<sup>5</sup> And, thirdly, these fibrils bind amyloid specific dyes like Congo Red<sup>6</sup> and Thioflavin T (ThT)<sup>7</sup>. ThT is widely used to determine the presence of amyloid fibrils and to examine the kinetics of fibril formation.<sup>5, 7-11</sup> The fluorescence of ThT is strongly enhanced by its specific binding to  $\beta$ -sheets. Since  $\beta$ -sheet formation takes place during fibril formation, the concentration of bound ThT molecules and therefore the fluorescent signal is proportional to the fibril concentration. Krebs et al.<sup>12</sup> proposed a binding mechanism of the ThT molecules to the  $\beta$ -sheets. It was suggested that the ThT molecule would insert itself into the channels, running along the  $\beta$ -sheets. These channels arise from neat rows formed by the side chains of the  $\beta$ -strands on each side of the  $\beta$ -sheet, running in the direction of the  $\beta$ -sheet.<sup>12</sup>

The amyloid fibrils are commonly associated with neurodegenerative diseases like Alzheimer's disease and type 2 diabetes where they occur in proteinaceous deposits called plaques. No medicines or therapeutic agents have been developed to cure or treat people that suffer from these diseases. Although the exact role of the amyloid fibrils in neurodegenerative diseases is still under discussion,<sup>13</sup> recent research has been focused on the inhibition of fibril formation and the destabilization of the existing fibrils.<sup>14-17</sup> This research area is becoming even more important nowadays, because of the population ageing in the world, which will lead to a large increase in the number of patients with these diseases.<sup>18-20</sup> In a recent study<sup>14</sup> the ThT assay was used to test a large amount of different compounds with biological activity on the ability to decrease the  $\beta$ -sheet content of aggregating A $\beta$ 1-42 (a peptide involved in

Alzheimer's disease). The molecule 4,5-dianilinophthalimide (DAPH) was reported to be the most effective compound in disaggregating the fibrils used in this study.

Beside these disease-associated proteins, also non-disease-associated proteins can lead to amyloid fibrils. For example, the globular whey protein  $\beta$ -lactoglobulin ( $\beta$ -lg) leads to fibrils when heated at 80°C and pH 2.<sup>21, 22</sup> It was recently shown by Akkermans et al. that not the intact protein is incorporated in the fibrils, but peptides derived from it by hydrolysis.<sup>23</sup> These fibrils show all the classical signatures of amyloid fibrils.<sup>5</sup> The protein  $\beta$ -lg has been excessively studied because it is readily available in large quantities and of its importance to the food industry.<sup>5</sup> This protein is therefore an excellent model protein for studying amyloid fibril formation. Due to the high aspect ratio of the fibrils, they could also be used in food products as structurant, for example as a thickening or gelling agent. For some of these applications it is desirable to break up the fibrils in their consisting peptides. Based on previous results<sup>14</sup> DAPH seems to be a promising candidate.

In our study we have investigated whether the compound DAPH was able to disaggregate the fibrils derived from  $\beta$ -lg. Apart from the ThT fluorescence assay, flow-induced birefringence was used as an independent technique to measure the total length concentration of the fibrils. An additional advantage of the latter technique is that not only the total length concentration, but also the length distribution of the fibrils can be measured. In addition rheological measurements and transmission electron microscopy (TEM) were used to determine the ability of DAPH to disaggregate the fibrils.

## Materials and Methods

### *Sample preparation*

$\beta$ -Lg was obtained from Sigma (product no. L0130, lot. no. 095K7006). A 2 % (w/w)  $\beta$ -lg solution at pH 2 was made by dissolving the protein powder into a HCl solution of pH 2 and adjusting the pH using a 6M HCl solution.

The DAPH was obtained from Sigma (product no. D3943) and was dissolved in dimethyl sulfoxide (DMSO). DMSO was obtained from Merck (product no. 102931). A DAPH stock solution was made by dissolving 5 mg DAPH in 1 ml DMSO (15.18 mM). The stock solution was diluted with DMSO prior to use.

The fibrils were made by heating and stirring the  $\beta$ -Ig solution at 80°C for 24 hours. Subsequently, DAPH was added to this fibril solution and the samples were incubated in a water bath at 35°C.

#### *ThT fluorescence assay*

A ThT stock solution (3.0 mM) was made by dissolving 7.9 mg ThT in 8 ml phosphate buffer (10 mM phosphate, 150 mM NaCl at pH 7.0). This stock solution was filtered through a 0.2  $\mu$ m filter (Schleicher & Schuell). The stock solution was diluted 50 times in a phosphate buffer (10 mM phosphate, 150 mM NaCl at pH 7.0) before use.

Small aliquots of the fibril samples (48  $\mu$ l) were mixed with 4 ml ThT solution and allowed to bind to the ThT for 1 minute. The fluorescence of the samples was measured using a fluorescence spectrophotometer (Perkin Elmer LS 50 B). The excitation wavelength was 460 nm (slit width 4.0 nm) and the emission wavelength was between 470 and 500 nm (slit width 2.5 nm) and a scanning speed 200 nm/min was used. The fluorescence intensity peak was determined at 482 nm. The fluorescence intensity of the ThT solution without any addition was subtracted from the fluorescence intensities of the samples to correct the samples for the background intensity.

#### *Flow-induced birefringence*

Flow-induced birefringence has proven to be an excellent method, not only for the determination of the total length concentration of fibrils, but also to measure the length distribution of fibrils<sup>24-26</sup> without, apart from dilution, any further sample preparation. By determining the length distribution using TEM pictures, there is

always the effect of the sample preparation, which can result in local concentration differences and large sample-to-sample variations leading to poor statistics. For example, on a TEM grid up to  $10^2$  fibrils can be distinguished, while with flow-induced birefringence typically  $10^{17}$  fibrils are monitored. The flow-induced birefringence and the decay curves of the flow-induced birefringence after the cessation of flow were measured with a strain-controlled ARES rheometer (Rheometrics Scientific) equipped with a modified optical analysis module.<sup>27</sup> The steady shear flow-induced birefringence is proportional to the total length concentration of the fibrils and from the decay curve of the flow-induced birefringence after the cessation of flow the length distribution of the fibrils can be determined.<sup>24</sup>

#### *Rheological measurements*

The viscosity as a function of shear rate was measured for fibril solutions incubated with and without DAPH. To show the effect of a 50% reduction in the amount of fibrils, a fibril solution, without DAPH was diluted twice (with pH 2 solution) before measuring. Shear rate sweeps were performed using a rheometer (PAAR Physica MCR 501) with a Couette geometry (CC10). The temperature was set at 20°C and the shear rate ranged from 0.1-10 s<sup>-1</sup> and was increased at logarithmically spaced intervals.

#### *Transmission electron microscopy (TEM)*

TEM pictures were taken from the fibrils which were incubated with and without DAPH. Before preparing the TEM samples by negative staining they were first diluted 50x or 100x. After dilution, a droplet of the diluted solution was put onto a carbon support film on a copper grid. The excess was removed after 15 s with a filter paper. Subsequently, a droplet of 2% uranyl acetate was put onto the grid and again removed after 15 s. Electron micrographs were taken using a JEOL electron microscope (JEM-1011, Tokyo, Japan) operating at 80 kV.

### *Far-UV circular dichroism (CD)*

CD spectra of the fibrils were recorded on a Jasco spectropolarimeter (J-715). Before measurement all samples were diluted to a protein concentration of 0.01 % (w/w). Far-UV (200-260 nm) CD measurements were performed at 20°C in quartz cuvettes with a path length of 0.1 cm, using a slit width of 5 nm and a scan speed of 100 nm/min. Each spectrum was obtained by averaging 40 scans and all values were corrected for solvent contributions (containing DMSO and/or DAPH).

## Results

### *Effect of DAPH monitored by ThT fluorescence assay*

Preformed fibrils derived from  $\beta$ -lg were incubated at different DAPH concentrations for 1 hour at 35°C and subsequently a ThT assay was performed. Upon increasing DAPH concentrations, the ThT fluorescence intensity decreased to less than 50% of the initial intensity at a DAPH concentration of 0.20 mM (Figure 1).

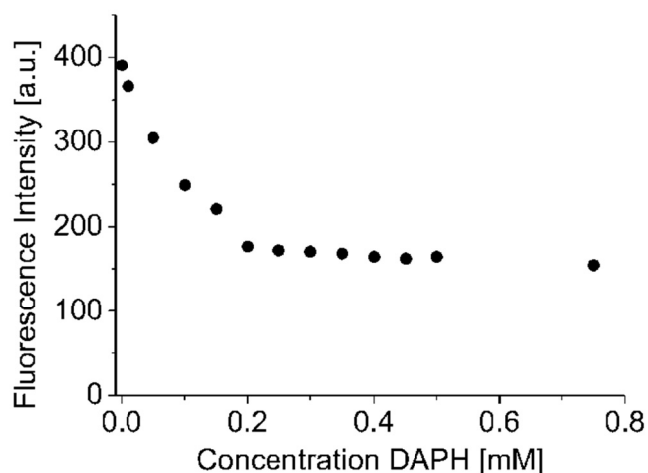


Figure 1. ThT fluorescence intensity of fibrils as a function of DAPH concentration. The fibril solutions were incubated at 35°C for 1 hour.

Higher concentrations of DAPH did not decrease the intensity any further. Incubation times of 25 hour were also investigated, by adding 0.23 mM DAPH to a preformed fibril solution. The fibrils were incubated in the presence of DMSO, in the presence of DMSO and DAPH or without any addition. During the incubation samples were taken and the ThT fluorescence intensity was measured (Figure 2).

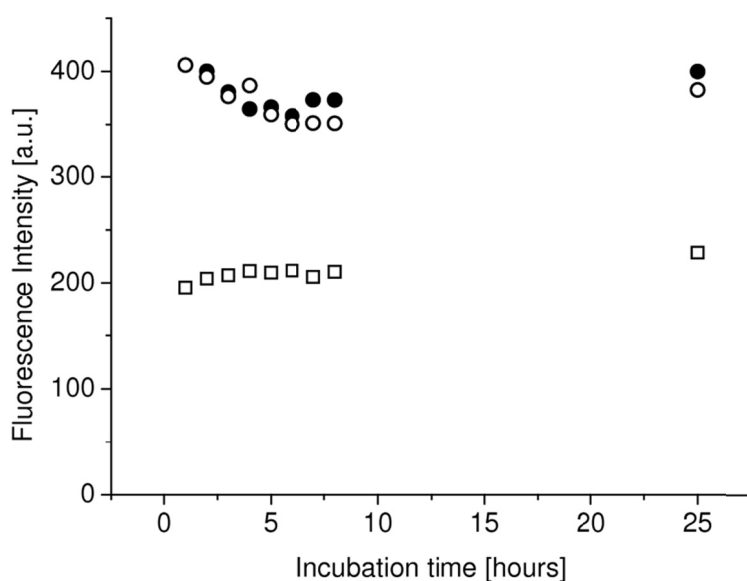


Figure 2. ThT fluorescence intensity of fibrils as a function of incubation time at 35°C. The fibrils are incubated in the presence of DMSO (○), in the presence of DMSO and 0.23 mM DAPH (□) or without any addition (●).

It can be seen that the ThT fluorescence intensity of the samples with DAPH already decreased with about 50% in the first hour of the incubation and did not decrease further upon longer incubation times. Assuming that a decrease in ThT fluorescence intensity is related to a decrease in  $\beta$ -sheet content and therefore the fibril concentration, these results strongly suggest that DAPH is indeed able to disaggregate the fibrils derived from  $\beta$ -lg to about 50%.

*Effect of DAPH monitored by flow-induced birefringence*

We also used flow-induced birefringence as an independent method to measure the total length concentration and the length distribution of the fibrils. The steady shear birefringence  $\Delta n$ , a quantity proportional to the total length concentration, of fibril solutions incubated with 0.23 mM DAPH did not show a significant decrease relative to the samples incubated without DAPH. Increasing the incubation time from 2 hours to 25 hours did not change this (see Figure 3) observation.

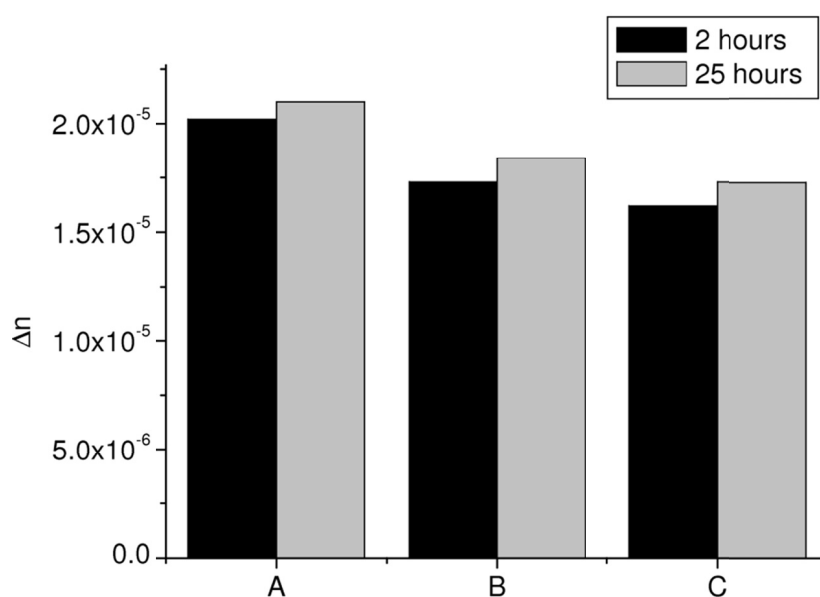


Figure 3. The steady-state flow birefringence of fibrils incubated at 35°C for 2 and 25 hours. The fibrils are incubated in the presence of DMSO (B), in the presence of DMSO and 0.23 mM DAPH (C) or without any addition (A).

The length distributions of the fibril solutions were determined from the decay curve of the birefringence after the cessation of flow. The length distributions of all the incubated samples were found to be identical, showing that no fibrils were disaggregated by DAPH (see Figure 4).

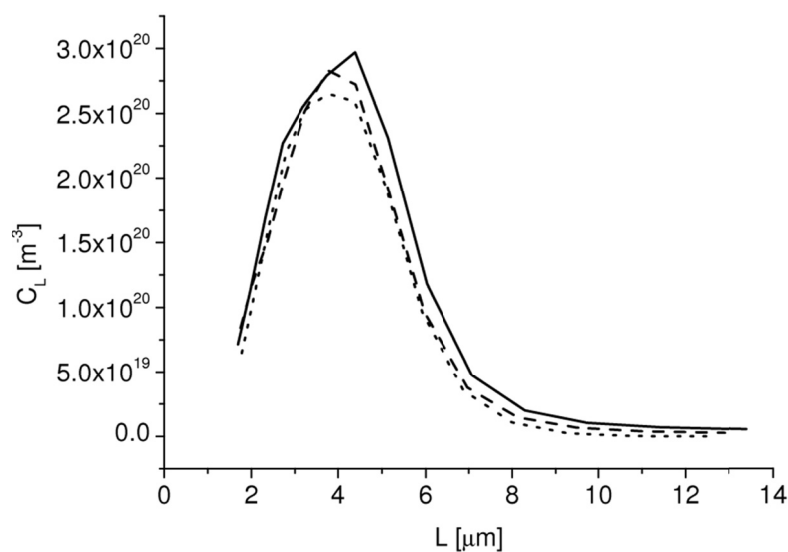


Figure 4. The length distribution of fibrils after 2 hours of incubation at 35°C. The length distribution curves correspond to the samples from Figure 3. The fibril solutions were incubated in the presence of DMSO (dashed line), in the presence of DMSO and 0.23 mM DAPH (dotted line) or without any addition (solid line). The results for the samples incubated for 25 hours were identical to these and not shown.

#### *Effect of DAPH monitored by rheological measurements*

The viscosity of the fibril solution is sensitive to the total amount and length distribution of fibrils (see e.g. Ref. 28). The viscosity of different fibril solutions incubated with and without DAPH was measured as a function of shear rate (Figure 5).

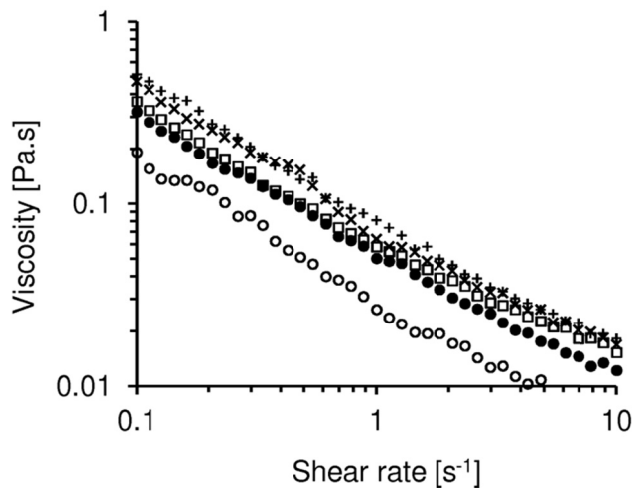


Figure 5. Viscosity as a function of shear rate. The fibrils are incubated in the presence of DMSO ( $\square$ ), in the presence of DMSO and 0.23 mM DAPH for 2 hours ( $\times$ ) and 24 hours ( $+$ ) or without any addition ( $\bullet$ ). Also a fibril solution without DAPH was diluted twice before measuring to show the effect of 50% reduction of the amount of fibrils on the viscosity ( $\circ$ ).

To show the effect of a 50% reduction in the amount of fibrils (as suggested by the ThT assay), a fibril solution was diluted twice. From Figure 5 it becomes clear that indeed a reduction of 50% in the concentration of fibrils lowers the viscosity. It is also clear from Figure 5 that the samples incubated with DAPH do not show a decrease in viscosity. This confirms the results of the flow-induced birefringence that the DAPH did not disaggregate the fibrils derived from  $\beta$ -lg.

#### *Effect of DAPH monitored by transmission electron microscopy (TEM)*

To visualize that DAPH indeed did not disaggregate the fibrils, TEM pictures were made of the fibril solutions incubated with and without DAPH (Figure 6). Although it is not straightforward to derive statistical significant data from these pictures, the results do not seem to contradict the finding that DAPH did not disaggregate the fibrils derived from  $\beta$ -lg. The pictures show that the fibrils in both solutions are present in equal amounts.

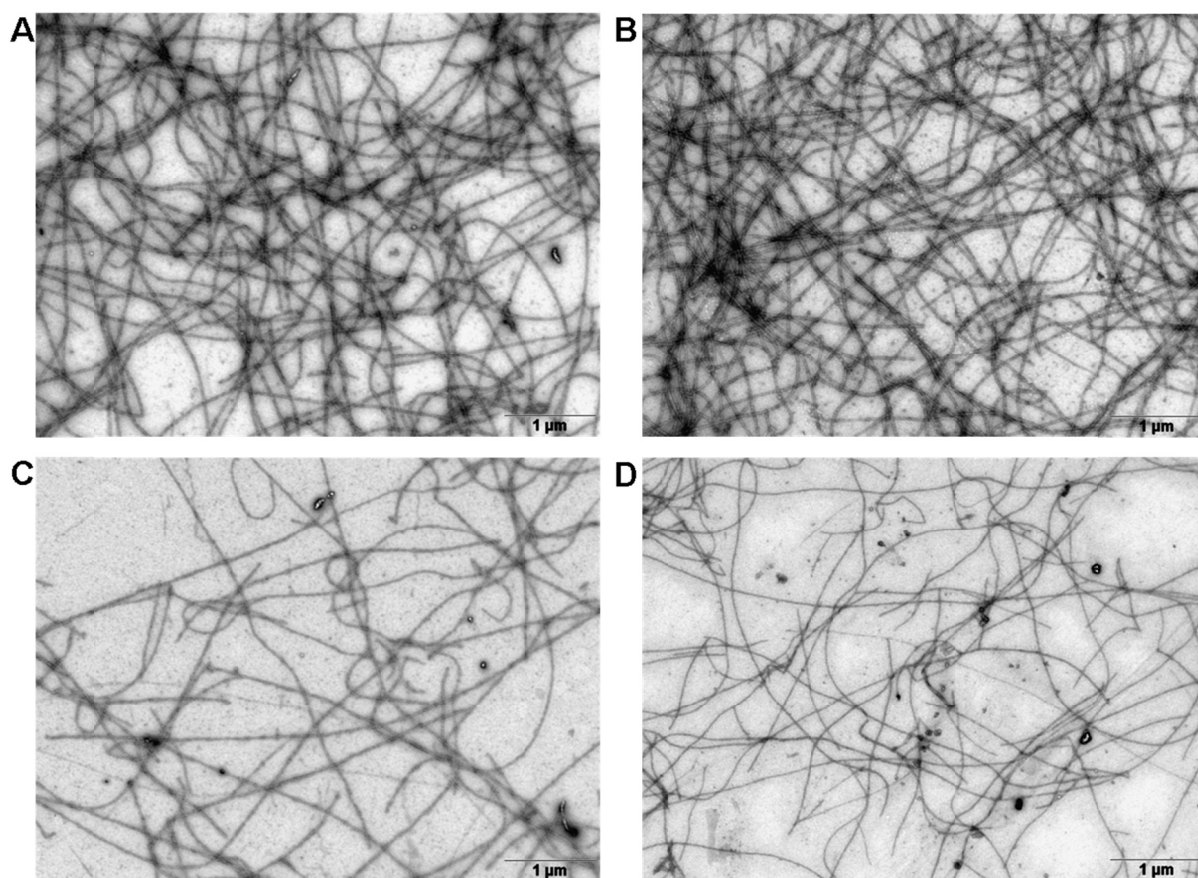


Figure 6. TEM pictures of the fibrils incubated with and without DAPH. Fibrils incubated without DAPH, diluted 50x (A) and diluted 100x (C). Fibrils incubated with DAPH, diluted 50x (B) and diluted 100x (D).

*Effect of DAPH monitored by far-UV circular dichroism (CD)*

Far-UV CD spectroscopy was used to assess the effect of DAPH on the secondary structure of the fibrils. The CD spectra (Figure 7) of the fibrils incubated with and without DAPH did not differ within the noise of the CD signal, showing that the secondary structure of the fibrils did not change upon incubation with DAPH.

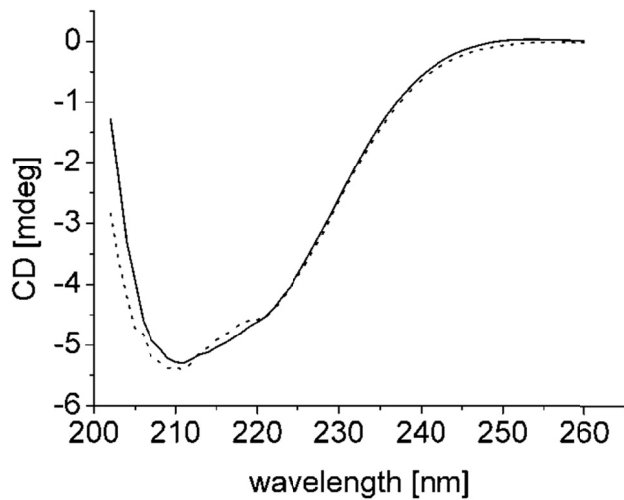


Figure 7. Far-UV CD spectra of fibrils incubated with (dashed line) and without (solid line) DAPH. The spectra were corrected for solvent contributions (containing DMSO and/or DAPH).

#### *Interference of DAPH in ThT fluorescence assay*

To better understand the physical basis of the interference of DAPH in the ThT assay, DAPH was added to a ThT solution that already contained fibrils (Figure 8). The DAPH was added in such an amount that the ratio DAPH / fibrils was the same as in the other experiments. Directly after adding the DAPH to the ThT-fibril mixture the fluorescence intensity decreased with about 50% and did not decrease any further.

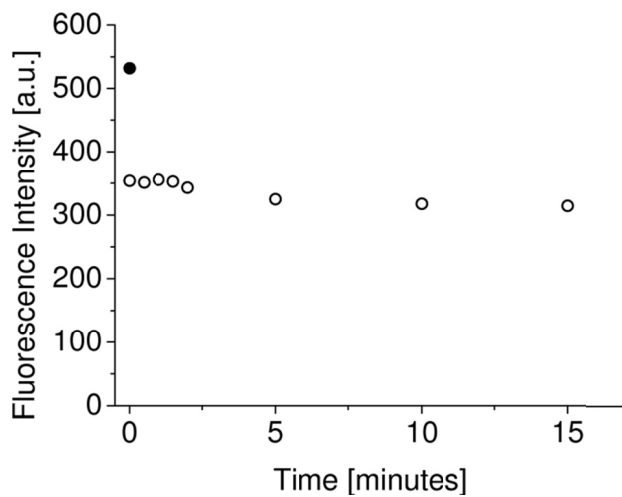


Figure 8. ThT fluorescence intensity of fibrils before (●) and after addition of DAPH (○). The DAPH was added to the ThT solution *after* the fibrils were added.

Furthermore, various ratios of DAPH were added to two ThT solutions containing different amounts of fibrils (48  $\mu\text{l}$  and 24  $\mu\text{l}$ , Figure 9). Again, in both solutions the decrease in fluorescence intensity did level off at about 50% of the initial intensity.

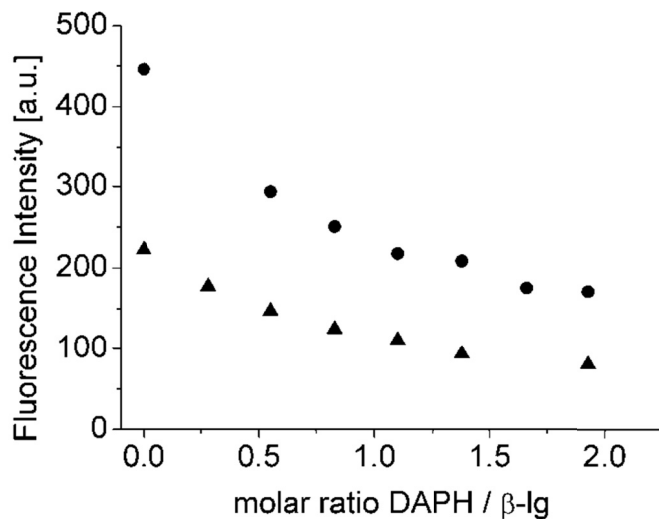


Figure 9. ThT fluorescence intensity of ThT solutions containing fibrils (● 48  $\mu\text{l}$ , ▲ 24  $\mu\text{l}$ ) and various concentrations of DAPH (added *after* the addition of the fibrils to the ThT solution).

## Discussion

Assuming that a decrease in ThT fluorescence intensity is related to a decrease in  $\beta$ -sheet content and therefore the fibril concentration, our results from the ThT assay alone strongly suggest that DAPH is indeed able to disaggregate the fibrils derived from  $\beta$ -lg to a large extent. However, based on the results obtained from flow-induced birefringence we conclude that DAPH did not disaggregate the fibrils derived from  $\beta$ -lg. <sup>§</sup> The rheological measurements and the TEM pictures both confirm this conclusion. The far-UV CD spectra did not show changes in secondary structure for the fibrils incubated with DAPH. A possible explanation for the decrease in ThT fluorescence intensity upon adding DAPH is that the DAPH molecules insert themselves in the channels running along the  $\beta$ -sheets in such a way that they hinder the ThT molecules in binding to the fibril. In this way, less ThT molecules are able to bind the  $\beta$ -sheets and a lower ThT fluorescence intensity is observed. In that respect it is interestingly to notice that the ThT fluorescence intensity levels off at approximately 50% of the initial intensity (see Figure 1 and 9), eliminating the possibility for a simple competition of ThT and DAPH molecules for the binding sites. Apparently the DAPH molecules do not occupy all the ThT binding sites, which is potentially related to the distribution of the hydrophobic and hydrophilic patches along the fibril and the hydrophobic character of the DAPH. DAPH is also capable of replacing part of about 50% of the already bound ThT molecules (Figure 8 and 9). Our findings show that the use of ThT fluorescent assay in order to probe the possible disaggregating, or even inhibiting effect on fibril formation, of certain compounds can be misleading.

## Acknowledgements

The authors acknowledge one of the referees for pointing out the relevance of Figure 1 in relation to the underlying binding mechanism and another for suggesting the

far-UV CD measurements. We thank Adrie Westphal and Carlo van Mierlo of the Wageningen Biochemistry group for their help with the far-UV CD measurements.

## References

1. Glenner, G. G., Amyloid deposits and amyloidosis - the beta-fibrilloses 1. *N. Engl. J. Med.* **1980**, 302, 1383-1292.
2. Glenner, G. G., Amyloid deposits and amyloidosis - the beta-fibrilloses 2. *N. Engl. J. Med.* **1980**, 302, (1333-1343).
3. Serpell, L. C.; Sunde, M.; Blake, C. C. F., The molecular basis of amyloidosis. *Cellular and Molecular Life Sciences* **1997**, 53, 871-887.
4. Nelson, R.; Sawaya, M. R.; Balbirnie, M.; Madsen, A. O.; Riek, C.; Grothe, R.; Eisenberg, D., Structure of the cross-beta spine of amyloid-like fibrils. *Nature* **2005**, 435, 773-778.
5. Bromley, E. H. C.; Krebs, M. R. H.; Donald, A. M., Aggregation across the length-scales in beta-lactoglobulin. *Faraday Discussions* **2005**, 128, 13-27.
6. Glenner, G. G.; Page, D. L.; Eanes, E. D., The relation of the properties of congo red-stained amyloid fibrils to the  $\beta$ -conformation. *Journal of Histochemistry & Cytochemistry* **1972**, 20, (10), 821-826.
7. Naiki, H. H., Fluorometric determination of amyloid fibrils in vitro using fluorescent dye, thioflavine T. *Analytical biochemistry* **1989**, 177, (2), 244.
8. Naiki, H.; Gejyo, F., [20] Kinetic analysis of amyloid fibril formation. *Methods in Enzymology* **1999**, 309, 305-318.
9. LeVine, H., Quantification of  $\beta$ -sheet amyloid fibril structures with Thioflavin T In *Methods in Enzymology: Amyloids, Prions and other Protein Aggregates*, Wetzel, R., Ed. Academic Press: London, 1999; Vol. 309, pp 285-305.
10. Nielsen, L. L.; Khurana, R. R.; Coats, A. A.; Frokjaer, S. S.; Brange, J. J.; Vyas, S. S.; Uversky, V. V. N.; Fink, A. A. L., Effect of environmental factors on the kinetics of

insulin fibril formation: elucidation of the molecular mechanism. *Biochemistry* **2001**, 40, (20), 6036-46.

11. Groenning, M.; Olsen, L.; van de Weert, M.; Flink, J. M.; Frokjaer, S.; Jørgensen, F. S., Study on the binding of Thioflavin T to beta-sheet-rich and non-beta-sheet cavities. *Journal of structural biology* **2007**, 158, 358-369.

12. Krebs, M. M. R. H.; Bromley, E. E. H. C.; Donald, A. A. M., The binding of thioflavin-T to amyloid fibrils: localisation and implications. *Journal of structural biology* **2005**, 149, (1), 30-7.

13. Lansbury, P. T.; Lashuel, H. A., A century-old debate on protein aggregation and neurodegeneration enters the clinic. *Nature* **2006**, 443, 774-779.

14. Blanchard, B. J.; Chen, A.; Rozeboom, L. M.; Stafford, K. A.; Weigele, P.; Ingram, V. M., Efficient reversal of Alzheimer's disease fibril formation and elimination of neurotoxicity by a small molecule. *PNAS* **2004**, 101, 14326-14332.

15. Porat, Y.; Abramowitz, A.; Gazit, E., Inhibition of Amyloid Fibril Formation by Polyphenols: Structural Similarity and Aromatic Interactions as a Common Inhibition Mechanism. *Chem. Biol. Drug Des.* **2006**, 67, 27-37.

16. Reches, M.; Gazit, E., Molecular self-assembly of peptide nanostructures: mechanism of association and potential uses. *Current Nanoscience* **2006**, 2, 105-111.

17. Zhu, J. T. T.; Choi, R. C. Y.; Chu, G. K. Y.; Cheung, A. W. H.; Gao, Q. T.; Li, J.; Jiang, Z. Y.; Dong, T. T. X.; Tsim, K. W. K., Flavonoids possess neuroprotective effects on cultured pheochromocytoma PC12 cells: a comparison of different flavonoids in activating estrogenic effect and in preventing  $\beta$ -amyloid-induced cell death. *J. Agric. Food Chem.* **2006**, 55, 2438-2445.

18. Brayne, C.; Gao, L.; Dewey, M.; Matthews, F. E.; Investigators, M. R. C. C. F. a. A. S., Dementia before Death in Ageing Societies—The Promise of Prevention and the Reality. *PLoS medicine* **2006**, 3, (10), 1922-1930.

19. Ferri, C. P.; Prince, M.; Brayne, C.; Brodaty, H.; Fratiglioni, L.; Ganguli, M.; Hall, K.; Hasegawa, K.; Hendrie, H.; Huang, Y.; Jorm, A.; Mathers, C.; Menezes, P. R.;

- Rimmer, E.; Scazufca, M., Global prevalence of dementia: a Delphi consensus study. *The Lancet* **2005**, 366, (9503), 2112-2117.
20. Qiu, C.; De Ronchi, D.; Fratiglioni, L., The epidemiology of the dementias: an update. *Current opinion in psychiatry* **2007**, 20, (4), 380-385.
21. Aymard, P.; Nicolai, T.; Durand, D., Static and Dynamic Scattering of *beta*-Lactoglobulin Aggregates Formed after Heat-Induced Denaturation at pH 2. *Macromolecules* **1999**, 32, 2542-2552.
22. Kavanagh, G. M.; Clark, A. H.; Ross-Murphy, S. B., Heat-induced gelation of globular proteins: part 3. Molecular studies on low pH *beta*-lactoglobulin gels. *International Journal of Biological Macromolecules* **2000**, 28, 41-50.
23. Akkermans, C.; Venema, P.; van der Goot, A. J.; Gruppen, H.; Bakx, E. J.; Boom, R. M.; van der Linden, E., Peptides are Building Blocks of Heat-Induced Fibrillar Protein Aggregates of  $\beta$ -Lactoglobulin Formed at pH 2. *Biomacromolecules* **2008**, 9, (5), 1474-1479.
24. Rogers, S. S.; Venema, P.; Sagis, L. M. C.; van der Linden, E.; Donald, A. M., Measuring length distribution of a fibril system: A flow birefringence technique applied to amyloid fibrils. *Macromolecules* **2005**, 38, 2948-2958.
25. Bolder, S. G.; Sagis, L. M. C.; Venema, P.; van der Linden, E., Effect of Stirring and Seeding on Whey Protein Fibril Formation. *Journal of agricultural and food chemistry* **2007**, 55, (14), 5661-5669.
26. Akkermans, C.; Venema, P.; Rogers, S. S.; van der Goot, A. J.; Boom, R. M.; van der Linden, E., Shear Pulses Nucleate Fibril Aggregation. *Food Biophysics* **2006**, 1, (144-150).
27. Klein van, C. O.; Venema, P.; Sagis, L. M. C.; Dusschoten, D. v.; Wilhelm, M.; Spiess, H. W.; Linden, E. v. d.; Rogers, S. S.; Donald, A. M., Optimized Rheo-optical Measurements Using Fast Fourier Transform and Oversampling. *Applied rheology* **2007**, 17, (4), 45210-1 - 45210-7.
28. Doi, M.; Edwards, S. F., The theory of polymer dynamics. *Oxford Science Press*, 1986.

## Footnote

§ To investigate the possibility that at pH 2 the efficient disaggregating effect of DAPH was prevented, all incubation experiments were repeated at pH 7.4. However, the results obtained at pH 7.4 (supplementary data) were similar to the results obtained at pH 2.

## Supplementary data

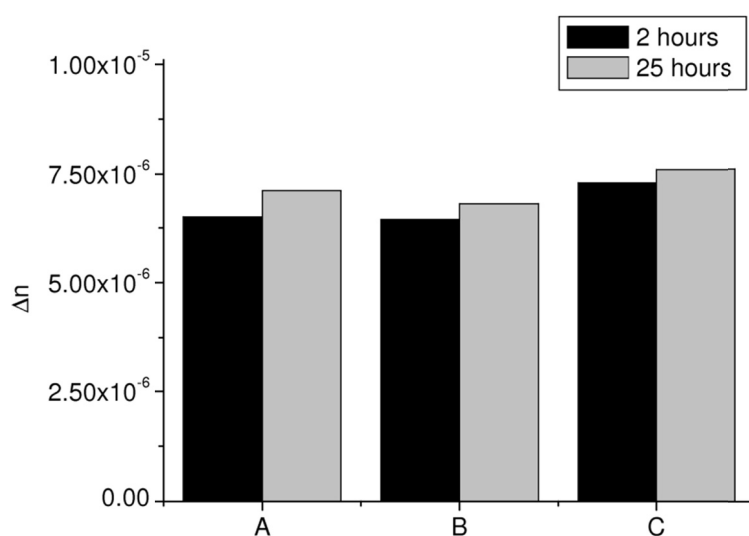


Figure I. The steady-state flow birefringence of fibrils incubated at 35°C and pH 7.4 for 2 and 25 hours. The fibrils are incubated in the presence of DMSO (B), in the presence of DMSO and 0.23 mM DAPH (C) or without any addition (A).

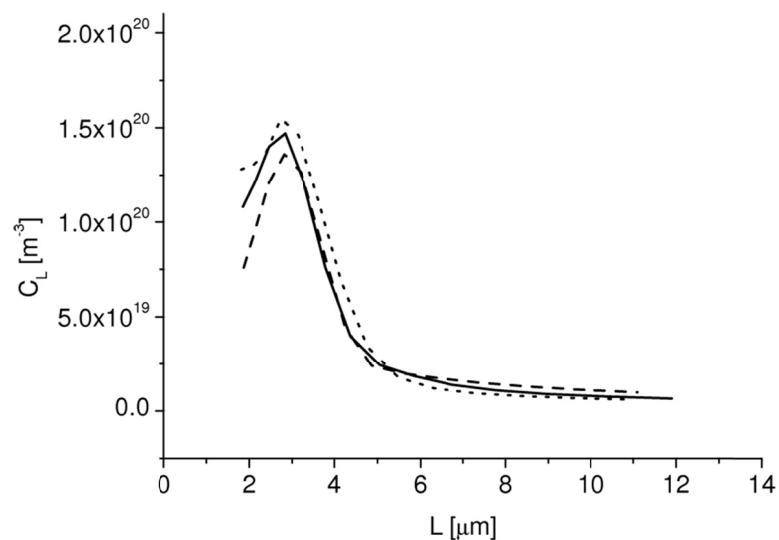


Figure II. The length distribution of fibrils after 2 hours of incubation at 35°C and pH 7.4. The length distribution curves correspond to the samples from Figure I. The fibril solutions were incubated in the presence of DMSO (dashed line), in the presence of DMSO and 0.23 mM DAPH (dotted line) or without any addition (solid line). The results for the samples incubated for 25 hours were identical to these and not shown.



Chapter 5 is published as: Kroes-Nijboer, A., Venema, P., Baptist, H., van der Linden, E. (2010) Fracture of protein fibrils as induced by elongational flow. *Langmuir* 26 (16) 13097-13101.

## *Chapter 5*

### **Fracture of protein fibrils as induced by elongational flow**

## Abstract

The length distribution of whey protein fibrils is important for application purposes. However, it is hard to influence the length distribution of whey protein fibrils during production. One way of influencing the length distribution of the mature fibrils is exposing them to an external field, like a flow field. In this research whey protein fibrils were exposed to elongational flow to fracture the fibrils. A simple experimental set-up was used to establish a range of elongational strain rates. The length distribution of the fractured fibrils was determined using transmission electron microscopy and was shown to be controllable at relatively low strain rates.

## Introduction

Proteins can form the basis for fibril formation under specific circumstances. For example, fibrils are formed when whey protein isolate (WPI) is heated for several hours at pH 2 and 80°C.<sup>1-3</sup> Such fibrils have a high aspect ratio, with a few nanometers thick and several micrometers long. The functionality of the fibrils, e.g. as thickeners or gelatinizers, makes the fibrils interesting candidates for the use in foods.<sup>1, 4-6</sup> The length distribution of the fibrils has a large influence on rheological properties like, for example, the viscosity. Since the fibrils are also semi-flexible,<sup>7</sup> the overlap concentration of the fibrils is low. Therefore the semi-dilute regime is easily reached, where the viscosity is predicted to scale with length as  $\eta \sim L^9$ .<sup>8</sup> Because of this large influence of the length on the viscosity it is important for application purposes to be able to influence the length distribution of the fibrils. Besides, recently fibrils have been used as coating material in the production of microcapsules.<sup>9,10</sup> For this application, the length of the fibrils is important for the coverage of the capsules, since short fibrils can be packed more effectively on a spherical surface than long ones.<sup>10</sup>

It is hard to influence the final length distribution of the fibrils obtained from WPI during production.<sup>11</sup> Although the use of shear can increase the final conversion of WPI into fibrils<sup>12-14</sup>, the fibrils obtained from WPI typically have a length between 2 and 4  $\mu\text{m}$ , regardless of the application of shear flow during fibril formation. The reason for this is that once the fibrils are formed, they remain stable. The fibrils do not fall apart upon dilution or pH changes.<sup>6</sup> One way of influencing the length distribution is exposing the mature fibrils after production to an external field, like shear flow. However, the mature fibrils are shown to be quite stable against shear forces. It was shown that fibrils did not fracture during shear treatment up to shear rates of at least 200  $\text{s}^{-1}$ .<sup>12, 15</sup> Only when very high shear rates are applied for several hours, fibril degradation was observed.<sup>14</sup> This stability against shear forces is because the fibrils align themselves along the flow lines of the shear flow and decrease

therefore their exposure to the elongational component of the shear. Elongational flow is much more effective in fracturing linear macromolecules.<sup>16</sup> Therefore, the effect of flow with a strong elongational component on fibril fracture was investigated here. This is not only relevant for the ability to tune the length of the fibrils, but will also give relevant information about the tensile strength of the fibrils. The required flow field was established with equipment that is available in most laboratories: a PEEK-tube connected to a syringe, and a texture analyzer to empty the syringe at constant discharge. The constriction caused by the difference in diameters between the syringe and the PEEK-tube is responsible for the formation of a flow with a strong elongational component. By varying the discharge of the texture analyzer and the diameter of the PEEK-tube, a range of strain rates could be established. Exposing the fibril solution to these strain rates and analyzing the length distributions of the resulting fracture products gave an estimate of the relation between the applied strain rate and the resulting fibril length. From the applied strain rates and the length of the fibrils exposed to these strain rates also a fracture force was estimated.<sup>17</sup>

## Materials and Methods

### *Fibril formation*

BiPRO whey protein isolate (WPI) was obtained from Davisco Foods International, Inc. (Le Sueur, MN). A stock solution (about 5 wt %) was made by dissolving the protein powder in demineralised water. The stock solution was purified by bringing the pH to 4.75 and centrifuged for 30 minutes at 22600 g. The supernatant was filtered through a protein filter (FD 30/0.45  $\mu\text{m}$  Ca-S from Schleicher & Schuell) and brought to pH 2 using 6 M HCl. The protein concentration of the stock solution was determined using an UV spectrophotometer (Cary 50 Bio, Varian) and a calibration curve of known WPI concentrations at a wavelength of 278 nm. The stock solution was diluted to a protein concentration of 2 wt % with HCl solution of pH 2. For the

fibril formation, the 2 wt % WPI solution was heated at 80°C for 16 hours. The solution was mildly stirred during heating.

*Fibril fracture*

For the establishment of the elongational flow field a PEEK-tube was connected to a syringe (Figure 1). The PEEK-tubes had various diameters (0.254, 0.508 and 0.762 mm) and had a fixed length of 235 mm. The syringe (50 mL) had a diameter of 26 mm. The syringe was vertically placed in a holder in a texture analyzer (TA.XT Plus, Stable Micro Systems) that was used to empty the syringe at constant discharge. In this way a flow with a strong elongational component was established at the transition area of syringe to PEEK-tube. Every sample was passed through the constriction 5 consecutive times.

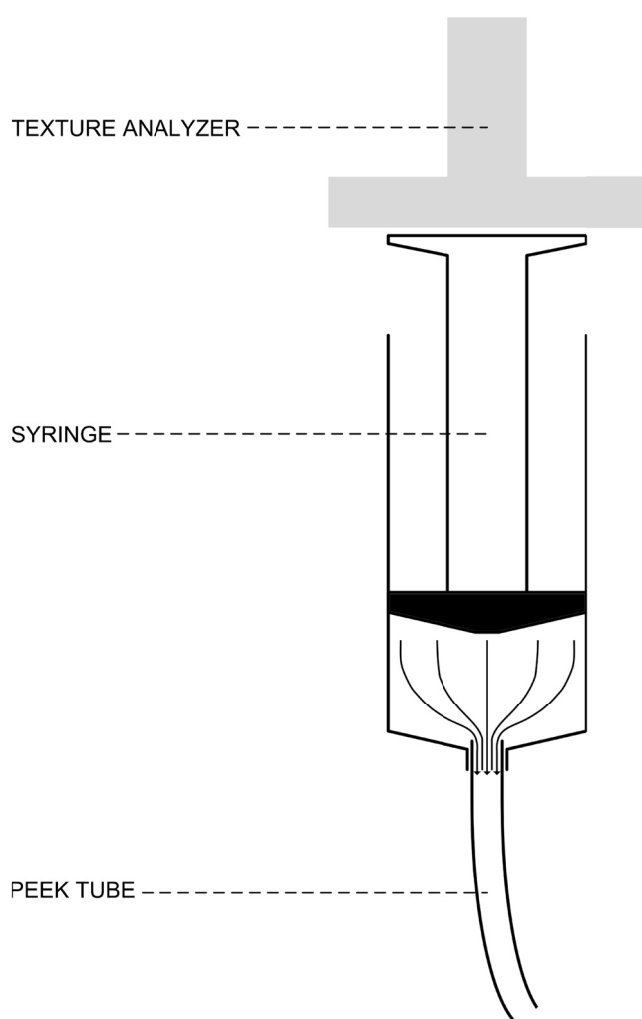


Figure 1. Schematic representation of the set-up to establish a flow with a strong elongational component.

The elongational strain rate is determined by the diameter of the syringe, the diameter of PEEK-tube and the discharge. The discharge and the diameter of the PEEK-tube were varied to obtain elongational strain rates, ranging from 8 to  $107 \text{ s}^{-1}$  (Table 1). For the calculation of the strain rate a Poiseuille flow was assumed in the PEEK-tube and the flow rate in the syringe was assumed to be negligible compared to the flow rate in the PEEK-tube. For the calculation of the strain rate the maximal velocity in the PEEK-tube was used, which is the velocity at the centre of the tube given by

$$v_{\max} = \frac{2D}{\pi \cdot R^2} \quad [1]$$

where  $v_{\max}$  is the maximal velocity,  $D$  is the discharge and  $R$  is the diameter of the tube. The velocity gradient between the syringe and the PEEK-tube is developing over a certain distance  $\Delta x$ . Following Boger (1987) this distance is estimated by<sup>18</sup>

$$\Delta x = (0.49 + 0.11 \cdot \text{Re}) \cdot R \quad [2]$$

where  $\Delta x$  is the distance from where the flow is being fully developed in the upstream to the point where the flow is being fully developed downstream.  $\text{Re}$  is the Reynolds number defined as

$$\text{Re} = \frac{\rho \cdot 2D}{\eta \cdot \pi \cdot R} \quad [3]$$

with the density  $\rho$  taken as 1000 kg/m<sup>3</sup> and the viscosity  $\eta$  taken as 1 mPa s.  $\text{Re}$  numbers were calculated to be in the range of 5-14 and  $\Delta x$  in the range of 0.5-0.8 mm. Now, using Equation 1 and 2 the elongational strain rate  $\varepsilon$  is given by

$$\varepsilon = \frac{v_{\max}}{\Delta x} \quad [4].$$

#### *Length distribution of the fibrils*

Transmission electron microscopy (TEM) pictures were taken from the fibrils in every sample to determine the length distribution of the fibrils. Before preparing the TEM samples by negative staining they were first diluted 1000x. After dilution, a droplet of the diluted solution was put onto a carbon support film on a copper grid. The excess was removed after 15 s with a filter paper. Subsequently, a droplet of 2% uranyl acetate was put onto the grid and again removed after 15 s. Electron

micrographs were taken using a JEOL electron microscope (JEM-1011, Tokyo, Japan) operating at 80 kV. About 20 to 25 pictures were taken per sample to be able to determine the number average length of at least 300 fibrils per sample.

Flow-induced birefringence can be used to efficiently measure the length distribution of a large number of fibrils at the same time.<sup>12,13,15</sup> However, this method is unsuitable for fibrils shorter than 2  $\mu\text{m}$ .<sup>15</sup> Therefore this method was only used to measure the length distribution of the initial fibril solution (strain rate 0  $\text{s}^{-1}$ ). The flow-induced birefringence and the decay curves of the flow-induced birefringence after the cessation of flow were measured with a strain-controlled ARES rheometer (Rheometrics Scientific) equipped with a modified optical analysis module.<sup>19</sup> The steady shear flow-induced birefringence is proportional to the total length concentration of the fibrils and from the decay curve of the flow-induced birefringence after the cessation of flow the length distribution of the fibrils can be determined.<sup>15</sup>

## Results

### *Fibril fracture*

The length distributions of the fibrils obtained from WPI, which were exposed to a range of strain rates, were analyzed using TEM (Figure 2). To verify if measuring more than 300 fibrils using TEM gives a reliable length distribution, the initial fibril solution (strain rate 0  $\text{s}^{-1}$ ) was analyzed in two ways: using TEM and flow-birefringence (Figure 3). The length distributions analyzed by TEM and by flow-birefringence gave similar results. Furthermore the effect of the number of passes was tested (Figure 4). As can be seen in Figure 4, the average length of the fibrils does not change significantly after 5 consecutive passes.

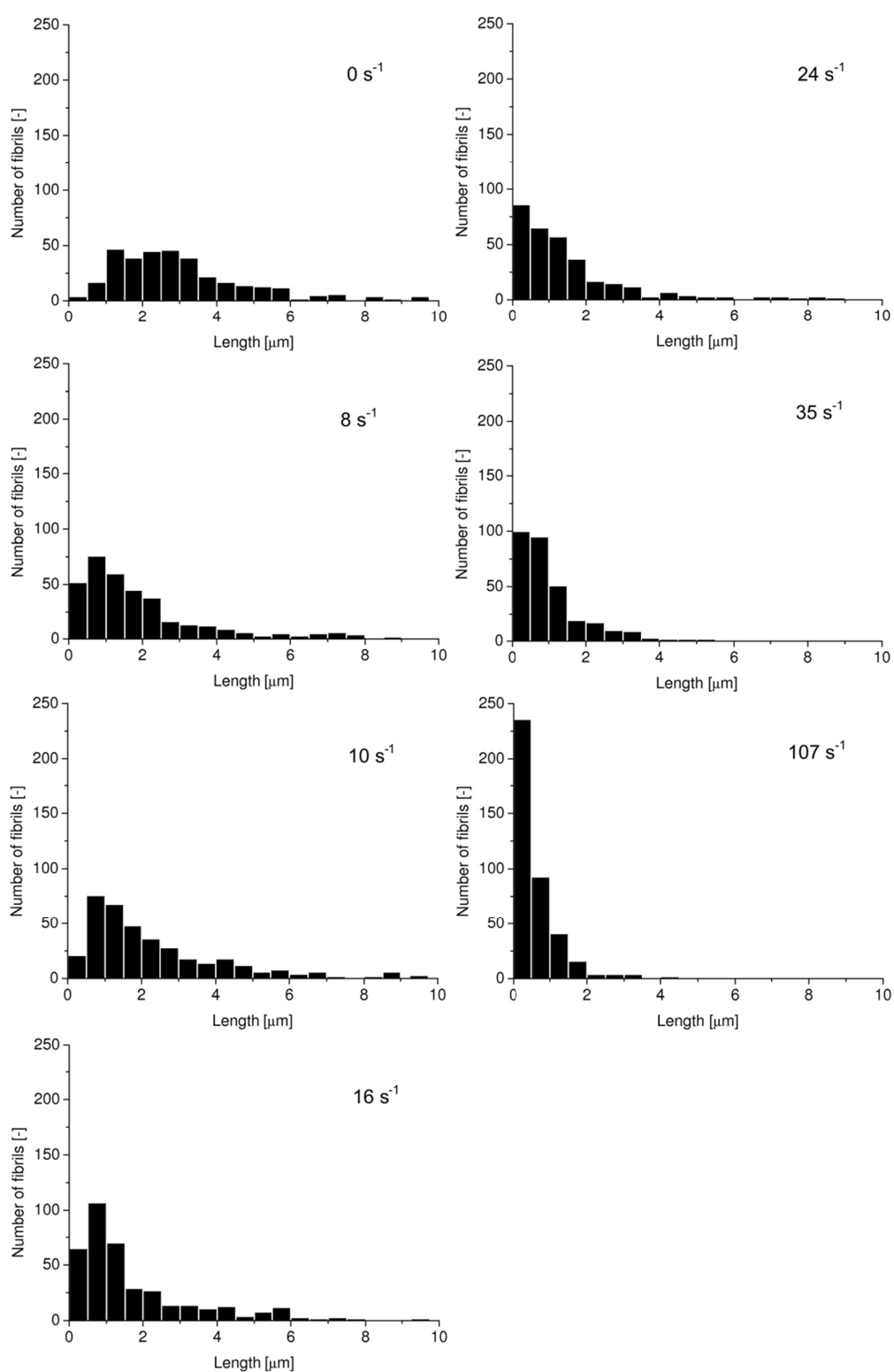


Figure 2. Length distributions of fibrils obtained from WPI. The fibrils were exposed to elongational strain rates of 0 s<sup>-1</sup>, 8 s<sup>-1</sup>, 10 s<sup>-1</sup>, 16 s<sup>-1</sup>, 24 s<sup>-1</sup>, 35 s<sup>-1</sup>, 107 s<sup>-1</sup>. Length distributions were analyzed using TEM.

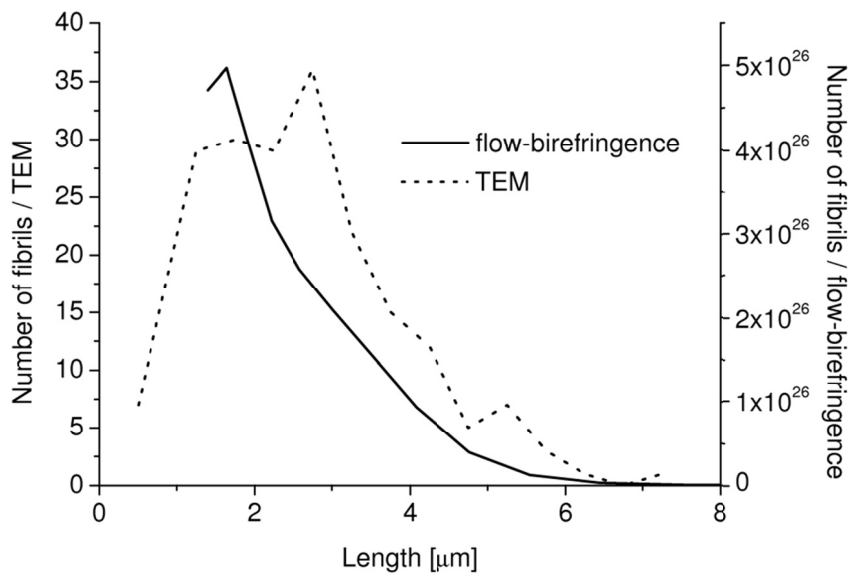


Figure 3. Length distributions of the initial fibril solution (strain rate  $0 \text{ s}^{-1}$ ) analyzed using both TEM and flow-birefringence.

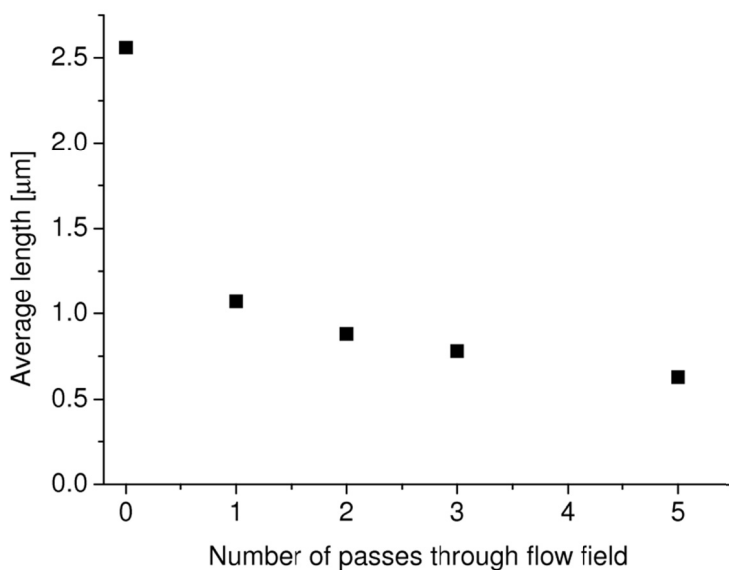


Figure 4. Average fibril length after passing the flow field 5 consecutive times.

As expected, a higher strain rate resulted in shorter fibrils (Figure 2). Even at strain rates of  $8 \text{ s}^{-1}$  fibrils were fractured. The length distribution of the fibril solutions shows a sharper peak at higher strain rates. The results in Figure 2 show that the

length of the fibrils can be influenced at relative low strain rates. Besides, the polydispersity in length of the fibrils can be decreased by using elongational flow.

Performing TEM on the same sample, one day and three days after fracture, did not show any changes in the length distribution, indicating that the fibrils did not recombine after fracture.

#### *Dependence of fibril length on strain rate at fracture*

When a polymer is subjected to elongational flow it will stretch as a result of the velocity gradient. At the moment that the strain rate is large enough and the residence time of the polymer in the flow field is sufficiently long to stretch the polymer, the polymer will finally fracture. Since the fibrils obtained from WPI are semi-flexible <sup>7</sup>, they do not need to fully unfold but only have to stretch to some extent in order to fracture.

To analyze the relation between the strain rate and the fibril length, the number average fibril length was used as a measure for the length (Table 1).

Table 1. Applied elongational strain rates and the resulting number average length of the fibrils obtained from WPI. More than 300 fibrils were measured per sample to obtain the number average length. For the determination of the strain rates, see the materials and methods section.

PEEK-tube $\varnothing$	Discharge	Strain rate	Number average fibril length
-	-	0	2.57 $\mu\text{m}$
0.762 mm	$5.56 \times 10^{-9} \text{ m}^3/\text{s}$	$8 \text{ s}^{-1}$	1.91 $\mu\text{m}$
0.762 mm	$1.08 \times 10^{-8} \text{ m}^3/\text{s}$	$10 \text{ s}^{-1}$	2.35 $\mu\text{m}$
0.762 mm	$9.22 \times 10^{-7} \text{ m}^3/\text{s}$	$16 \text{ s}^{-1}$	1.82 $\mu\text{m}$
0.508 mm	$5.56 \times 10^{-9} \text{ m}^3/\text{s}$	$24 \text{ s}^{-1}$	1.53 $\mu\text{m}$
0.508 mm	$9.22 \times 10^{-7} \text{ m}^3/\text{s}$	$35 \text{ s}^{-1}$	1.07 $\mu\text{m}$
0.254 mm	$5.56 \times 10^{-9} \text{ m}^3/\text{s}$	$107 \text{ s}^{-1}$	0.63 $\mu\text{m}$

In Figure 5 the log of the strain rates are plotted against the log of the number average fibril lengths of the fibrils that were exposed to these strain rates. As can be seen in Figure 5, the strain rate for fracture as a function of the length of the fibrils scales as

$$\varepsilon_f \propto L^{-1.9} \quad [6]$$

where  $L$  is the number average length of the fibrils exposed to elongational strain rate for fracture  $\varepsilon_f$ .

This is in accordance with theoretical predictions where the fracture strain rate for polymers in elongational flow is predicted to be proportional to the inverse square of the molecular weight of the polymers.<sup>17, 20</sup> This scaling behaviour was also experimentally confirmed for synthetic polymers such as polystyrene (PS) and polyethylene oxide (PEO), for which also exponents close to -2 were found.<sup>17, 21</sup>

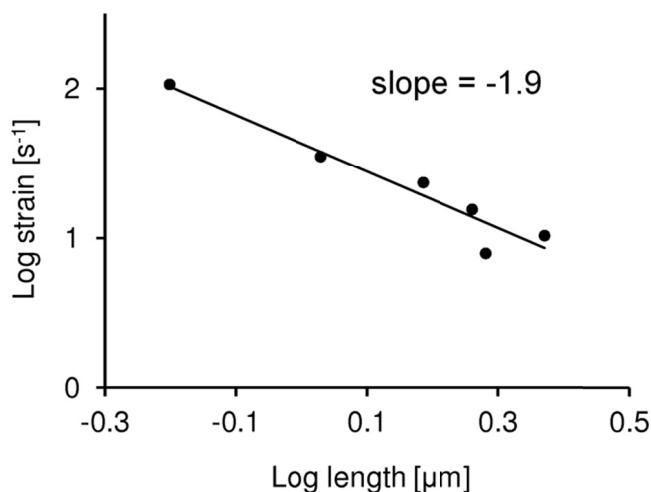


Figure 5. Relation between the log of the elongational strain rate for fracture,  $\varepsilon_f$ , and the log of the number average length of the fibrils exposed to this elongational strain rate,  $L$ .

*Fracture force*

In order to estimate the fracture force  $F_f$ , which is needed to fracture the fibrils, we follow the analysis given by Odell & Keller in their anticipation of a simple Stokes bead-rod model in extensional flow.<sup>17</sup> In this model the fibril is considered as a string of beads exposed to an elongational flow.

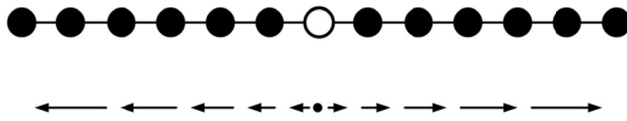


Figure 6. Schematic picture of the stretched-out fibril represented as a bead-rod model in extensional flow. The arrows represent the direction and magnitude of the relative velocity. (adapted from Ref. 17)

Due to the elongational flow, there will be a relative velocity difference between the fibril and the fluid in two directions, which gives frictional forces along the fibril with the direction of the forces leaving from the midpoint towards the tips of the fibril (Figure 6). As a result, the maximum stress will occur at the centre of the fibril. To calculate the force at the centre of the chain  $F_c$ , we have to sum all the hydrodynamics forces acting on the beads, leading to<sup>17</sup>:

$$F_c = \frac{6\pi}{8} \cdot \eta_0 \cdot S \cdot \frac{b}{a} \cdot \varepsilon \cdot L^2 \quad [7]$$

here  $\eta_0$  is the solvent viscosity,  $a$  is the radius of the bead,  $b$  is the separation between midpoints of two neighbouring beads,  $S$  is the hydrodynamic shielding factor,  $\varepsilon$  is the elongational strain rate and  $L$  is the length of the fibril. Breakage will

occur as soon as  $F_c \geq F_f$ . Note that Equation 7 predicts  $\varepsilon_f \propto L^{-2}$ , close to our experimental result  $\varepsilon_f \propto L^{-1.9}$ , supporting the assumption of midpoint fracture.

The occurrence of midpoint fracture was also experimentally shown for PS<sup>22-24</sup> and PEO<sup>17</sup>, where the fracture products had a molecular weight that was  $1/2$ ,  $1/4$ ,  $1/8$ , etc. of the molecular weight of the original polymers. We could not observe this phenomenon as clearly in our length distributions (Figure 2) as was the case in Ref. 17, 22-24. However, in contrast with the polydispersity in length of the fibrils used in this study, these samples were monodisperse in molecular weight. Besides, some of the fibrils might contain weak points resulting from stacking faults, causing these fibrils to fracture at other points than the midpoint of the fibril.

Although the values for the different parameters in Equation 7 are rather uncertain, we use the following estimates in order to estimate the order of magnitude for the fracture force  $F_f$ : the solvent viscosity  $\eta_0 = 1$  mPas, the radius of the bead  $a = 2$  nm (based on the typical thickness of the fibrils)<sup>25</sup> and the separation between midpoints of two neighbouring beads  $b = 2$  nm (based on the line density of the fibrils)<sup>25</sup>. Similarly as in Ref. 17 we ignore hydrodynamic screening and choose the shielding factor  $S = 1$ . Combining this with the result shown in Figure 5, we find a fracture force for the fibrils of  $\sim 0.1$  pN.

Since the fibrils are stable against the thermal force, the fracture force  $F_f$  must be at least as large as  $kT/a$ . Again using 2 nm as a typical length scale leads to a thermal force of about 4 pN, showing that the Stokes' bead-rod model underestimates the fracture force with the chosen parameters. However, by changing the parameters in the Stokes' bead-rod model within realistic bounds, we do not expect the fracture force to exceed the pN range. We therefore expect the fracture force to be only slightly larger than the thermal force, that is around 10 pN. This value for the fracture force is in line with the result that one can break up the fibrils at relatively low elongational strain rates.

## Discussion

The strain rates used to fracture the fibrils are much lower than the strain rates that were used to fracture covalently bound polymers. Odell & Keller and also Nguyen & Kausch used strain rates in the order of  $10\,000\text{ s}^{-1}$  for the fracturing of PS and PEO in typically half of their original size.<sup>17, 26, 27</sup> The length of these synthetic polymers was in the order of  $8\text{ }\mu\text{m}$ ,<sup>17</sup> which is close to the length of the WPI fibrils. Also for the fracturing of DNA in elongational flow, strain rates in the order of  $10\,000\text{ s}^{-1}$  were used to fracture them.<sup>28, 29</sup> In regard to the fact that we showed fibril fracture at a strain rate as low as  $8\text{ s}^{-1}$  these strain rates are a factor 1000 higher. Also initial experiments in our laboratory with xanthan, using the same set-up and conditions that were used for the fibrils, did not show any fracture of xanthan. Thus, the fibrils are evidently not as stable against fracture in elongational flow as some covalently bound polymers are. In addition we show that the length of the fibrils can be shortened in a controlled way at relatively low elongational strain rates that can be generated in a simple experiment.

The elongational strain rate for fracture as a function of the length of the fibrils scaled as  $\varepsilon_f \propto L^{-1.9}$ . The exponent of -1.9 is close to the predicted value and also the experimentally found value for other polymers of -2.<sup>17, 20, 21</sup> The fact that the exponent is close to -2 is in line with the assumption that the fibrils fracture in the centre, as was already shown for covalently bound polymers in elongational flow.<sup>22-24</sup>

The estimated fracture force, which was estimated to be around  $10\text{ pN}$ , is low compared to fracture forces measured for other polymers. For PS, forces of  $2.6\text{-}13.4\text{ nN}$  were needed to fracture the polymers in elongational flow, which are forces needed to break a covalent C-C bond.<sup>17</sup> This is in accordance with the higher strain rates that were needed to fracture these polymers. Also with atomic force microscopy (AFM) it was shown that to be able to fracture covalent bonds, forces in the order of  $\text{nN}$  are required.<sup>30</sup>

The difference in fracture force might be due to the type of polymer. PS, PEO and xanthan are covalently bound polymers, whereas the fibrils are linear protein based aggregates. The fibrils are composed of peptides which are formed during the acid hydrolysis reaction that takes place in the fibril formation process.<sup>31</sup> The peptides in the fibrils are held together by intermolecular  $\beta$ -sheets,<sup>32, 33</sup> where hydrogen bonds are involved. Hydrogen bonds are much weaker than covalent bonds,<sup>34</sup> which explains the lower fracture force that was found for the fibrils compared to fracture forces measured for covalently bound polymers. For insulin amyloid fibrils, forces that were required to fracture the fibrils mechanically using AFM ranged from 0.3 to 0.5 nN.<sup>35</sup> However, this could be due to the fact that Smith et al. did only measure the two-filament insulin fibrils and that the fracture mechanism in their case is different.<sup>35</sup> In their AFM method the fibrils are cut in the direction perpendicular to the fibril axis, whereas in our case the fibrils are fractured in elongational flow, where in the force is applied along the fibril axis.

## Conclusion

In contrast to fibrils under shear flow, fibrils obtained from WPI did fracture when they were exposed to flow with a strong elongational character. This flow was created using a simple set-up. Strain rates of  $8 \text{ s}^{-1}$  to  $107 \text{ s}^{-1}$  were able to fracture the fibrils, with the resulting length distributions depending on the strain rate. The strain rate for fracture as a function of the length of the fibrils scales as  $\dot{\epsilon}_f \propto L^{-1.9}$ , which is close to the scaling predicted theoretically and shown experimentally for other polymers, like PS and PEO.

The fact that relatively low strain rates could be used to fracture the fibrils compared to strain rates that were used to fracture other polymers, indicates that the fibrils are much weaker than covalently bound polymers. This was confirmed by the fact that a fracture force for the fibrils was estimated to be in the order of 10 pN, whereas forces in the order of nN are required to break covalent bonds.

We showed a way to influence the length distribution of the fibrils in a controlled way at relatively low strain rates. This result is of importance for application purposes of the fibrils.

## References

1. Bolder, S. G. S. G.; Hendrickx, H. H.; Sagis, L. M. L. M. C.; van der Linden, E. E., Fibril assemblies in aqueous whey protein mixtures. *Journal of agricultural and food chemistry* **2006**, 54, (12), 4229-34.
2. Ikeda, S.; Morris, V. J., Fine-Stranded and Particulate Aggregates of Heat-Denatured Whey Proteins Visualized by Atomic Force Microscopy. *Biomacromolecules* **2002**, 3, (2), 382-389.
3. Langton, M.; Hermansson, A.-M., Fine-stranded and particulate gels of  $\beta$ -lactoglobulin and whey protein at varying pH. *Food Hydrocolloids* **1992**, 5, 523-539.
4. Bolder, S. G.; Hendrickx, H.; Sagis, L. M. C.; van der Linden, E.,  $\text{Ca}^{2+}$ -induced cold-set gelation of whey protein isolate fibrils. *Applied Rheology* **2006**, 16, (5), 258-264.
5. Veerman, C.; Sagis, L.M.C.; van der Linden, E., Gels at Extremely Low Weight Fractions Formed by Irreversible Self-Assembly of Proteins. *Macromolecular bioscience* **2003**, 3, (5), 243.
6. Veerman, C. C.; Baptist, H. H.; Sagis, L. M. L. M. C.; van der Linden, E. E., A new multistep  $\text{Ca}^{2+}$ -induced cold gelation process for beta-lactoglobulin. *Journal of agricultural and food chemistry* **2003**, 51, (13), 3880-5.
7. Sagis, L. M. C.; Veerman, C.; van der Linden, E., Mesoscopic Properties of Semiflexible Amyloid Fibrils. *Langmuir* **2004**, 20, 924-927.
8. Doi, M.; Edwards, S. F., Dynamics of Rod-like Macromolecules in Concentrated Solution. Part 2. **1978**, 918-932.
9. Sagis, L. M. C.; de Ruiter, R.; Miranda, F. J. R.; de Ruiter, J.; Schroen, K.; van Aelst, A. C.; Kieft, H.; Boom, R.; van der Linden, E., Polymer Microcapsules with a Fiber-Reinforced Nanocomposite Shell. *Langmuir* **2008**, 24, (5), 1608-1612.

10. Humblet-Hua, K. N. P.; Scheltens, G.; van der Linden, E. Sagis, L. M. C., Encapsulation systems based on ovalbumin fibrils and high methoxyl pectin. *Food Hydrocolloids*, **2011**, 25, (4), 569-576.
11. Akkermans, C.; van der Goot, A. J.; Venema, P.; van der Linden, E.; Boom, R. M., Formation of fibrillar whey protein aggregates: Influence of heat and shear treatment, and resulting rheology. *Food Hydrocolloids* **2008**, 22, (7), 1315-1325.
12. Akkermans, C.; Venema, P.; Rogers, S.; van der Goot, A.; Boom, R.; van der Linden, E., Shear Pulses Nucleate Fibril Aggregation. *Food Biophysics* **2006**, 1, (3), 144-150.
13. Bolder, S. G.; Sagis, L. M. C.; Venema, P.; van der Linden, E., Effect of Stirring and Seeding on Whey Protein Fibril Formation. *Journal of agricultural and food chemistry* **2007**, 55, (14), 5661-5669.
14. Hill, E. K.; Krebs, B.; Goodall, D. G.; Howlett, G. J.; Dunstan, D. E., Shear Flow Induces Amyloid Fibril Formation. *Biomacromolecules* **2006**, 7, (1), 10-13.
15. Rogers, S. S.; Venema, P.; Sagis, L. M. C.; van der Linden, E.; Donald, A. M., Measuring length distribution of a fibril system: A flow birefringence technique applied to amyloid fibrils. *Macromolecules* **2005**, 38, 2948-2958.
16. Clay, J. D.; Koelling, K. W., Molecular degradation of concentrated polystyrene solutions in a fast transient extensional flow. *Polym. Eng. Sci.* **1997**, 37, 789-800.
17. Odell, J. A.; Keller, A., Flow-induced chain fracture of isolated linear macromolecules in solution. *J. Polym. Sci. (B)* **1986**, 24, 1889-1916.
18. Boger, D. V., Viscoelastic flows through contractions. *Annu. Rev. Fluid Mech.* **1987**, 19, 157-182.
19. Klein van, C. O.; Venema, P.; Sagis, L. M. C.; Dusschoten, D. v.; Wilhelm, M.; Spiess, H. W.; Linden, E. v. d.; Rogers, S. S.; Donald, A. M., Optimized Rheo-optical Measurements Using Fast Fourier Transform and Oversampling. *Applied rheology* **2007**, 17, (4), 45210-1 - 45210-7.

20. Odell, J. A.; Keller, A.; Rabin, Y., Flow-induced scission of isolated macromolecules. *J. Chem. Phys.* **1988**, *88*, 4022-4028.
21. Keller, A.; Odell, J. A., The extensibility of macromolecules in solution; A new focus for macromolecular science. *Colloid Polym. Sci.* **1985**, *263*, 181-201.
22. Horn, A. F.; Merrill, E. W., Midpoint scission of macromolecules in dilute solution in turbulent flow. *Nature* **1984**, *312*, 140-141.
23. Merrill, E. W.; Horn, A. F., Scission of macromolecules in dilute solution: extensional and turbulent flows. *Polym. Commun.* **1984**, *25*, 144-146.
24. Odell, J. A.; Keller, A.; Miles, M. J., A method for studying flow-induced polymer degradation: verification of chain halving. *Polym. Commun.* **1983**, *24*, 7-10.
25. Aymard, P.; Nicolai, T.; Durand, D., Static and Dynamic Scattering of *beta*-Lactoglobulin Aggregates Formed after Heat-Induced Denaturation at pH 2. *Macromolecules* **1999**, *32*, 2542-2552.
26. Nguyen, T. Q.; Kausch, H.-H., Chain scission in transient extensional flow kinetics and molecular weight dependence. *J. Non-Newtonian Fluid Mech.* **1988**, *30*, 125-140.
27. Nguyen, T. Q.; Kausch, H.-H., Effects of solvent viscosity on polystyrene degradation in transient elongational flow. *Macromol.* **1990**, *23*, 5137-5145.
28. Atkins, E. D. T.; Taylor, M. A., Elongational flow studies on DNA in aqueous solution and stress-induced scission of the double helix. *Biopolym.* **1992**, *32*, 911-923.
29. Reese, H. R.; Zimm, B. H., Fracture of polymer chains in extensional flow: Experiments with DNA, and a molecular-dynamics simulation. *J. Chem. Phys.* **1990**, *92*, 2650-2662.
30. Grandbois, M.; Beyer, M.; Rief, M.; Clausen-Schaumann, H.; Gaub, H. E., How Strong Is a Covalent Bond? *Science* **1999**, *283*, 1727-1730.
31. Akkermans, C.; Venema, P.; van der Goot, A. J.; Gruppen, H.; Bakx, E. J.; Boom, R. M.; van der Linden, E., Peptides are Building Blocks of Heat-Induced Fibrillar Protein Aggregates of  $\beta$ -Lactoglobulin Formed at pH 2. *Biomacromolecules* **2008**, *9*, (5), 1474-1479.

32. Kavanagh, G. M.; Clark, A. H.; Ross-Murphy, S. B., Heat-induced gelation of globular proteins: part 3. Molecular studies on low pH beta-lactoglobulin gels. *International Journal of Biological Macromolecules* **2000**, *28*, 41-50.
33. Lefèvre, T.; Subirade, M., Molecular differences in the formation and structure of fine-stranded and particulate beta-lactoglobulin gels. *Biopolymers* **2000**, *54*, (7), 578-586.
34. Israelachvili, J., Chapter 16: Thermodynamic principles of self-assembly, in *Intermolecular & Surface Forces*, **1992**, (Academic Press, California, USA), 341-365.
35. Smith, J. F.; Knowles, T. P. J.; Dobson, C. M.; MacPhee, C. E.; Welland, M. E., Characterization of the nanoscale properties of individual amyloid fibrils. *PNAS* **2006**, *103*, 15806-15811.





## *Chapter 6*

### **The behaviour of fibril-peptide mixtures at varying pH**

## Abstract

Fibrils are formed when  $\beta$ -lactoglobulin is heated at pH 2 and 80°C for several hours. These fibrils can be used as structurants in foods. Since most foods have a pH between 4 and 7, the stability of the fibrils upon pH change is important. Previous research showed that the fibril solutions become turbid around pH 5, suggesting that the fibrils aggregate around this pH. However, recently it was found that the fibrils consist of peptides derived from the hydrolysis of  $\beta$ -lactoglobulin and that the fibril solutions are actually mixtures of fibrils and non-aggregated peptides. A priori, it is unclear what fraction is causing the turbidity. Therefore, the fibrils and the non-aggregated peptides were separated to obtain three different fractions: a solution only containing fibrils (so-called pure fibril solution), a solution only containing non-aggregated peptides (so-called pure non-aggregated peptides solution) and the original fibril solution containing both the fibrils and the non-aggregated peptides. The stability of these three solutions upon pH changes was analyzed. It was found that most of the turbidity at pH 5 was caused by the non-aggregated peptides, and that the fibrils have a tendency to form aggregates themselves around that pH.

## Introduction

In solution, the whey protein  $\beta$ -lactoglobulin ( $\beta$ -lg) forms fibrils when heated at pH 2 and 80°C for several hours.<sup>1, 2</sup> The fibrils that are formed are several micrometers long, and only a few nanometers thick.<sup>3</sup> This makes them interesting candidates as thickeners or gelling agents in foods. Several researchers have investigated the transparent fine stranded gels that are formed when beta-lactoglobulin is heated at pH 2 and concentrations above 6 wt %.<sup>1, 2, 4-10</sup> Next to these transparent gels, the fibrils could also be used to produce gels with very low volume fractions in a so-called cold set gelation process.<sup>11</sup> For these cold-set gels a fibril solution was brought to pH 7 and subsequently the fibrils were cross-linked by addition of CaCl<sub>2</sub>. Akkermans et al showed that the viscosity and gel strength of whey protein isolate (WPI) solutions was increased upon addition of fibrils.<sup>12</sup>

The fibrils are produced at pH 2, but most food products have a pH between 3 and 7. Therefore the stability of the fibrils upon pH changes is important. Although the fibrils do not fall apart upon dilution or pH changes,<sup>11-13</sup> fibril solutions become turbid around pH 5, close to the iso-electric point of  $\beta$ -lg.<sup>12, 14</sup> These results are suggesting that the fibrils aggregate around pH 5. However, recently it was found that the fibril solutions contain a mixture of fibrils and non-aggregated peptides. It was shown that the fibrils consist of peptides derived from the acidic hydrolysis of  $\beta$ -lg at pH 2. Not all the peptides that are produced assemble into fibrils; only ~40% of the peptides are being incorporated into the fibrils. These peptides were found to be the more hydrophobic peptides with a high ability to form  $\beta$ -sheets.<sup>15</sup> The rest of the material remains in the solution as non-aggregated peptides. It has not been addressed which fraction is causing the turbidity around pH 5.

Therefore, the aim of this research was to analyze the stability relative to pH changes for the different fractions that are present in the initial fibril solution. First the fibrils and non-aggregated material were separated to be able to analyze the behaviour of the pure fibrils, the non-aggregated peptides and the initial fibril solution separately.

Three different methods were investigated on their ability to separate the two fractions. The first method uses centrifugal filtration and is based on the method that Bolder et al. used to determine the conversion of protein into fibrils.<sup>16</sup> Next to this method also dialysis and ultracentrifugation were tested on their ability to separate the fibrils and the non-aggregated peptides. Subsequently, the behaviour of the initial fibril solution and both the pure fibrils and the non-aggregated material were analyzed within a pH range between 2 and 8.

## Materials and Methods

### *Fibril formation*

$\beta$ -Lg was obtained from Sigma (product no. L0130, lot. no. 095K7006). A stock solution (about 6 wt %) was made by dissolving the protein powder in HCl solution of pH 2. The pH of the protein solution was adjusted to pH 2 with 6M HCl solution. Subsequently, this stock solution was filtered through a protein filter (FD 30/0.45  $\mu$ m Ca-S from Schleicher & Schuell) to remove any traces of undissolved protein. The protein concentration of the stock solution was determined using an UV spectrophotometer (Cary 50 Bio, Varian) and a calibration curve of known  $\beta$ -lg concentrations at a wavelength of 278 nm. The stock solution was diluted to a protein concentration of 2 wt % with HCl solution of pH 2.

The  $\beta$ -Lg solution was heated in small glass vials (20 ml) in a metal stirring and heating plate for 20 hours at 80°C. The protein solution was mildly stirred during heating.

### *Separation fibrils and non-aggregated peptides*

#### **Centrifugal Filtration**

For the first method to separate the fibrils and the non-aggregated peptides, centrifugal filters were used. This separation method is based on the method developed by Bolder et al. to determine the conversion of protein into fibrils.<sup>16</sup> To

separate the fibrils from the non-aggregated peptides, the fibril solution was diluted to a protein concentration of 0.2 wt % with HCl solution of pH 2. The solution was divided over 6 centrifugal filters (Amicon Ultra 100K - 15 Centrifugal Filters) and centrifuged at 3000 g and 15°C for 30 minutes (Allegra X-22R Centrifuge, Beckman Coulter). After the centrifugation the filtrate was removed from the tubes and the retentate (containing the fibrils) was resuspended in ~10 ml of fresh pH 2 solution. Subsequently the samples were centrifuged again at 3000 g and 15C for 30 min. In total 4 centrifugation steps were used. After the fourth centrifugation step the retentate was resuspended in 2 ml pH 2 solution instead of the original 15 ml.

### **Dialysis**

The second method used to separate the fibrils and the non-aggregated peptides was dialysis. To see whether it is an option to separate the fibrils and the non-aggregated peptides by dialysis, first it was investigated if the non-aggregated peptides would pass the dialysis tube. For this, the non-aggregated protein fraction (obtained by the ultracentrifugation method) was dialyzed against HCl solution of pH 2 overnight (MWCO 12-14 kDa). The protein concentration of the solution before and after dialysis was determined.

### **Ultracentrifugation**

The third method used to separate the fibrils and the non-aggregated protein was ultracentrifugation. To separate the fibrils from the non-aggregated protein, the fibril solution was diluted to a protein concentration of 1 wt % with HCl solution of pH 2. The solution was divided over 6 centrifuge tubes and centrifuged at 90100 g and 15C for 90 minutes. After the centrifugation the supernatant was immediately removed from the tubes and the pellets were resuspended in their original volume in a fresh pH 2 solution and stored overnight in a cold room (UCF 1). For 4 of the 6 tubes one extra washing step was performed by repeating the ultracentrifugation and

resuspending step (UCF 2). For two of these 4 tubes, a third washing step was performed (UCF 3).

### **Protein concentration**

The protein concentration of the various samples were determined using an UV spectrophotometer (Cary 50 Bio, Varian) using a calibration curve of known  $\beta$ -lg concentrations at a wavelength of 278 nm.

### **ThT Fluorescence**

To analyze the different fractions for fibrils after separation by ultracentrifugation, the various solutions were analyzed using a ThT assay. A ThT stock solution (3.0 mM) was made by dissolving 7.9 mg ThT in 8 ml phosphate buffer (10 mM phosphate, 150 mM NaCl at pH 7.0). This stock solution was filtered through a 0.2  $\mu$ m filter (Schleicher & Schuell). The stock solution was diluted 50x in a phosphate buffer (10 mM phosphate, 150 mM NaCl at pH 7.0) before use.

Aliquots of the solutions (48  $\mu$ l) were mixed with 4 ml ThT solution and allowed to bind to the ThT for 1 minute. The fluorescence of the samples was measured using a fluorescence spectrophotometer (Perkin Elmer LS 50 B). The excitation wavelength was set on 460 nm (slit width 4.0 nm) and the emission spectrum was recorded between 470 and 500 nm (slit width 2.5 nm) at a scanning speed of 200 nm/min. The fluorescence intensity peak was determined at 482 nm. The fluorescence intensity of the ThT solution itself was subtracted as a background. All samples were measured in duplicates.

### **Flow-induced birefringence**

Flow-induced birefringence was used to analyze the length distribution of the fibrils that were present in the various fractions after ultracentrifugation. This method can be used to efficiently measure the length distribution of a large number of fibrils at the same time.<sup>17-19</sup> The decay curves of the flow-induced birefringence after the

cessation of flow were measured with a strain-controlled ARES rheometer (Rheometrics Scientific) equipped with a modified optical analysis module.<sup>20</sup> From these decay curves the length distribution of the fibrils can be determined.<sup>19</sup>

### **Gel Electrophoresis (SDS-PAGE)**

To check whether all non-aggregated peptides were removed from the fibril solution with the separation based on ultracentrifugation, SDS-PAGE was performed on the various fractions. For the gel electrophoresis a XCell *SureLock*<sup>TM</sup> Mini-Cell (Invitrogen Corporation, Carlsbad, California 92008, USA) was used. Samples were run on NuPAGE® Novex 4-12% Bis-Tris gels with NuPAGE® MES SDS running buffer (Invitrogen Corporation) under non-reducing conditions (no S-bonds are broken). The gels were stained with SimplyBlue<sup>TM</sup> SafeStain (Invitrogen Corporation).

### *Behaviour of the fibrils as a function of pH*

#### **Conversion of protein into fibril**

The conversion of protein into fibrils was calculated using the various fractions obtained by centrifugal filtration. From the protein concentration of the various fractions and the weight of these fractions the conversion of protein into fibrils could be calculated as

$$C = \frac{P - (F_1 + F_2 + F_3 + F_4)}{P} \times 100\%$$

where  $C$  is the conversion of protein in fibrils in wt %,  $F_1$  is the weight of protein in filtrate 1 (g),  $F_2$  is the weight of protein in filtrate 2 (g), etc., and  $P$  is the weight of the initial amount of protein in the solution (g).

### **Visual appearance**

For the visual observations, the initial fibril solution, the pure fibril solution and the solution containing the non-aggregated peptides were diluted to 0.1 wt % protein and brought to pH 5 and pH 8 using 0.1M NaOH. The appearance of the various fractions at a protein concentration of 0.1 wt % and pH 2, 5 and 8 were analyzed visually and digitally recorded.

### **TEM**

TEM pictures were taken from all fractions at pH 2, 5 and 8 (protein concentration 0.01 wt %). A droplet of the solution was put onto a carbon support film on a copper grid. The excess was removed after 15 s with a filter paper. Subsequently, a droplet of 2% uranyl acetate was put onto the grid and again removed after 15 s. Electron micrographs were taken using a JEOL electron microscope (JEM-1011, Tokyo, Japan) operating at 80 kV.

### **Mobility**

For the electrophoretic mobility measurements, all fractions were diluted to 0.01 wt % protein with milliQ water. Samples at various pH were prepared by adding 0.1M HCl or 0.1 - 0.01M NaOH. The electrophoretic mobility of the different fractions at various pH was measured using a Zetasizer Nano (Malvern Instruments Ltd, Worcestershire, UK). Samples were measured in 5-fold.

### *Preventing aggregation*

In analogy to the work of Jung et al. we investigated the addition of SDS to the various fractions to prevent clustering of the protein material in the solutions.<sup>14</sup> For this experiment the fibrils and the non-aggregated peptides were separated using ultracentrifugation. First a series of SDS solutions at pH 2 was made with SDS concentrations from 0 to 0.02M. The initial fibril solution, the pure fibril solution and the solution containing the non-aggregated peptides were added so that the final

protein concentration of the solutions was 0.005 wt %. The pH of all the samples were set at pH 3 using NaOH. The electrophoretic mobility of the samples were measured using a Zetasizer Nano (Malvern Instruments Ltd, Worcestershire, UK). Samples were measured in 5-fold.

Next, the solutions that contained enough SDS to prevent the fibrils and non-aggregated peptides from aggregation were adjusted to a range of pH values between 3 and 8 using NaOH. Also the electrophoretic mobility of these samples was measured.

## Results and Discussion

### *Separation of fibrils and non-aggregated peptides*

#### **Centrifugal filtration**

The first method that was used to separate the fibrils from the non-aggregated peptides was based on the method as introduced by Bolder et al. to determine the conversion of protein into fibrils.<sup>17</sup> In this method the fibrils and the non-aggregated peptides are separated using centrifugal filters. Four washing steps were performed to remove all the non-aggregated peptides from the fibril solution. No protein was found by UV spectroscopy measurements in the filtrate after the 4<sup>th</sup> washing step, indicating that the pure fibril solution was free from non-aggregated peptides after four washing steps. Besides, the fibrils do not pass the filters<sup>15, 17</sup> and therefore no fibrils will be present in the filtrate.

#### **Dialysis**

The second method that was tested to separate the fibrils and the non-aggregated peptides was to dialyse the fibril solutions. To check whether the non-aggregated peptides would actually pass the dialysis tube, a prerequisite for this method, a solution containing the non-aggregated peptides (the supernatant obtained from the ultracentrifugation) was dialyzed against an HCl solution of pH 2. The protein

concentration that was measured in the dialysis tube remained the same before and after dialysis, indicating that the non-aggregated peptides did not pass the dialysis tube and therefore making dialysis under the conditions used in this experiment unsuitable for the separation of the fibrils and the non-aggregated peptides. To be able to separate the non-aggregated peptides and the fibrils by dialysis, dialysis tubing with a higher MWCO than 12-14 kDa and longer dialysis times than ~12 hours might be necessary. Jordens et al. dialysed a fibril solution against milliQ water of pH 2 for 7 days using dialysis tubing with a MWCO of 100 kDa to remove unreacted protein and low molecular weight residual peptides.<sup>21</sup> Since this method would become much more time consuming compared to the other separation methods, the separation based on dialysis was not further investigated.

### **Ultracentrifugation**

The third method that was tested to separate the fibrils and the non-aggregated peptides was ultracentrifugation (~90 000 g for 90 min). After the first centrifugation step, the supernatant was removed and kept separate for further analysis. The transparent pellet that was obtained was resuspended in a fresh HCl solution of pH 2. These steps were repeated twice in an attempt to separate all the non-aggregated peptides from the fibrils. Protein concentration measurements showed that after three ultracentrifugation steps, still protein was present in the supernatant. The protein in the supernatant can be present in the form non-aggregated peptides or fibrils that were not completely spun down. Therefore, a ThT fluorescence assay was performed to see in which fractions fibrils were present after the centrifugation steps (Figure 1).

Figure 1 shows that the supernatant after each centrifugation step still showed a fluorescence signal, indicating the presence of fibrils. It is estimated that in total about 60% of the fibrils remain in the supernatants.

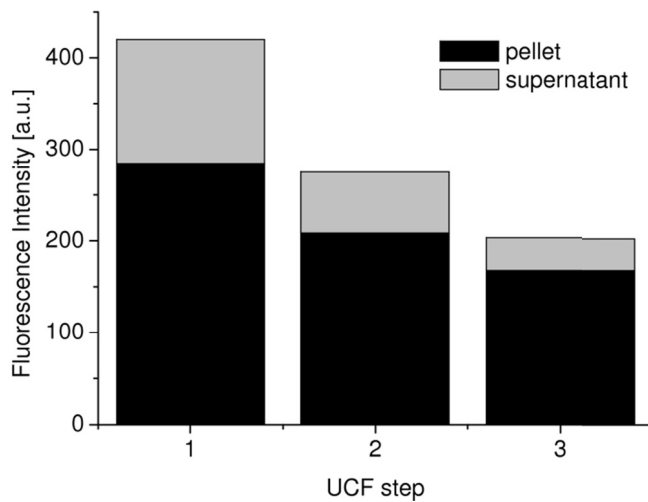


Figure 1. ThT Fluorescence intensities of the pellet and the supernatant after the 3 UCF steps.

Flow-induced birefringence measurements confirmed that indeed fibrils were present in the supernatant (Figure 2), showing that after three ultracentrifugation steps no solution could be obtained containing only the non-aggregated peptides.

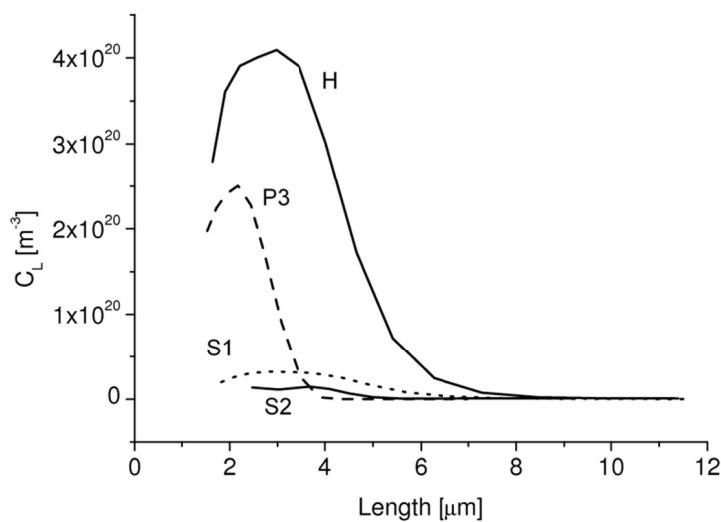


Figure 2. Length distributions of the heated sample (H), pellet after 3x UCF (P3), supernatant after 1x UCF (S1), supernatant after 2x UCF (S2).

Conversely, to check whether all the non-aggregated peptides were removed from the fibril solution, SDS PAGE was performed (Figure 3) on the final resuspended pellet (P3). Figure 3 shows that the final resuspended pellet (P3) indeed does not contain any detectable amount of small peptides, indicating that after three ultracentrifugation steps a pure fibril solution could be obtained.

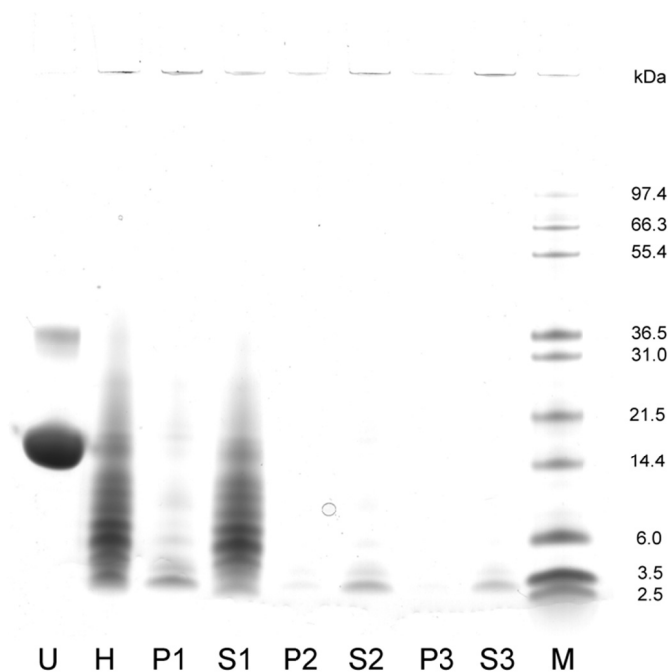


Figure 3. SDS-Page. Unheated sample (U), heated sample (H), pellet after 1x UCF (P1), supernatant after 1x UCF (S1), pellet after 2x UCF (P2), supernatant after 2x UCF (S2), pellet after 3x UCF (P3), supernatant after 3x UCF (S3), marker (M).

From the ThT assay, the flow-induced birefringence and the SDS-PAGE it can be concluded that ultracentrifugation is a suitable method to remove all the non-aggregated material from the fibril solution to obtain a pure fibril solution. The drawback from this method is that it was not possible to obtain a solution that only contained non-aggregated peptides, since there were still fibrils present in the supernatant.

Comparing the separation using centrifugal filters with the other two methods, the separation using centrifugal filtration is more efficient in the sense that no fibrils are present in the non-aggregated peptide fraction and no non-aggregated peptides are present in the pure fibril solution. Therefore, the fractions obtained using centrifugal filtration were used to analyze the behaviour of the different fractions as a function of pH.

*Behaviour of the various fractions as a function of pH*

**Conversion of protein into fibrils**

Based on the separation using the centrifugal filters three different solutions were now obtained:

- (A) the initial fibril solution containing a mixture of fibrils and non-aggregated peptides,
- (B) a solution containing only fibrils,
- (C) a solution containing only the non-aggregated peptides.

Using the weight and protein concentration that were obtained during the separation process, it was determined that about 46% (w/w) of the initial protein was present in the form of fibrils, whereas the rest of the protein material was present as small peptides. The behaviour of the three solutions A, B and C was analyzed as a function of pH. All solutions were transparent at pH 2.

**Visual appearance as a function of pH**

The turbidity of the various fractions was visually inspected at pH 2, 5 and 8 and protein concentrations of 0.1 wt % (Figure 4). It is found from Figure 4 that solution A is transparent at pH 2, becomes turbid around pH 5, and becomes transparent again at pH 8. This behaviour was also observed by other researchers.<sup>12, 14</sup> For solution C, a similar behaviour is seen, with the turbidity even more pronounced at pH 5. This more pronounced turbidity in solution C is possibly due to the fact that

solution A and C have the same protein concentration, but in solution C all proteinaceous material exists of the non-aggregates peptides whereas in solution A also fibrils are present. In contrast to solution A and solution C, solution B stayed transparent at pH 5, only showing a slight haze. This is confirming that the peptides are the main cause for the turbidity around pH 5.

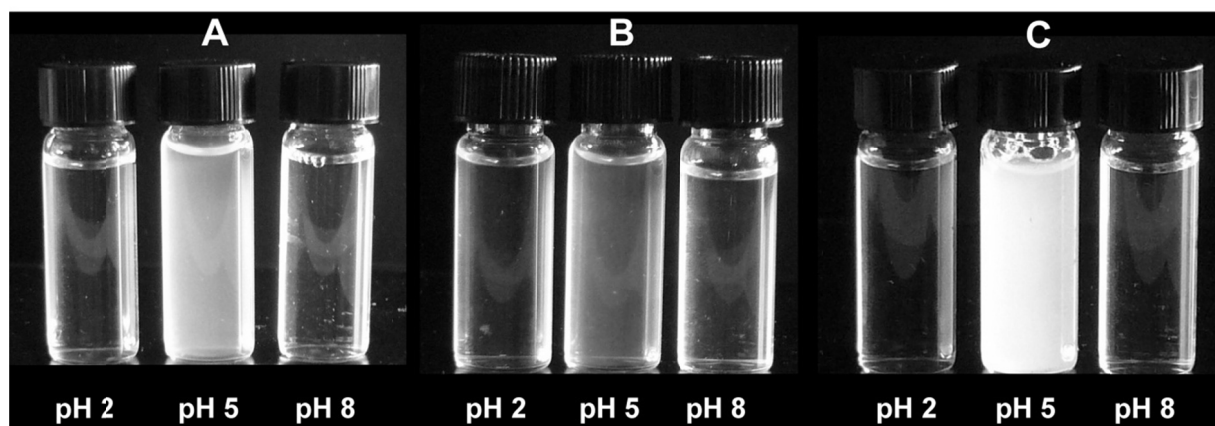


Figure 4. Visual observations of solutions A, B and C at pH 2, 5 and 8, and 0.1 wt % protein.

### TEM as a function of pH

To analyze the samples on a microscopic scale in the solutions, TEM pictures were taken from the different fractions at pH 2, 5 and 8. The results are shown in Figure 5. Linear fibrils are visible in the TEM pictures at pH 2 and pH 8 of solution A and solution B. At these pH values the fibrils are charged and the solutions were stable and transparent in line with the visual observations (Figure 4). As expected in the TEM picture of solution C no fibrils were visible, confirming the efficiency of the separation.

In the TEM picture of solution A at pH 5, aggregates of fibrils were observed. Only spots of collapsed fibrils are visible and no elongated fibrils could be observed. In solution B, fibrils were visible at pH 5, but these fibrils looked smaller. In solution B, also aggregates of fibrils were visible at pH 5, however the aggregates look more open compared to the aggregates in solution A. These results are in agreement with

the visual observations, where solution A was turbid, whereas solution B was still transparent at pH 5. The aggregates in solution B apparently are not optically dense enough to scatter light, resulting in a transparent solution. In these transparent pure fibril solutions at pH 5 some gel like particles were observed. The formation of these open aggregates might be caused by the separation method in which the fibrils have to be resuspended in the pH 2 solution after every washing step. However, it is more likely that the fibrils in solution B form aggregates because their net charge is close to zero at pH 5.

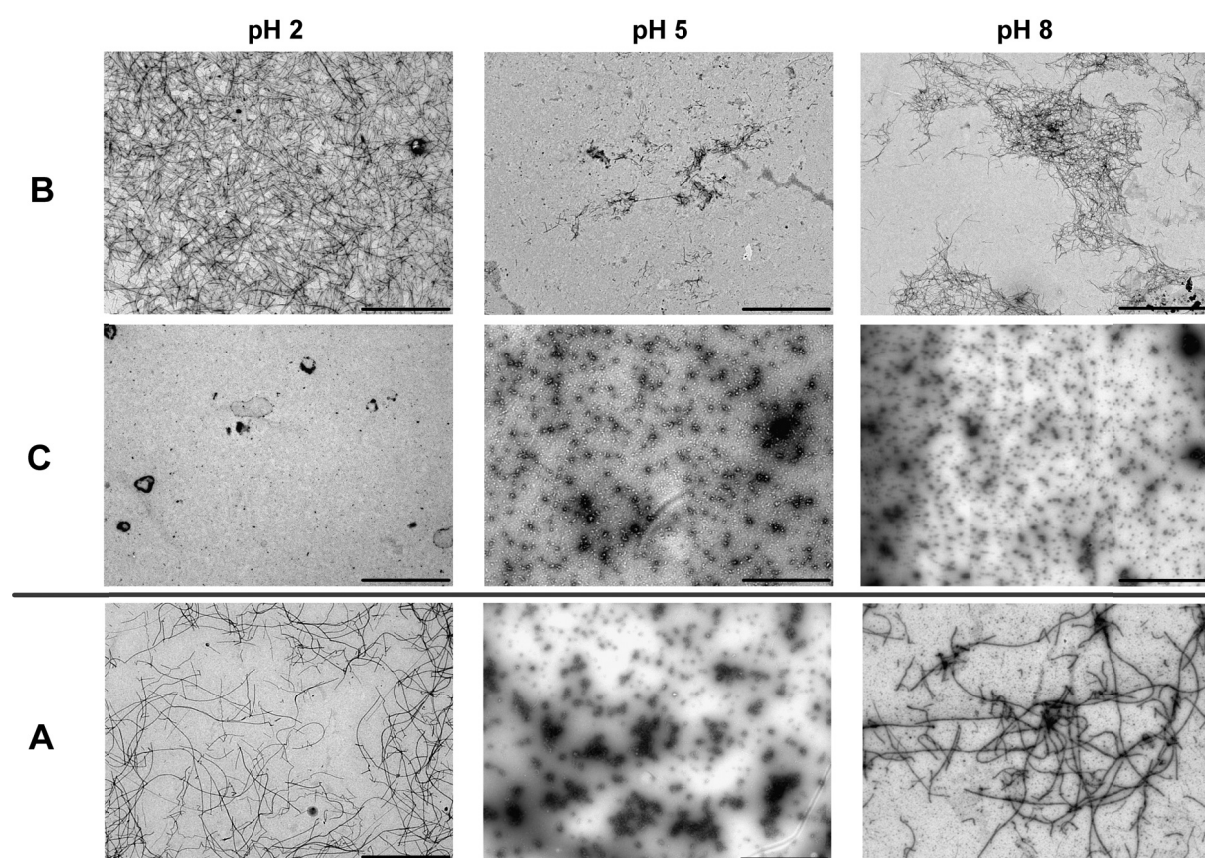


Figure 5. TEM pictures of solutions A, B and C at pH 2, 5 and 8. Scale bars represent 2  $\mu\text{m}$ .

In solution C at pH 5 small aggregates are visible with a diameter of about 20 nm. At pH 8 also some small spherical aggregated were visible in this fraction, but these

were much smaller than the ones at pH 5. This is in accordance with the visual observations that solution C is turbid at pH 5 and transparent at pH 8. The aggregates in solution C at pH 5 were large enough to scatter light in the visible wavelength, whereas the aggregates at pH 8 were too small to do this, resulting in a turbid solution at pH 5 and a transparent solution at pH 8.

### Electrophoretic mobility as a function of pH

The electrophoretic mobility as a function of pH was measured for all solutions: A, B and C (Figure 6).

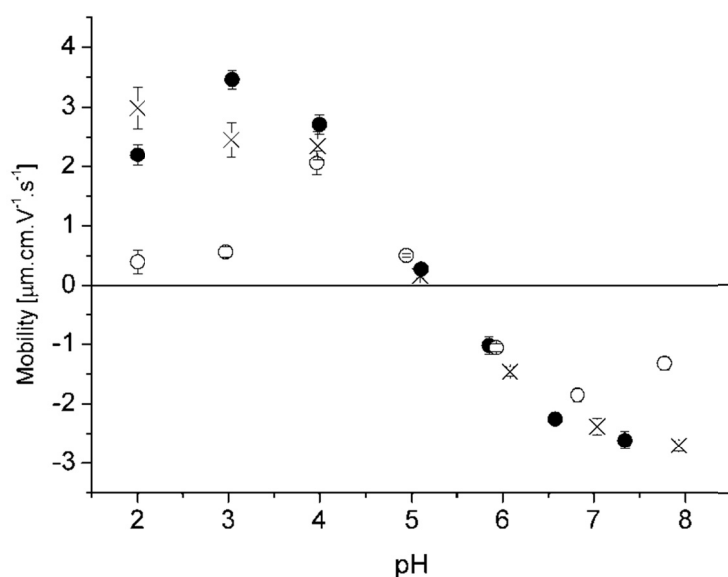


Figure 6. Electrophoretic mobility of solution A (x), solution B (●) and solution C (○) as a function of pH. Protein concentrations are 0.01 wt %.

Although the curves of the various fractions are not exactly the same over the whole pH range, the pH where the mobility of the samples is zero is for all fractions around pH 5, close to the iso-electric point of  $\beta$ -lg.<sup>22</sup> This is in agreement with the TEM pictures which showed that at pH 5 in all the fractions aggregates were present, indicating that both the non-aggregated peptides and the pure fibrils have no net

charge at this pH. Furthermore, the curves of solution A and solution B are quite similar, compared to the curve of solution C. Note that more than 50% of the protein material in solution A is consisting of non-aggregated peptides.

### *Preventing of aggregation*

#### **Coating with sodium dodecyl sulphate (SDS)**

It is shown that the turbidity is mainly coming from the non-aggregated peptides in the initial fibril solution and this can be avoided by removing the non-aggregated peptides. Yet it is also shown that the fibrils still form aggregates in the pure fibril solution around pH 5. One way to prevent the aggregation of the fibrils would be to coat the fibrils using anionic surfactants. This was investigated by Jung et al. who used sodium dodecyl sulfate (SDS) to coat the fibrils.<sup>14</sup> Two stages were distinguished in this study. In the first stage the SDS concentration is high enough to neutralize the charges of the protein, which is the case at SDS concentrations of  $9 \times 10^{-4}$  M, at 0.1 wt % protein. At this point a so-called SDS single layer is formed around the fibrils and precipitation of the coated fibrils is visible. At higher SDS concentrations, of 2 mM, a SDS double layer was formed around the fibrils and the coated fibrils could be completely redispersed in water.

In analogy to Jung et al. we investigated various concentrations of SDS to our solutions A, B and C (Figure 7). Note that the fibril solution used by Jung et al. can be compared with solution A in our research. By measuring the mobility as a function of the SDS concentration we observe a change in mobility for solution A, B and C from  $+1.5 \mu\text{m cm V}^{-1} \text{s}^{-1}$  at low SDS concentrations to a mobility of  $-2 \mu\text{m cm V}^{-1} \text{s}^{-1}$  at SDS concentrations of around 7 mM. No clear difference could be seen between the solutions A, B and C in their change in mobility as a function of SDS concentration. To investigate whether the coated fibrils and peptides would stay negatively charged over the whole pH range, solutions A, B and C containing 7 mM SDS were adjusted to a range of pH values between 3 and 8 using NaOH. SDS concentrations of 7 mM, only slightly below the critical micelle concentration of SDS (CMC  $\sim$  8 mM)<sup>14, 23</sup>

could prevent the aggregation of both the pure fibrils and the non-aggregated peptides over the whole pH range at protein concentrations of 0.005 wt % (Figure 8). All these samples were transparent over the whole pH range. With respect to food grade applications, alternative molecules should be tested that can coat and solubilize the fibrils and thereby prevent aggregation of the fibrils.

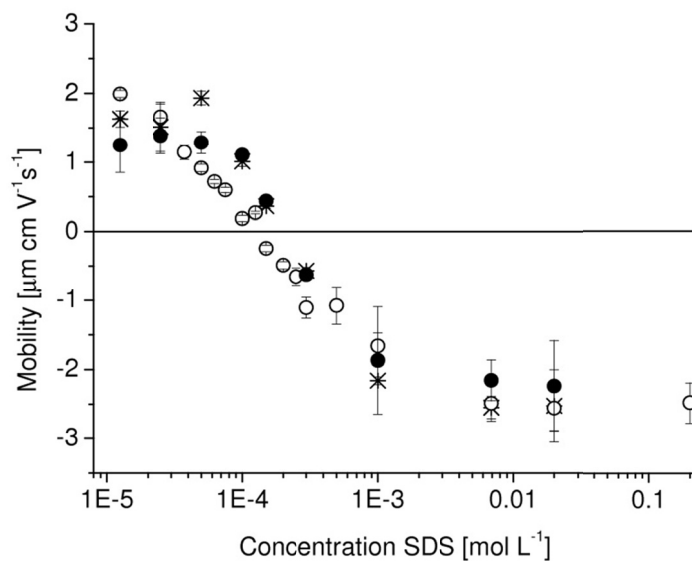


Figure 7. Electrophoretic mobility of solution A (×), solution B (●) and solution C (○) as a function of SDS concentration at pH 3. Protein concentrations were 0.005 wt %.

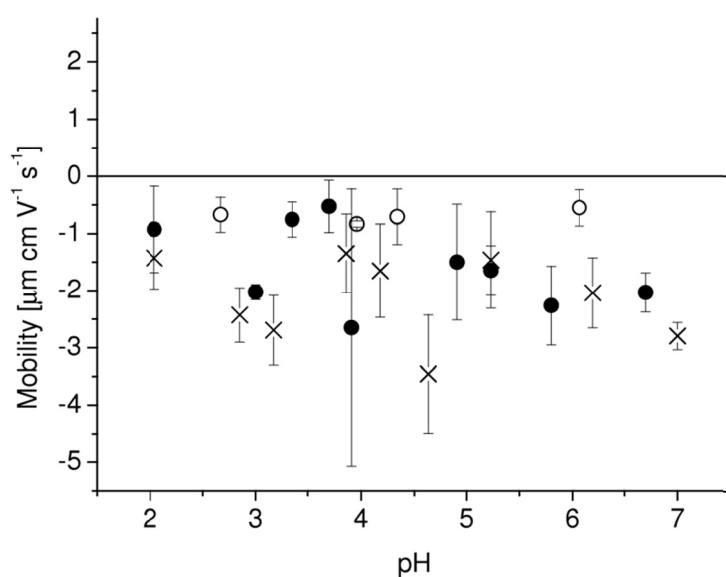


Figure 8. Electrophoretic mobility of solution A (×), solution B (●) and solution C (○) as a function of pH, all containing 7 mM SDS. Protein concentrations were 0.005 wt %.

## Conclusions

The turbidity of a fibril solution at pH 5 is mainly caused by the aggregation of the non-aggregated peptides and can be prevented by removing the non-aggregated peptides from the fibril solution using centrifugal filters. The fibrils in the pure fibril solution still have the tendency to aggregate around pH 5, however these aggregates only scatter the light to a small extent. SDS is capable in solubilizing both the pure fibrils and the non-aggregated peptides.

## References

1. Aymard, P.; Nicolai, T.; Durand, D., Static and Dynamic Scattering of *beta*-Lactoglobulin Aggregates Formed after Heat-Induced Denaturation at pH 2. *Macromolecules* **1999**, 32, 2542-2552.

2. Kavanagh, G. M.; Clark, A. H.; Ross-Murphy, S. B., Heat-induced gelation of globular proteins: part 3. Molecular studies on low pH beta-lactoglobulin gels. *International Journal of Biological Macromolecules* **2000**, *28*, 41-50.
3. Bromley, E. H. C.; Krebs, M. R. H.; Donald, A. M., Aggregation across the length-scales in beta-lactoglobulin. *Faraday Discussions* **2005**, *128*, 13-27.
4. Clark, A. H.; Kavanagh, G. M.; Ross-Murphy, S. B., Globular protein gelation - theory and experiment. *Food Hydrocolloids* **2001**, *15*, 383-400.
5. Gosal, W. S.; Clark, A. H.; Pudney, P. D. A.; Ross-Murphy, S. B., Novel amyloid fibrillar networks derived from a globular protein: B-lactoglobulin. *Langmuir* **2002**, *18*, 7174-7181.
6. Gosal, W. S.; Ross-Murphy, S. B., Globular protein gelation. *Current opinion in colloid & interface science* **2000**, *5*, 188-194.
7. Langton, M.; Hermansson, A.-M., Fine-stranded and particulate gels of  $\beta$ -lactoglobulin and whey protein at varying pH. *Food Hydrocolloids* **1992**, *5*, 523-539.
8. Renard, D.; Lefebvre, J., Gelation of globular proteins: effect of pH and ionic strength on the critical concentration for gel formation. A simple model and its application to [beta]-lactoglobulin heat-induced gelation. *International Journal of Biological Macromolecules* **1992**, *14*, (5), 287-291.
9. Stading, M.; Hermansson, A.-M., Viscoelastic behaviour of [beta]-lactoglobulin gel structures. *Food Hydrocolloids* **1990**, *4*, (2), 121-135.
10. Veerman, C. C.; Ruis, H. H.; Sagis, L. M. L. M. C.; van der Linden, E. E., Effect of electrostatic interactions on the percolation concentration of fibrillar beta-lactoglobulin gels. *Biomacromolecules* **2002**, *3*, (4), 869.
11. Veerman, C. C.; Baptist, H. H.; Sagis, L. M. L. M. C.; van der Linden, E. E., A new multistep Ca<sup>2+</sup>-induced cold gelation process for beta-lactoglobulin. *Journal of agricultural and food chemistry* **2003**, *51*, (13), 3880-5.
12. Akkermans, C.; Van der Goot, A. J.; Venema, P.; Van der Linden, E.; Boom, R. M., Properties of protein fibrils in whey protein isolate solutions: Microstructure, flow behaviour and gelation. *International Dairy Journal* **2008**, *18*, (10-11), 1034-1042.

13. Bolder, S. G.; Hendrickx, H.; Sagis, L. M. C.; van der Linden, E., Ca<sup>2+</sup> -induced cold-set gelation of whey protein isolate fibrils. *Applied Rheology* **2006**, 16, (5), 258-264.
14. Jung, J.-M.; Savin, G.; Pouzot, M.; Schmitt, C.; Mezzenga, R., Structure of Heat-Induced Î<sup>2</sup>-Lactoglobulin Aggregates and their Complexes with Sodium-Dodecyl Sulfate. *Biomacromolecules* **2008**, 9, (9), 2477-2486.
15. Akkermans, C.; Venema, P.; van der Goot, A. J.; Gruppen, H.; Bakx, E. J.; Boom, R. M.; van der Linden, E., Peptides are Building Blocks of Heat-Induced Fibrillar Protein Aggregates of Î<sup>2</sup>-Lactoglobulin Formed at pH 2. *Biomacromolecules* **2008**, 9, (5), 1474-1479.
16. Bolder, S. G., Heat-induced whey protein isolate fibrils: Conversion, hydrolysis, and disulphide bond formation. *International dairy journal* **2007**, 17, (7), 846.
17. Bolder, S. G.; Sagis, L. M. C.; Venema, P.; van der Linden, E., Effect of Stirring and Seeding on Whey Protein Fibril Formation. *Journal of agricultural and food chemistry* **2007**, 55, (14), 5661-5669.
18. Akkermans, C.; Venema, P.; Rogers, S. S.; van der Goot, A. J.; Boom, R. M.; van der Linden, E., Shear Pulses Nucleate Fibril Aggregation. *Food Biophysics* **2006**, 1, (144-150).
19. Rogers, S. S.; Venema, P.; Sagis, L. M. C.; van der Linden, E.; Donald, A. M., Measuring length distribution of a fibril system: A flow birefringence technique applied to amyloid fibrils. *Macromolecules* **2005**, 38, 2948-2958.
20. Klein van, C. O.; Venema, P.; Sagis, L. M. C.; Dusschoten, D. v.; Wilhelm, M.; Spiess, H. W.; Linden, E. v. d.; Rogers, S. S.; Donald, A. M., Optimized Rheo-optical Measurements Using Fast Fourier Transform and Oversampling. *Applied rheology* **2007**, 17, (4), 45210-1 - 45210-7.
21. Jordens, S.; Adamcik, J.; Amar-Yuli, I.; Mezzenga, R., Disassembly and Reassembly of Amyloid Fibrils in Water–Ethanol Mixtures. *Biomacromolecules* **2010**, 12, (1), 187-193.

22. Verheul, M.; Pedersen, J. S.; Roefs, S. P. F. M.; de Kruif, K. G., Association behavior of native  $\beta$ -lactoglobulin. *Biopolymers* **1999**, 49, (1), 11-20.
23. Moroi, Y.; Motomura, K.; Matuura, R., The critical micelle concentration of sodium dodecyl sulfate-bivalent metal dodecyl sulfate mixtures in aqueous solutions. *Journal of Colloid and Interface Science* **1974**, 46, (1), 111-117.





## *Chapter 7*

### **General discussion**

## Introduction

Under the appropriate conditions, proteins can assemble into structures called fibrils. Assembly of proteins or peptides into fibrils is an important subject of study in various research fields. Not only in biomedical sciences where the so-called amyloid fibrils are studied intensively since they are being associated with neurodegenerative diseases,<sup>1-4</sup> but also in the field of material sciences fibrils are receiving increased attention.<sup>5-7</sup> They are used in the fabrication of for example metal nanowires, bionanotubes, nanometer thick coatings, three-dimensional peptide scaffolds, and vehicles for bioactives.<sup>5-7</sup> Various food proteins lead to assembly into fibrils, as was shown for egg proteins,<sup>8-12</sup> soy proteins<sup>13</sup> and milk proteins<sup>14-31</sup>. Therefore it is not surprising that the ability of proteins to form fibrils is suggested to be a generic form of protein aggregation.<sup>32, 33</sup>

The most studied milk proteins with respect to fibril formation are the whey proteins. Whereas the whey used to be a waste-product from the cheese production and casein manufacturing, nowadays whey proteins are becoming increasingly important proteins for the food industry. The whey proteins are receiving increased attention, because of their nutritional and functional properties.<sup>34</sup> In acidified milk drinks stabilizers like pectin are needed to prevent aggregation of the casein at the low pH 3.4-4.6.<sup>35-37</sup> Replacing the casein by whey proteins is a good alternative, since whey proteins are more stable against aggregation at these low pH values.

Fibrils are e.g. formed when whey protein isolate (WPI) in solution is heated to 80°C for several hours, at pH 2. WPI consists of about 60 % beta-lactoglobulin ( $\beta$ -lg), a globular protein that was found to be the only fibril forming protein in WPI at pH 2 and 80°C.<sup>38</sup> Other proteins that are present in WPI are alpha-lactalbumin ( $\alpha$ -lac), bovine serum albumin (BSA) and immunoglobulins. For  $\alpha$ -lac and BSA was found that they can also form fibrils, but in that case other conditions are required.<sup>30, 39</sup>

The fibrils derived from  $\beta$ -lg or WPI are long and thin (Figure 1). This high ratio of the length versus the diameter of the fibrils makes them promising candidates for

using them as structurants in foods. Akkermans et al. showed that upon addition of fibrils, the viscosity and gel strength of WPI solutions could be increased, making them suitable as thickening or gelling agent.<sup>40</sup> Besides, the fibrils can be used as stabilizer of foams where the fibrils are increasing the viscosity of the liquid phase, slowing down the drainage, forming a film around the air bubbles, thereby preventing collapse of the bubbles. In emulsions the fibrils can be used to increase the viscosity of the continuous phase. At a given concentration range, the fibrils act as a very effective depletion flocculant.<sup>41</sup> In emulsions the fibrils can also adsorb on the oil/water interface to form a coating around the oil droplets. This propensity of the fibrils to adsorb at the oil/water interface is also being used in the production of microcapsules, where capsules are produced by depositing layers of fibrils on oil droplets in oil-in-water emulsions, leading to specific capsule properties in terms of permeability and mechanical strength.<sup>42-45</sup>

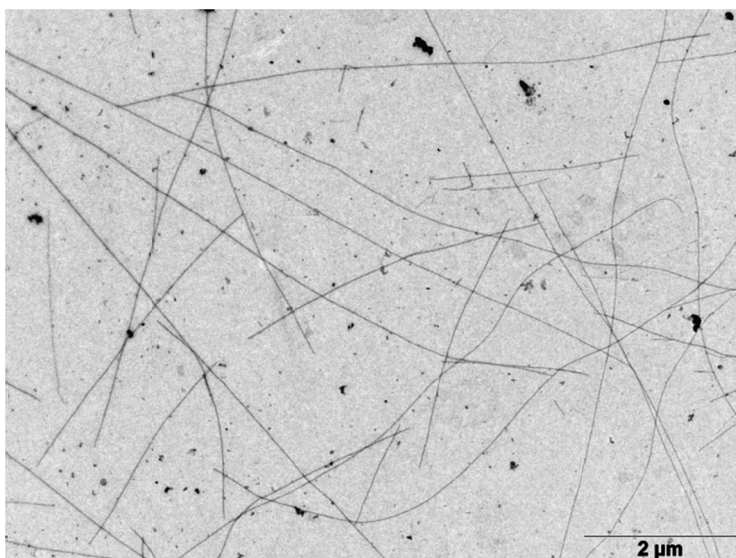


Figure 1. Fibrils produced by heating a  $\beta$ -lg solution to 80°C for several hours, at pH 2.

For the applications of  $\beta$ -lg fibrils in food products, it is important to have the ability to control the formation of the fibrils and to be able to influence the properties of the

fibrils. These properties will determine the functionality of the fibrils. The length distribution of the fibrils in combination with the thickness of the fibrils will for example influence the gel efficiency. The length distribution of the fibrils will also determine the rheological properties and the isotropic-nematic phase transition of the fibril solutions. Besides, when the fibrils are used in the production of microcapsules, the length distribution in combination with the flexibility of the fibrils is important for covering of microcapsules, thereby influencing the strength and permeability of the capsules. The charge of the fibrils as a function of pH is also an important factor in the layer-by-layer process to make microcapsules, where the different layers have opposite charges. Also for fibrils in solution, the charge of the fibrils as a function of pH is important, since it determines whether aggregation will take place.

It is clear from the above paragraph that the properties of the fibrils will determine their functionality. Therefore, more knowledge about the properties of the fibrils will not only give more fundamental knowledge about the fibril formation, but also helps to fine tune the functionality of the fibrils. Therefore this last chapter describes the impact of the previous chapters on the general view of the process of fibril formation from  $\beta$ -lg and the properties of the fibrils that are formed, leading to controlled applications of the fibrils. Although the focus of this general discussion will be mainly on the formation and properties of fibrils, at higher concentrations of fibrils also other structures exist like spherulites and nematic phases.

## Formation

The formation of the fibrils is accomplished by heating a  $\beta$ -lg solution for several hours at low pH. When the protein concentration is high enough, typically 5-8 wt %, <sup>22, 27, 46</sup> fine stranded gels are formed. Early research focused on these fine stranded gels that are transparent, in contrast to the particulate gels, which are opaque and are formed when  $\beta$ -lg is heated at pH 4-6.<sup>23, 27, 46</sup> The transparency of the gels formed at low pH and low ionic strength was originally explained by a strong electrostatic

repulsion that is originating from the charged proteins far from the iso-electric point.<sup>16, 27, 47</sup> Here it was conjectured that at low pH electrostatic repulsive forces hinder the formation of random aggregates and as a consequence more ordered linear polymers were formed.<sup>48</sup> These fibrillar aggregates are too thin to scatter the light, resulting in transparent solutions or gels. The gelation behaviour of  $\beta$ -lg at low pH and high temperatures was investigated<sup>20, 22, 23, 27, 46, 47</sup> as well as the properties of the gels that are formed under these conditions.<sup>19, 20, 31, 46</sup> Next to the heat set gels that were formed at protein concentrations of about 5 wt % and higher, solutions of fibrils with a lower protein concentrations were also used to form cold-set gels. This was done by increasing the pH from pH 2 to 7 and adding calcium chloride. In this way weak gels with extremely low volume fractions down to 0.07 wt % could be made.<sup>49-51</sup>

To have a better understanding of the relation between the molecular and macroscopic characteristics of the  $\beta$ -lg gels, it was important not only to study the gels that were composed of fibrils, but also to study the fibril formation process itself. To produce fibrils from  $\beta$ -lg, protein solutions must be heated for several hours at low pH and temperatures around 80°C. In this way micrometers long linear aggregates are formed with a rigid rod-like local structure depending on the ionic strength.<sup>16, 22, 29</sup> Adamcik<sup>52</sup> showed that the fibrils consist of multiple protein filaments that associate laterally to form twisted ribbons with a helical structure. During the fibril formation at low pH intermolecular  $\beta$ -sheets are formed.<sup>16, 22, 26</sup>

Under certain conditions so-called spherulites were observed, depending on the  $\beta$ -lg or WPI concentration, ionic strength and the use of flow.<sup>38, 53-55</sup> These spherulites were 20 to 100  $\mu\text{m}$  in size, therefore visible by the naked eye. A Maltese cross extinction pattern was observed when the spherulites were analyzed under the microscope using crossed polarizers.<sup>38</sup> Similarly, spherulite formation was also studied extensively in bovine insulin solutions. These spherulites are different from spherulites of  $\beta$ -lg in the sense that they have a large amorphous core of irregularly oriented protein.<sup>55</sup> It was also shown that the observed Maltese cross pattern is

originating from the radially arrangement of fibrils with a central core, where the arrangement of the fibrils is fairly compact.<sup>54-58</sup> The formation of spherulites could be prevented by applying flow during the formation of the fibrils.<sup>53</sup>

The fibril formation process of  $\beta$ -lg is generally described by a nucleation growth mechanism.<sup>14, 16, 54, 59, 60</sup> In such a mechanism first nuclei are being formed, which is usually the rate limiting step of fibril formation. The nucleation phase is followed by the growth phase in which fibrils start to grow from the nuclei. Bolder et al. proposed a model where also an activation step was added prior to the nucleation phase and a termination step after the growth phase.<sup>53</sup> In this four-step mechanism the role of the hydrolysis of  $\beta$ -lg when the protein is heated at low pH and high temperatures was also taken into account. In the proposed activation step, native  $\beta$ -lg monomers are activated by heat-denaturation at low pH and these active monomers are able to form the nuclei in the nucleation step. After the growth phase a termination step was suggested in which monomers would be inactivated due to prolonged heating at pH 2, thereby terminating the fibril formation. The tips of the fibrils could also be inactivated due to hydrolysis of the fibril tips after prolonged heating.<sup>53</sup> This termination step gave a possible explanation for the conversion levels that were found to be substantial lower than 100% for the fibril formation of  $\beta$ -lg or WPI at pH 2.<sup>31, 53</sup> However, recently it was found that the hydrolysis plays a more prominent role in the fibril formation. Akkermans et al. showed that the fibrils are composed of peptides that result from the cleavage of the bonds before or after aspartic acid residues in  $\beta$ -lg.<sup>61</sup> The cleavage of these specific peptide bonds is caused by acidic hydrolysis at pH 2 and 80°C, but can also be induced by enzymatic hydrolysis using the enzyme AspN.<sup>62</sup> This enzyme is cleaving the same bonds that are cleaved during the acidic hydrolysis of  $\beta$ -lg at pH 2 and 80 °C. In both hydrolysis processes peptides are produced that can act as building blocks for the fibrils.<sup>61, 62</sup> This important role of hydrolysis was also previously shown for hen egg white lysozyme.<sup>63, 64</sup> Fibrils formed from HEWL also consist of peptides that are produced by hydrolysis of the

HEWL monomer. Besides, it was shown that addition of the intact full monomer was slowing down the fibril formation,<sup>64</sup> suggesting that only peptides produced by the hydrolysis of the full HEWL can be efficiently incorporated into the fibril. Recently, Lara et al. also confirmed that the hydrolysis of both the globular proteins  $\beta$ -lg and HEWL plays a central role in their fibril formation.<sup>65</sup> The fact that the fibrils are composed of small peptides gives important information about the structure of the fibrils, but also has implications for the fibril formation process. From the above it becomes clear that the fibril formation process is still not fully understood, and that the new insights need to be incorporated in the overall picture of formation of fibrils from  $\beta$ -lg. Therefore the first part of this thesis focuses on the fibril formation process.

Several researchers have looked at the effect of the concentration of  $\beta$ -lg on the fibril formation at pH 2, however, none of them has actually determined a critical aggregation concentration (CAC) at a certain temperature at low pH.<sup>14, 38, 66</sup> The CAC is defined as the  $\beta$ -lg concentration below which no fibrils are formed. The CAC for the fibril formation is an important parameter, since it gives information about the binding energy that is involved in the fibril formation. The temperature dependence of the CAC gives information about the driving mechanism behind the fibril formation. The CAC for the fibril formation of  $\beta$ -lg at pH 2 was determined in Chapter 2. From the CAC measurements the binding energy was determined to be  $\sim 13$  kT. This binding energy represents the change in Gibbs free energy of the overall system when a fibril is extended by one building block. After this initial binding intermolecular  $\beta$ -sheets are formed<sup>22, 26</sup> making the binding irreversible. Covalent disulphide bonds are not expected to be formed under these acidic conditions at pH 2, and therefore only hydrogen bonds are formed upon fibril formation at this pH. By measuring the CAC as a function of temperature one can determine the change of entropy and enthalpy upon binding. It was found that upon binding there was an increase in entropy and no change in enthalpy. As a result one can conclude that the

fibril formation of  $\beta$ -lg at pH 2 is driven by an increase in entropy. This is in agreement with the claim that hydrophobic interactions are the driving force for the fibril formation at pH 2.<sup>67, 68</sup>

In view of the finding that the fibrils are being composed of small peptides, the kinetics of the fibril formation was revisited in this thesis. Several researchers have studied the kinetics of fibril formation of  $\beta$ -lg at pH 2 and fit these results to a model.<sup>14, 16, 54, 59, 60</sup> However, none of these physical models took the hydrolysis of  $\beta$ -lg explicitly into account. Therefore in Chapter 3 both the hydrolysis of the  $\beta$ -lg and the fibril growth were analyzed. Next, to quantify the effect of the hydrolysis of the protein on the fibril growth kinetics a simple polymerization model was forwarded that took the hydrolysis explicitly into account. In Figure 2 a schematic representation is given of the 2 steps in this model. First, the  $\beta$ -lg monomers are hydrolyzed into small peptides by acidic hydrolysis at pH 2 and temperatures around 80°C with rate constant  $k_h$ . Second, specific peptides with a high hydrophobicity and capacity to form beta-sheets assemble into fibrils with rate constant  $k_2$ .

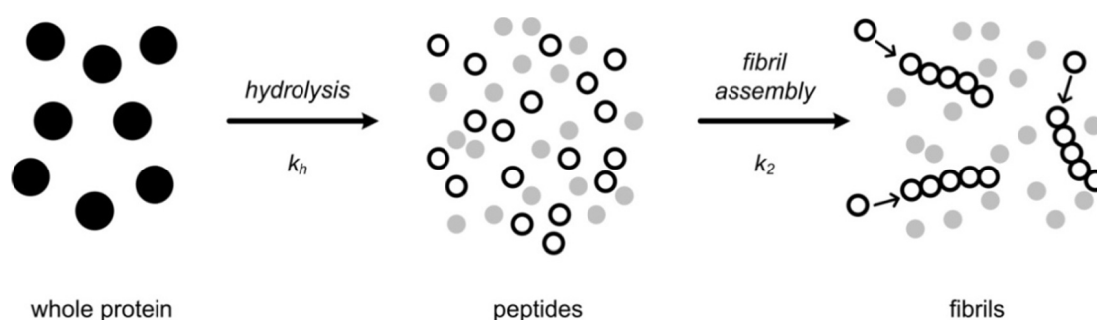


Figure 2. Schematic representation of the fibril formation of  $\beta$ -lg at pH 2: First, the  $\beta$ -lg is hydrolysed into peptides with rate constant  $k_h$ , and second, some of these peptides assembly into fibrils with rate constant  $k_2$ .

The results of the model show that at low protein concentrations, the incorporation of peptides into fibrils is the rate limiting step for the fibrillar growth, while at high concentrations the hydrolysis becomes rate limiting. One can use this information to speed up the process of fibril formation at high concentrations by increasing the temperature to increase the hydrolysis rate. However, it was also found that although the process of fibril formation might go faster at these higher temperatures, the final amount of fibrils formed is maximal around 80°C (Chapter 2). Apparently, when the temperature becomes too high, the protein may become completely hydrolysed before the peptides can be incorporated into the fibrils.

Although the mechanism of fibril formation of  $\beta$ -lg is generally described as a nucleation growth mechanism,<sup>14, 16, 54, 59, 60</sup> it was found that the fibril formation could be described with a simple polymerization model, including the hydrolysis, but without the necessity to include a nucleation step. Only at very low protein concentrations, the model starts to deviate from the measured fibril growth data. At these low concentrations nucleation effects might start to play a role.

## Properties and function

For a successful application of the fibrils in food products, it is important to have a proper understanding of the physical properties of the fibrils and to have the ability to influence these properties and thereby the functionality of the fibrils. The fibrils formed at low pH and low ionic strength have a diameter of only about 2-4 nanometers,<sup>14, 21</sup> whereas they are several micrometers long.<sup>17, 19, 31, 66</sup> This high aspect ratio, together with their semi-flexibility is mainly determining their behaviour as a function of concentration.

The fibril solutions can be divided into four different concentration regimes (Figure 3).<sup>69</sup> In the dilute regime, the fibrils can rotate freely without interacting with the other fibrils. However, since the fibrils are long, thin and rigid, their overlap concentration  $c^*$  is quite low, since the overlap concentration scales with length as

$c^* \sim 1/L^3$ . Therefore  $c^*$  is already reached at fibril concentrations of about  $1.4 \times 10^{-4}$  wt % fibrils. At these concentrations the semi-dilute regime starts where the rotation of the individual fibrils is not severely restricted yet, but the dynamical properties of the solutions are completely changed.<sup>69</sup> This is for example reflected in the zero shear viscosity which is predicted to scale with length as  $\eta \sim L^9$  in the semi-dilute regime.<sup>70</sup> When the fibril concentration is further increased, the so-called concentrated isotropic regime is reached.<sup>69</sup> In this regime the fibrils start to have a tendency to orient in the same direction as the neighboring fibrils, however the concentration is still too low to align and to form anisotropic solutions.<sup>69</sup> Upon further increasing of the fibril concentration, the nematic regime is reached where the number of polymers per volume is given by  $v \geq 1/bL^2$ , where  $b$  is the diameter of the fibrils.<sup>69</sup> In this regime the fibrils align more or less parallel but do not show positional ordering (Figure 4a). In general the fibrils are produced in this nematic regime. When the samples are observed between crossed polarizers this nematic phase is visible as bright domains of macroscopic scale in which the fibrils are aligned (Figure 4b). The transition from the isotropic to the nematic regime for fibrils solutions at pH 2 and low ionic strength, was determined to be at fibril concentrations  $c^{I-N}$  of  $\sim 0.4$  wt % fibrils.<sup>71</sup>

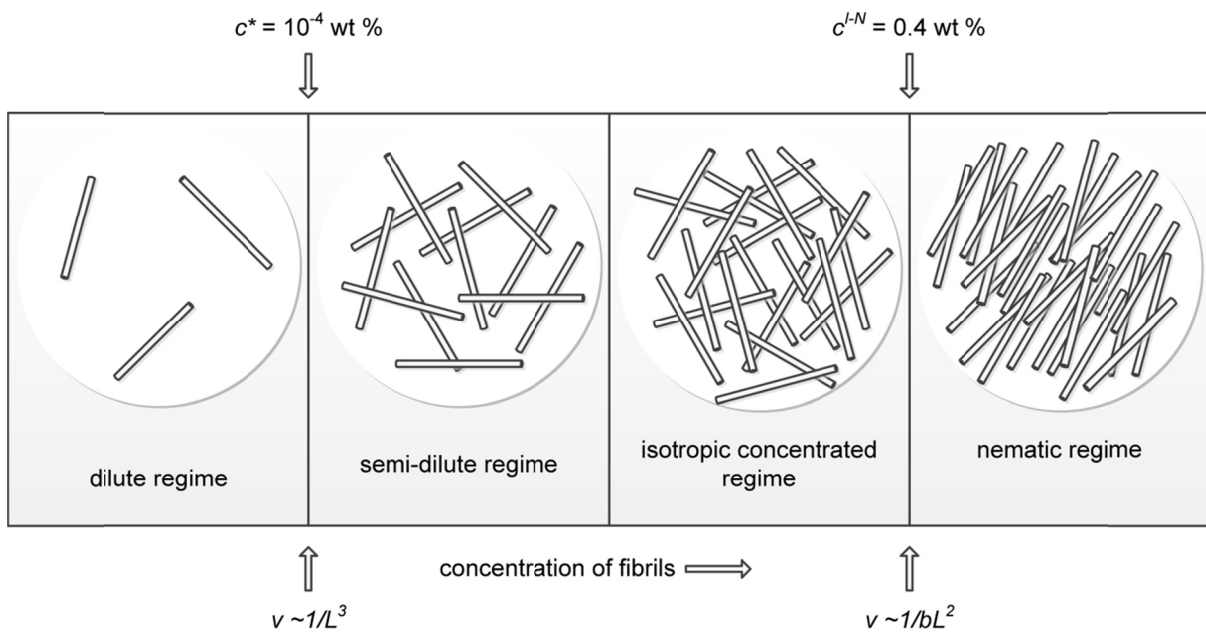


Figure 3. Different concentration regimes for fibril solutions derived from  $\beta$ -lg. After reference.<sup>69</sup>

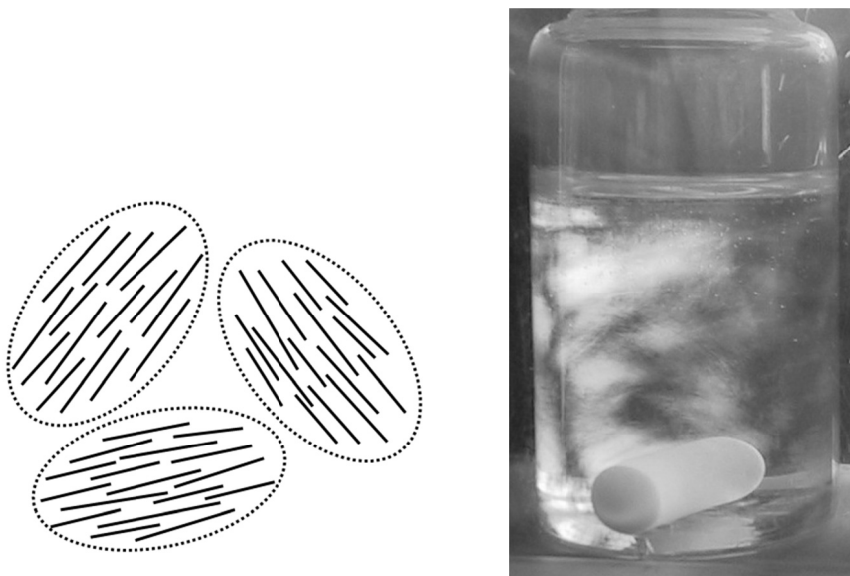


Figure 4. Fibril solution in the nematic regime: a) schematic representation of a nematic phase, b) picture of a 2 wt %  $\beta$ -lg solution that was heated at pH 2 and 80°C for about 20 hours, observed between cross-polarizers to show that the solution is birefringent.

The total length concentration of fibrils in a fibril solution is high. For instance, a 1 ml fibril solution at a concentration of 1 wt % contains  $10^5$  km fibril, approximately 10-fold the circumference of the earth. However, since the length distribution of the fibrils is polydisperse and the rheological properties strongly depend on the length distribution, it is important to also have information about the length distribution of the fibrils. Rogers et al. developed a technique that efficiently measures the length distribution of the fibrils.<sup>66</sup> For this analysis shear flow is used to align the fibrils and thereby inducing birefringence at fibril concentrations in the semi-dilute regime. From the decay of the flow-induced birefringence, after the cessation of the flow, the length distribution of the fibrils in the solution can be determined. Using this technique, the length distribution of a large amount of fibrils in a relatively short time can be analyzed. Whereas with conventional methods like TEM the length distribution of up to  $10^2$  fibrils per grid can be measured, with flow-induced birefringence typically  $10^{17}$  fibrils are simultaneously monitored, leading to much better statistics. The length distributions measured using flow-induced birefringence show that the fibrils obtained from  $\beta$ -lg typically have a length between 2 and 4  $\mu\text{m}$ .<sup>53, 66, 72</sup> Figure 5 shows a typical example of such a length distribution curve for  $\beta$ -lg fibrils.

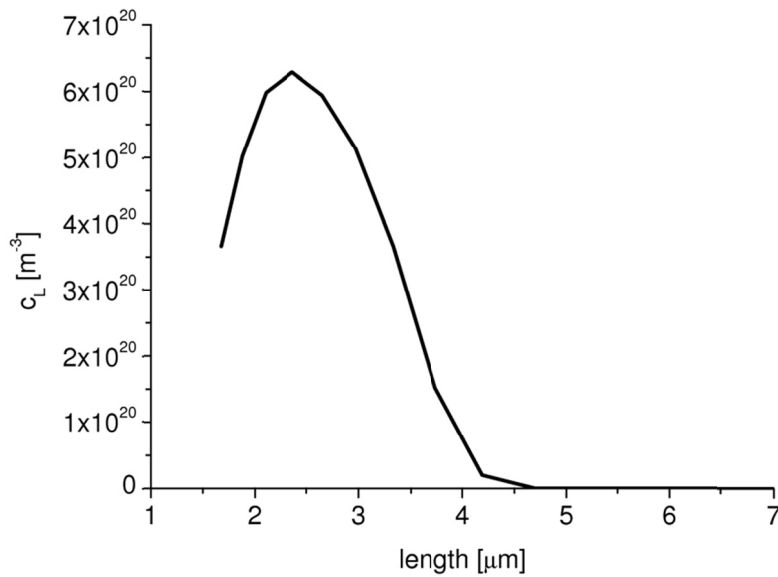


Figure 5. Length distribution of protein fibrils derived from 3 wt %  $\beta$ -lg heated for 22 hours at 80°C and pH 2, presented as the number of fibrils per  $\text{m}^3$  with a length between  $L$  and  $dL$ .

The length distribution of the fibrils is an important parameter influencing the properties of the final product. Not only does the length distribution of the fibrils has a large effect on the properties of a fibril solution, it is also important when the fibrils are used in the production of microcapsules where they should not be too long for an effective coverage of the spherical surface.<sup>12, 42-44</sup> The ability to tune the length distribution of the fibrils is therefore important, however it is hard to significantly influence the length distribution during the production of the fibrils. In contrast to the fibril formation of henn egg white lysozyme,<sup>12</sup> the final length distribution of the fibrils derived from  $\beta$ -lg is hardly influenced by the use of shear flow during fibril formation.<sup>72</sup> Therefore a different approach was taken in Chapter 5 by applying elongational flow on beta-lactoglobulin fibrils. A simple experimental set-up was built to create a flow with a high elongational component. Using this technique it was possible to tune the length distribution of the fibrils, and additional information about the strength of the fibrils was obtained. When the tensile stress on the fibrils that is created by the flow is exceeding the tensile strength of the fibrils, the fibrils are

expected to fracture exactly in the middle.<sup>73</sup> The tensile strength of the fibrils were found to be much lower than that of commonly used thickeners and stabilizers like gums as e.g. xanthan. These gums consist of covalently bound polysaccharides, whereas the fibrils are stabilized by  $\beta$ -sheets held together by hydrogen bonds. The relatively low tensile strength of the fibrils is an important aspect that needs to be taken into account when the fibrils are utilized in food processes, where large elongational flow rates are present, like in mixing, stirring, and homogenization.

Another approach to break down fibrils is inspired by the biomedical research area, where bioactive compounds are tested on their ability to disaggregate amyloid fibrils. Although it is still under discussion if the fibrils themselves are infectious or that they act like a sink for infectious peptides in neurodegenerative diseases,<sup>1</sup> several research groups are looking for compounds that are able to disaggregate amyloid fibrils. Flavonoids, like catechins, which are flavonoids abundantly present in e.g. green tea, are forwarded to be potential therapeutic agents against amyloid diseases.<sup>74-78</sup> Another compound that was reported to disaggregate amyloid fibrils involved in Alzheimer's disease is 4,5-dianilinophthalimide (DAPH).<sup>79</sup> The ability of DAPH to disaggregate fibrils derived from  $\beta$ -lg was investigated and it was found that DAPH could not disaggregate these fibrils (Chapter 4). The results from a Thioflavin T (ThT) assay did suggest that DAPH could disaggregate the fibrils. However, flow-induced birefringence, far-UV circular dichroism and transmission electron micrographs showed that DAPH did not disaggregate the fibrils derived from  $\beta$ -lg. It was concluded that DAPH interfered with the ThT assay in this study, giving misleading results.

Another interesting approach to break down the fibrils was shown by Rühls et al., using the so-called supramolecular bottle-brush approach.<sup>80</sup> In this approach, negatively charged polyethyleneglycol (PEG) chains are ionically attached to the positively charged fibrils to form a bottle-brush. In this bottle-brush conformation the

PEG chains stretch out due to excluded volume interaction, resulting in an entropy loss, causing breakage of the fibril.

Furthermore, from a food technology perspective the research of Bateman et al. is of importance in which they show that fibrils derived from  $\beta$ -lg could be digested by the enzyme pepsin in simulated gastric fluid.<sup>81</sup>

In principle fibrils could be used as food additives. Since the fibrils are produced at pH 2, and most food products have a pH between 4 and 7, knowledge about the stability of the fibril solutions to pH changes is necessary. At these pH values between 4 and 7 the fibrils are stable in the sense that the fibrils do not fall apart upon dilution or pH changes.<sup>40, 50, 51</sup> However, next to the stability against break down of the fibrils upon pH changes, the stability against clustering of the fibrils need to be investigated. Jung et al. and Akkermans et al. analyzed the behaviour of fibril solutions from  $\beta$ -lg and WPI at various pH.<sup>40, 82</sup> These results show that there is an important challenge for the application of fibrils made from  $\beta$ -lg at pH 2, since the solutions become turbid around pH 5.<sup>40, 82</sup> The results are suggesting that the fibrils form clusters around pH 5 which are causing the turbidity, but Akkermans also showed that fibril solutions actually contain a mixture of fibrils and non-aggregated peptides.<sup>61</sup> From this perspective that the fibrils are composed of small peptides, and that other non-aggregated peptides are present in the fibril solutions, the behaviour of the various fractions (fibril solution, pure fibril solution, non-aggregated peptide solution) as a function of pH was investigated (Chapter 6). The turbidity of the fibril solutions around pH 5 could be decreased by removing the non-aggregated fraction from the solutions, indicating that the non-aggregated fraction is mainly causing the turbidity. However, zeta-measurements showed that the net charge of fibrils is zero around pH 5 and TEM pictures showed that the fibrils are clustering around this pH. In these TEM pictures the fibril clusters look like open clusters, which explain the transparency of the pure fibril samples around pH 5. Removal of the non-aggregated fraction could therefore avoid the turbidity, but not the clustering around pH 5, and

it is this clustering that will influence the properties of the solutions. One way to prevent this clustering of the fibrils around the iso-electric point is to coat the fibrils using anionic molecules. This was shown by Jung et al. who used sodium dodecyl sulfate (SDS) to coat the fibrils, which charges the fibrils even at the pH where the fibrils themselves exhibit net zero charge.<sup>82</sup> In Chapter 6 it was shown that the SDS is coating both the pure fibrils and the non-aggregated material. With respect to food grade applications, alternative molecules should be tested that can coat the fibrils and thereby prevent clustering and eventual precipitation of the fibrils. Possibly, the non-aggregated peptides also have interesting properties, which widens the application window.

## Outlook

In this thesis the focus has been mainly on the formation and properties of whey protein fibrils, since it is essential to understand the formation and properties of the fibrils for successful application of the fibrils in food products. In future research the focus should be shifted more towards the application of the fibrils, as is already the case in for example the production of microcapsules. Also in Chapter 6 of this thesis some progress has been made towards fibrils in more complex systems. It is important to have knowledge about the behaviour of the fibrils in a system containing other particles, like for example in emulsions. Next to other proteins, also fat and carbohydrates might be present in food, and it is important to have knowledge about both the chemical and physical interaction of the fibrils with those compounds. From the perspective of sustainable food production one needs to consider plant proteins for texturizing. As a special case, to learn more about the assembly of such plant based compounds, one needs to consider fibril formation based on plant based proteins.

It was shown that fibrils can be produced from soy proteins and kidney bean proteins,<sup>13, 83, 84</sup> but this field is still fairly unexplored.

The work in this thesis forms an important basis for the route towards more application oriented research of fibrils derived from  $\beta$ -Ig and at the same time it forms a basis to explore the formation and properties of other fibrils derived from, for example, plant proteins.

## References

1. Lansbury, P. T.; Lashuel, H. A., A century-old debate on protein aggregation and neurodegeneration enters the clinic. *Nature* **2006**, 443, 774-779.
2. Sipe, J. D.; Cohen, A. S., Review: History of the amyloid fibril. *Journal of Structural Biology* **2000**, 130, 88-98.
3. Sunde, M.; Blake, C.; Frederic M. Richards, D. S. E.; Peter, S. K., The Structure of Amyloid Fibrils by Electron Microscopy and X-Ray Diffraction. In *Advances in Protein Chemistry*, Academic Press: 1997; Vol. Volume 50, pp 123-124, C11-C12, 125-159.
4. Uversky, V. N.; Fink, A. L., Conformational constraints for amyloid fibrillation: the importance of being unfolded. *Biochimica et Biophysica Acta (BBA) - Proteins & Proteomics* **2004**, 1698, (2), 131-153.
5. Gazit, E., Use of biomolecular templates for the fabrication of metal nanowires. *FEBS Journal* **2007**, 274, (2), 317-322.
6. Livney, Y. D., Milk proteins as vehicles for bioactives. *Current Opinion in Colloid & Interface Science* **2010**, 15, (1-2), 73-83.
7. Zhang, S., Fabrication of novel biomaterials through molecular self-assembly. **2003**, 21, (10), 1171-1178.
8. Arnaudov, L. N.; de Vries, R., Thermally Induced Fibrillar Aggregation of Hen Egg White Lysozyme. *Biophysical Journal* **2005**, 88, (1), 515-526.
9. Krebs, M. R. H.; Wilkins, D. K.; Chung, E. W.; Pitkeathly, M. C.; Chamberlain, A. K.; Zurdo, J.; Robinson, C. V.; Dobson, C. M., Formation and seeding of amyloid fibrils from wild-type hen lysozyme and a peptide fragment from the [beta]-domain. *Journal of Molecular Biology* **2000**, 300, (3), 541-549.

10. Veerman, C.; de Schiffart, G.; Sagis, L. M. C.; van der Linden, E., Irreversible self-assembly of ovalbumin into fibrils and the resulting network rheology. *International Journal of Biological Macromolecules* **2003**, *33*, 121-127.
11. Weijers, M.; Velde, v. d. F.; Stijnman, A.; Pijpekamp, A.; Visschers, R. W., Structure and rheological properties of acid-induced egg white protein gels. *Food Hydrocolloids* **2005**, 1-14.
12. Humblet-Hua, N.-P.; Sagis, L. M. C.; van der Linden, E., Effects of Flow on Hen Egg White Lysozyme (HEWL) Fibril Formation: Length Distribution, Flexibility, and Kinetics. *Journal of Agricultural and Food Chemistry* **2008**, *56*, (24), 11875-11882.
13. Akkermans, C.; Van der Goot, A. J.; Venema, P.; Gruppen, H.; Vereijken, J. M.; Van der Linden, E.; Boom, R. M., Micrometer-Sized Fibrillar Protein Aggregates from Soy Glycinin and Soy Protein Isolate. *Journal of agricultural and food chemistry* **2007**, *55*, (24), 9877-9882.
14. Arnoudov, L. N.; Vries, d. R.; Ippel, H.; Mierlo, v. C. P. M., Multiple steps during the formation of beta-lactoglobulin fibrils. *Biomacromolecules* **2003**, *4*, 1614-1622.
15. Aymard, P.; Durand, D.; Nicolai, T., The effect of temperature and ionic strength on the dimerisation of [beta]-lactoglobulin. *International Journal of Biological Macromolecules* **1996**, *19*, (3), 213-221.
16. Aymard, P.; Nicolai, T.; Durand, D., Static and Dynamic Scattering of beta-Lactoglobulin Aggregates Formed after Heat-Induced Denaturation at pH 2. *Macromolecules* **1999**, *32*, 2542-2552.
17. Durand, D.; Christophe Gimel, J.; Nicolai, T., Aggregation, gelation and phase separation of heat denatured globular proteins. *Physica A: Statistical Mechanics and its Applications* **2002**, *304*, (1-2), 253-265.
18. Gimel, J. C.; Durand, D.; Nicolai, T., Structure and distribution of aggregates formed after heat-induced denaturation of globular proteins. *Macromolecules* **1994**, *27*, (2), 583-589.

19. Gosal, W. S.; Clark, A. H.; Pudney, P. D. A.; Ross-Murphy, S. B., Novel amyloid fibrillar networks derived from a globular protein: B-lactoglobulin. *Langmuir* **2002**, *18*, 7174-7181.
20. Gosal, W. S.; Ross-Murphy, S. B., Globular protein gelation. *Current opinion in colloid & interface science* **2000**, *5*, 188-194.
21. Ikeda, S.; Morris, V. J., Fine-Stranded and Particulate Aggregates of Heat-Denatured Whey Proteins Visualized by Atomic Force Microscopy. *Biomacromolecules* **2002**, *3*, (2), 382-389.
22. Kavanagh, G. M.; Clark, A. H.; Ross-Murphy, S. B., Heat-induced gelation of globular proteins: part 3. Molecular studies on low pH beta-lactoglobulin gels. *International Journal of Biological Macromolecules* **2000**, *28*, 41-50.
23. Langton, M.; Hermansson, A.-M., Fine-stranded and particulate gels of  $\beta$ -lactoglobulin and whey protein at varying pH. *Food Hydrocolloids* **1992**, *5*, 523-539.
24. Le Bon, C.; Nicolai, T.; Durand, D., Kinetics of Aggregation and Gelation of Globular Proteins after Heat-Induced Denaturation. *Macromolecules* **1999**, *32*, 6120-6127.
25. Le Bon, C.; Nicolai, T.; Durand, D., Growth and structure of aggregates of heat-denatured beta-Lactoglobulin. *International Journal of Food Science and Technology* **1999**, *34*, 451-465.
26. Lefèvre, T.; Subirade, M., Molecular differences in the formation and structure of fine-stranded and particulate beta-lactoglobulin gels. *Biopolymers* **2000**, *54*, (7), 578-586.
27. Renard, D.; Lefebvre, J., Gelation of globular proteins: effect of pH and ionic strength on the critical concentration for gel formation. A simple model and its application to [beta]-lactoglobulin heat-induced gelation. *International Journal of Biological Macromolecules* **1992**, *14*, (5), 287-291.
28. Renard, D.; Lefebvre, J.; Griffin, M. C. A.; Griffin, W. G., Effects of pH and salt environment on the association of beta-lactoglobulin revealed by intrinsic fluorescence studies. *International Journal of Biological Macromolecules* **1998**, *22*, 41-49.

29. Schokker, E. P., Heat-induced aggregation of beta-lactoglobulin AB at pH 2.5 as influenced by ionic strength and protein concentration. *International dairy journal* **2000**, 10, (4), 233.
30. Veerman, C.; Sagis, L. M. C.; Heck, J.; van der Linden, E., Mesostructure of fibrillar bovine serum albumin gels. *International Journal of Biological Macromolecules* **2003**, 31, 139-146.
31. Veerman, C. C.; Ruis, H. H.; Sagis, L. M. L. M. C.; van der Linden, E. E., Effect of electrostatic interactions on the percolation concentration of fibrillar beta-lactoglobulin gels. *Biomacromolecules* **2002**, 3, (4), 869.
32. Chiti, F.; Dobson, C. M., Protein Misfolding, Functional Amyloid, and Human Disease. *Annual Review of Biochemistry* **2006**, 75, 333-366.
33. Dobson, C. M., Protein folding and misfolding. *Nature* **2003**, 426, (6968), 884.
34. Smithers, G. W., Whey and whey proteins--From '['gutter-to-gold'. *International Dairy Journal* **2008**, 18, (7), 695-704.
35. Laurent, M. A.; Boulenguer, P., Stabilization mechanism of acid dairy drinks (ADD) induced by pectin. *Food Hydrocolloids* **2003**, 17, (4), 445-454.
36. Nakamura, A.; Yoshida, R.; Maeda, H.; Corredig, M., The stabilizing behaviour of soybean soluble polysaccharide and pectin in acidified milk beverages. *International Dairy Journal* **2006**, 16, (4), 361-369.
37. Tromp, R. H.; de Kruif, C. G.; van Eijk, M.; Rolin, C., On the mechanism of stabilisation of acidified milk drinks by pectin. *Food Hydrocolloids* **2004**, 18, (4), 565-572.
38. Bolder, S. G. S. G.; Hendrickx, H. H.; Sagis, L. M. L. M. C.; van der Linden, E. E., Fibril assemblies in aqueous whey protein mixtures. *Journal of agricultural and food chemistry* **2006**, 54, (12), 4229-34.
39. Graveland-Bikker, J. F.; Ipsen, R.; Otte, J.; de Kruif, C. G., Influence of Calcium on the Self-Assembly of Partially Hydrolyzed  $\alpha$ -Lactalbumin. *Langmuir* **2004**, 20, (16), 6841-6846.

40. Akkermans, C.; Van der Goot, A. J.; Venema, P.; Van der Linden, E.; Boom, R. M., Properties of protein fibrils in whey protein isolate solutions: Microstructure, flow behaviour and gelation. *International Dairy Journal* **2008**, *18*, (10-11), 1034-1042.
41. Blijdenstein, T. B. J.; Veerman, C.; van der Linden, E., Depletion–Flocculation in Oil-in-Water Emulsions Using Fibrillar Protein Assemblies. *Langmuir* **2004**, *20*, (12), 4881-4884.
42. Humblet-Hua, N.-P.; Sagis, L. M. C.; Scheltens, G.; Yi, L.; van der Linden, E. In *Encapsulation systems based on proteins, polysaccharides, and protein-polysaccharide complexes*, 5th International Symposium on Food Rheology and Structure, Zurich, Switzerland, 2009; Fischer, P.; Pollard, M.; Windhab, E. J., Eds. Zurich, Switzerland, 2009; pp 180-183.
43. Sagis, L. M. C.; de Ruiter, R.; Miranda, F. J. R.; de Ruiter, J.; Schroen, K.; van Aelst, A. C.; Kieft, H.; Boom, R.; van der Linden, E., Polymer Microcapsules with a Fiber-Reinforced Nanocomposite Shell. *Langmuir* **2008**, *24*, (5), 1608-1612.
44. Rossier-Miranda, F. J.; Schroën, K.; Boom, R., Mechanical Characterization and pH Response of Fibril-Reinforced Microcapsules Prepared by Layer-by-Layer Adsorption. *Langmuir* **2010**, *26*, (24), 19106-19113.
45. Jung, J.-M.; Gunes, D. Z.; Mezzenga, R., Interfacial Activity and Interfacial Shear Rheology of Native  $\beta$ -Lactoglobulin Monomers and Their Heat-Induced Fibers. *Langmuir* **2010**, *26*, (19), 15366-15375.
46. Stading, M.; Hermansson, A.-M., Viscoelastic behaviour of [ $\beta$ ]-lactoglobulin gel structures. *Food Hydrocolloids* **1990**, *4*, (2), 121-135.
47. Clark, A. H.; Kavanagh, G. M.; Ross-Murphy, S. B., Globular protein gelation - theory and experiment. *Food Hydrocolloids* **2001**, *15*, 383-400.
48. Doi, E., Gels and gelling of globular proteins. *Trends in Food Science & Technology* **1993**, *4*, (1), 1-5.
49. Veerman, C., Gels at Extremely Low Weight Fractions Formed by Irreversible Self-Assembly of Proteins. *Macromolecular bioscience* **2003**, *3*, (5), 243.

50. Veerman, C. C.; Baptist, H. H.; Sagis, L. M. L. M. C.; van der Linden, E. E., A new multistep Ca<sup>2+</sup>-induced cold gelation process for beta-lactoglobulin. *Journal of agricultural and food chemistry* **2003**, 51, (13), 3880-5.
51. Bolder, S. G.; Hendrickx, H.; Sagis, L. M. C.; van der Linden, E., Ca<sup>2+</sup> -induced cold-set gelation of whey protein isolate fibrils. *Applied Rheology* **2006**, 16, (5), 258-264.
52. Adamcik, J.; Jung, J.-M.; Flakowski, J.; De Los Rios, P.; Dietler, G.; Mezzenga, R., Understanding amyloid aggregation by statistical analysis of atomic force microscopy images. *Nature Nanotechnology* **2010**, 5, (6), 423-428.
53. Bolder, S. G.; Sagis, L. M. C.; Venema, P.; van der Linden, E., Effect of Stirring and Seeding on Whey Protein Fibril Formation. *Journal of agricultural and food chemistry* **2007**, 55, (14), 5661-5669.
54. Bromley, E. H. C.; Krebs, M. R. H.; Donald, A. M., Aggregation across the length-scales in beta-lactoglobulin. *Faraday Discussions* **2005**, 128, 13-27.
55. Domike, K. R.; Donald, A. M., Thermal Dependence of Thermally Induced Protein Spherulite Formation and Growth: Kinetics of  $\beta$ -lactoglobulin and Insulin. *Biomacromolecules* **2007**, 8, (12), 3930-3937.
56. Krebs, M. R. H., The formation of spherulites by amyloid fibrils of bovine insulin. *Proceedings of the National Academy of Sciences of the United States of America* **2004**, 101, (40), 14420.
57. Krebs, M. R. H.; Bromley, E. H. C.; Rogers, S., Samson; Donald, A. M., The mechanism of amyloid spherulite formation by bovine insulin. *Biophysical Journal* **2005**, 88, 2013-2021.
58. Rogers, S. S.; Krebs, M. R. H.; Bromley, E. H. C.; van der Linden, E.; Donald, A. M., Optical Microscopy of Growing Insulin Amyloid Spherulites on Surfaces In Vitro. *Biophysical Journal* **2006**, 90, (3), 1043-1054.
59. Arnaudov, L. N.; Vries, R. d., Theoretical modeling of the kinetics of fibrillar aggregation of bovine beta-lactoglobulin at pH 2. *The Journal of Chemical Physics* **2007**, 126, (14), 145106.

- 
60. Loveday, S. M.; Wang, X. L.; Rao, M. A.; Anema, S. G.; Creamer, L. K.; Singh, H., Tuning the properties of [beta]-lactoglobulin nanofibrils with pH, NaCl and CaCl<sub>2</sub>. *International Dairy Journal* **2010**, *20*, (9), 571-579.
61. Akkermans, C.; Venema, P.; van der Goot, A. J.; Gruppen, H.; Bakx, E. J.; Boom, R. M.; van der Linden, E., Peptides are Building Blocks of Heat-Induced Fibrillar Protein Aggregates of  $\beta$ -Lactoglobulin Formed at pH 2. *Biomacromolecules* **2008**, *9*, (5), 1474-1479.
62. Akkermans, C.; Venema, P.; van der Goot, A.; Boom, R.; van der Linden, E., Enzyme-Induced Formation of  $\beta$ -Lactoglobulin Fibrils by AspN Endoproteinase. *Food Biophysics* **2008**, *3*, (4), 390-394.
63. Frare, E.; Polverino de Laureto, P.; Zurdo, J.; Dobson, C. M.; Fontana, A., A Highly Amyloidogenic Region of Hen Lysozyme. *Journal of Molecular Biology* **2004**, *340*, (5), 1153-1165.
64. Mishra, R.; Sorgjerd, K.; Nystrom, S.; Nordigarden, A.; Yu, Y.-C.; Hammarstrom, P., Lysozyme Amyloidogenesis Is Accelerated by Specific Nicking and Fragmentation but Decelerated by Intact Protein Binding and Conversion. *Journal of Molecular Biology* **2007**, *366*, 1029-1044.
65. Lara, C. c.; Adamcik, J.; Jordens, S.; Mezzenga, R., General Self-Assembly Mechanism Converting Hydrolyzed Globular Proteins Into Giant Multistranded Amyloid Ribbons. *Biomacromolecules* **2011**, *12*, (5), 1868-1875.
66. Rogers, S. S.; Venema, P.; Sagis, L. M. C.; van der Linden, E.; Donald, A. M., Measuring length distribution of a fibril system: A flow birefringence technique applied to amyloid fibrils. *Macromolecules* **2005**, *38*, 2948-2958.
67. Nicolai, T.; Britten, M.; Schmitt, C., [beta]-Lactoglobulin and WPI aggregates: Formation, structure and applications. *Food Hydrocolloids* **2011**, *25*, (8), 1945-1962.
68. Meersman, F.; Dobson, C. M., Probing the pressure-temperature stability of amyloid fibrils provides new insights into their molecular properties. *Biochimica et Biophysica Acta (BBA) - Proteins & Proteomics* **2006**, *1764*, (3), 452-460.

69. Doi, M.; Edwards, S. F., Semidilute solutions of rigid rodlike polymers. In *The theory of polymer dynamics*, Adair, R. K.; Elliott, R. J.; Ehrenreich, H.; Llewellyn Smith, C. H.; Marshall, W.; Rees, M., Eds. Oxford University Press: New York, 1986; pp 324-349.
70. Doi, M.; Edwards, S. F., Dynamics of Rod-like Macromolecules in Concentrated Solution. Part 2. **1978**, 918-932.
71. Mezzenga, R.; Jung, J.-M.; Adamcik, J., Effects of Charge Double Layer and Colloidal Aggregation on the Isotropic–Nematic Transition of Protein Fibers in Water. *Langmuir* **2010**, 26, (13), 10401-10405.
72. Akkermans, C.; van der Goot, A. J.; Venema, P.; van der Linden, E.; Boom, R. M., Formation of fibrillar whey protein aggregates: Influence of heat and shear treatment, and resulting rheology. *Food Hydrocolloids* **2008**, 22, (7), 1315-1325.
73. Odell, J. A.; Keller, A., Flow-induced chain fracture of isolated linear macromolecules in solution. *Journal of Polymer Science: Part B: Polymer Physics* **1986**, 24, 1889-1916.
74. He, J.; Xing, Y.-F.; Huang, B.; Zhang, Y.-Z.; Zeng, C.-M., Tea Catechins Induce the Conversion of Preformed Lysozyme Amyloid Fibrils to Amorphous Aggregates. *Journal of Agricultural and Food Chemistry* **2009**, 57, (23), 11391-11396.
75. Ehrnhoefer, D. E.; Bieschke, J.; Boeddrich, A.; Herbst, M.; Masino, L.; Lurz, R.; Engemann, S.; Pastore, A.; Wanker, E. E., EGCG redirects amyloidogenic polypeptides into unstructured, off-pathway oligomers. **2008**, 15, (6), 558-566.
76. Lin, C.-L.; Chen, T.-F.; Chiu, M.-J.; Way, T.-D.; Lin, J.-K., Epigallocatechin gallate (EGCG) suppresses [beta]-amyloid-induced neurotoxicity through inhibiting c-Abl/FE65 nuclear translocation and GSK3[beta] activation. *Neurobiology of Aging* **2009**, 30, (1), 81-92.
77. Lee, Y. K.; Yuk, D. Y.; Lee, J. W.; Lee, S. Y.; Ha, T. Y.; Oh, K. W.; Yun, Y. P.; Hong, J. T., (-)-Epigallocatechin-3-gallate prevents lipopolysaccharide-induced elevation of beta-amyloid generation and memory deficiency. *Brain Research* **2009**, 1250, 164-174.

78. Rezai-Zadeh, K.; Arendash, G. W.; Hou, H.; Fernandez, F.; Jensen, M.; Runfeldt, M.; Shytle, R. D.; Tan, J., Green tea epigallocatechin-3-gallate (EGCG) reduces [beta]-amyloid mediated cognitive impairment and modulates tau pathology in Alzheimer transgenic mice. *Brain Research* **2008**, 1214, 177-187.
79. Blanchard, B. J.; Chen, A.; Rozeboom, L. M.; Stafford, K. A.; Weigele, P.; Ingram, V. M., Efficient reversal of Alzheimers's disease fibril formation and elimination of neurotoxicity by a small molecule. *PNAS* **2004**, 101, 14326-14332.
80. Ruhs, P. A.; Adamcik, J.; Bolisetty, S.; Sanchez-Ferrer, A.; Mezzenga, R., A supramolecular bottle-brush approach to disassemble amyloid fibrils. *Soft Matter* **2011**, 7, (7), 3571-3579.
81. Bateman, L.; Ye, A.; Singh, H., In Vitro Digestion of  $\beta$ -Lactoglobulin Fibrils Formed by Heat Treatment at Low pH. *Journal of Agricultural and Food Chemistry* **2010**, 58, (17), 9800-9808.
82. Jung, J.-M.; Savin, G.; Pouzot, M.; Schmitt, C.; Mezzenga, R., Structure of Heat-Induced  $\beta$ -Lactoglobulin Aggregates and their Complexes with Sodium-Dodecyl Sulfate. *Biomacromolecules* **2008**, 9, (9), 2477-2486.
83. Tang, C.-H.; Wang, C.-S., Formation and Characterization of Amyloid-like Fibrils from Soy  $\beta$ -Conglycinin and Glycinin. *Journal of Agricultural and Food Chemistry* **2010**, 58, (20), 11058-11066.
84. Tang, C.-H.; Zhang, Y.-H.; Wen, Q.-B.; Huang, Q., Formation of Amyloid Fibrils from Kidney Bean 7S Globulin (Phaseolin) at pH 2.0. *Journal of Agricultural and Food Chemistry* **2010**, 58, (13), 8061-8068.



# Summary

## Summary

Fibrils can be formed from various food proteins. Fibrils are linear aggregates that have a length in the order of several micrometers whereas they are only a few nanometers thick. In this thesis fibrils were produced from whey protein isolate (WPI) and  $\beta$ -lactoglobulin ( $\beta$ -lg) by heating the protein solution at low pH and low ionic strength for several hours. The dimensions of the fibrils make them interesting as food ingredient, as for example thickening agent or encapsulation material. However, for a successful application of the fibrils it is important to know how the fibrils are formed and to know how to influence the properties of the fibrils. Therefore the aim of this thesis was to unravel the fibril formation process of  $\beta$ -lactoglobulin at pH 2, to analyze some of the properties of the fibrils and to investigate the possibilities to influence these properties.

In the first part of this thesis the process of fibril formation of  $\beta$ -lg at pH 2 is analyzed in terms of thermodynamics (Chapter 2) and kinetics (Chapter 3). In Chapter 2 the critical aggregation concentration (CAC) is determined for the fibrils formation of  $\beta$ -lg at pH 2 and 343, 353, 358, 363, 383K. This was done by extrapolating the relation between the protein concentration and the conversion to zero conversion. The accuracy of the CAC was increased by measuring the conversion into fibrils at different stirring speeds. From the CAC a binding energy could be determined, which was found to be independent of temperature. This temperature independency of the binding energy indicates that the fibril formation of  $\beta$ -lg at pH 2 and the used temperature range is an entropy-driven process.

Whereas Chapter 2 is related to the thermodynamic aspects of the self-assembly of the peptides into fibrils, in Chapter 3 the focus is on the kinetics of the fibril formation process. In Chapter 3 the influence of the hydrolysis of  $\beta$ -lg on the kinetics of the fibril formation is investigated. Both the hydrolysis of the  $\beta$ -lg and the growth of the fibrils were followed as a function of time and temperature. To quantify the

effect of the hydrolysis on the fibrillar growth a simple polymerization model including a hydrolysis step is forwarded. The results show that at low protein concentrations the incorporation of peptides into the fibrils is rate limiting, while at higher concentrations the hydrolysis becomes rate limiting. This crossover shifts towards higher concentrations with increasing temperature.

In the second part of this thesis, the properties of the fibrils are investigated (Chapter 4 to 6). In Chapter 4 the possible disaggregation of the fibrils by 4,5-dianilinophthalimide (DAPH) is investigated, a bioactive compound that was found to disaggregate protein fibrils involved in neurodegenerative diseases. Although the results from a commonly used Thioflavin T (ThT) assay were suggesting that DAPH could disaggregate the fibrils, the results from flow-induced birefringence measurements, rheological measurements and transmission electron microscopy (TEM) showed that DAPH was not able to disaggregate the fibrils. Chapter 4 shows that the use of a ThT assay in order to probe the possible disaggregating effect of certain compounds can give misleading results.

Since the length distribution of the fibrils is influencing the properties of the final product to a large extent, it is important to be able to influence the length of the fibrils. In Chapter 5 it is shown that in contrast to fibrils under shear flow, fibrils obtained from WPI did fracture when they were exposed to elongational flow. Using a simple experimental setup, the fibrils could be exposed to a range of elongational strain rates. The length distributions of the fibrils were determined using TEM and the fibrils were found to fracture at relatively low strain rates. From the applied strain rates and the length distribution of the fibrils exposed to these strain rates the tensile strength of the fibrils was estimated. The tensile strength of the fibrils was found to be much lower than that of commonly used thickeners and stabilizers like gums as e.g. xanthan.

The stability of the fibrils upon pH changes is important in view of their use in food products. Therefore, in Chapter 6 the stability of the fibril solutions upon pH changes

is investigated, thereby focusing on the aggregation of the different fractions that are present in the solutions around pH 5. To investigate their behaviour as a function of pH, the fibrils and the non-aggregated peptides were first separated. The results showed that the turbidity around pH 5 can be prevented by removing the non-aggregated peptides from the fibril solution, but the fibrils still have the tendency to aggregate around this pH. The aggregation of both the fibrils and the non-aggregated peptides can be prevented by coating them with anionic molecules like sodium dodecyl sulfate.

Finally, Chapter 7 provides a general discussion on how the results of the previous chapters contribute to the field of fibril formation and their properties.

# Samenvatting

## Samenvatting

Fibrillen kunnen worden gevormd van verschillende soorten voedsleiwitten. Fibrillen zijn lineaire aggregaten met een lengte van een aantal micrometers, terwijl ze maar een aantal nanometers dik zijn. In dit proefschrift werden fibrillen gemaakt van wei eiwit isolaat (WPI) en  $\beta$ -lactoglobuline ( $\beta$ -lg) door de eiwitoplossingen verscheidene uren te verhitten bij lage pH en lage ionsterkte. De dimensies van de fibrillen maken de fibrillen interessant als voedsel ingrediënt, als bijvoorbeeld verdikkingsmiddel of materiaal voor incapsulering. Echter, voor een succesvolle toepassing van de fibrillen is het belangrijk om te weten hoe de fibrillen worden gevormd en hoe de eigenschappen van de fibrillen beïnvloed kunnen worden. Daarom was het doel van dit proefschrift om het fibrilvormingsproces van  $\beta$ -lactoglobuline bij pH 2 te ontravellen, een aantal eigenschappen van de fibrillen te analyseren en de mogelijkheden om die eigenschappen te beïnvloeden te onderzoeken.

In het eerste gedeelte van dit proefschrift werd het fibrilvormingsproces van  $\beta$ -lg bij pH 2 geanalyseerd in termen van thermodynamica (Hoofdstuk 2) en kinetica (Hoofdstuk 3). In Hoofdstuk 2 werd de kritische aggregatie concentratie (CAC) voor de fibrilvorming van  $\beta$ -lg bij pH 2 en 343, 353, 358, 363 en 383K bepaald. Dit werd gedaan door de relatie tussen de eiwitconcentratie en de conversie te extrapoleren naar nul conversie. De nauwkeurigheid van de CAC werd verhoogd door de conversie naar fibrillen te meten bij verschillende roersnelheden. Met behulp van de CAC kon een bindingsenergie bepaald worden, die onafhankelijk van de temperatuur bleek te zijn. Deze temperatuursonafhankelijkheid van de bindingsenergie geeft aan dat de fibrilvorming van  $\beta$ -lg bij pH 2 in de temperatuurs range die hier gebruikt is een entropie gedreven proces is.

Daar waar Hoofdstuk 2 gerelateerd is aan de thermodynamische aspecten van het zelf-assembleren van peptiden in fibrillen, ligt de focus in Hoofdstuk 3 op de kinetica

van het fibrilvormings proces. In Hoofdstuk 3 is de invloed van de hydrolyse van  $\beta$ -lg op de kinetica van de fibrilvorming onderzocht. De hydrolyse van de  $\beta$ -lg en de groei van de fibrillen zijn beide gevolgd als functie van tijd en temperatuur. Om het effect van de hydrolyse op de fibrilvorming te quantificeren is een simpel polymerisatiemodel gepresenteerd dat een hydrolyse stap bevat. De resultaten laten zien dat bij lage eiwitconcentratie het inbouwen van peptiden in de fibrillen snelheidsbepalend is, terwijl bij hogere concentraties de hydrolyse snelheidsbepalend wordt. Deze cross-over verschuift naar hogere concentraties bij hogere temperatuur.

In het tweede deel van dit proefschrift werden de eigenschappen van de fibrillen onderzocht (Hoofdstuk 4 tot 6). In Hoofdstuk 4 werd de mogelijke afbraak van fibrillen door 4,5-dianilinophthalimide (DAPH) onderzocht, een bioactieve stof waarvan is aangetoond dat het eiwitfibrillen afbreekt die betrokken zijn bij neurodegeneratieve ziekten. Ondanks dat de resultaten van een veel gebruikte Thioflavin T (ThT) assay suggereerden dat DAPH de fibrillen kon afbreken, lieten de resultaten van stromings-geïnduceerde birefringence metingen, rheologische metingen en transmissie elektronen microscopie (TEM) zien dat DAPH niet in staat was de fibrillen af te breken. Hoofdstuk 4 laat zien dat het gebruik van een ThT assay om de mogelijke afbraak-effecten van sommige stoffen te onderzoeken misleidende resultaten kan geven.

De lengteverdeling van de fibrillen beïnvloedt de eigenschappen van het eindproduct in grote mate, daarom is het belangrijk om de lengte van de fibrillen te kunnen beïnvloeden. In Hoofdstuk 5 werd laten zien dat in tegenstelling tot fibrillen onder afschuifstroming, fibrillen (verkregen uit WPI) breken wanneer ze worden blootgesteld aan elongatiestroming. Gebruikmakend van een simpele experimentele opstelling, konden de fibrillen worden blootgesteld aan een serie sterktes van de elongatiestroming. De lengteverdelingen van de fibrillen werd bepaald met behulp van TEM en de fibrillen bleken te breken bij relatief lage vervormingssnelheden. Met

behulp van de toegepaste vervormingssnelheden en de lengteverdeling van de fibrillen die zijn blootgesteld aan deze vervormingssnelheden werd de treksterkte ingeschat. De treksterkte van de fibrillen bleek veel lager dan die van veel gebruikte verdikkingsmiddelen en stabilisatoren zoals gummen, bijvoorbeeld xanthaan.

De stabiliteit van de fibrillen ten opzichte van pH veranderingen is belangrijk met het oog op het gebruik van fibrillen in levensmiddelen. Daarom is in Hoofdstuk 6 de stabiliteit van fibriloplossingen ten opzichte van pH veranderingen onderzocht, waarbij de focus lag op de aggregatie van de verschillende fracties die aanwezig zijn in de oplossingen rond pH 5. Om het gedrag als functie van pH te onderzoeken werden de fibrillen en niet-geaggregeerde peptiden eerst gescheiden. De resultaten laten zien dat de turbiditeit rond pH 5 voorkomen kan worden door de niet-geaggregeerde peptiden te verwijderen uit de fibriloplossing, maar dat de fibrillen nog steeds de neiging hebben te aggregeren rond deze pH. De aggregatie van zowel de fibrillen als de niet-geaggregeerde peptiden kan worden voorkomen door ze te coaten met anionische moleculen zoals sodiumdodecylsulfaat.

Tot slot geeft Hoofdstuk 7 een algemene discussie over hoe de resultaten uit de vorige hoofdstukken bijdragen aan het onderzoeksveld van fibrilvorming en fibrileigenschappen.

# Dankwoord

## Dankwoord

Eindelijk is het zover, mijn proefschrift is af! Natuurlijk zijn er een heleboel mensen die op een of andere manier hebben bijgedragen aan het tot stand komen hiervan. Die mensen wil ik hier graag bedanken, al heb ik geen illusies dat deze lijst volledig is.

Allereerst wil ik Paul en Erik bedanken. Paul, je was een inspirerende begeleider en had altijd tijd om te helpen. Ik vond het leuk om te zien hoe je altijd weer nieuwe ideeën had. En als ik het eventjes niet meer zag, na gesprekje met jou was alles weer mogelijk. Erik, bedankt voor jou vertrouwen in een goede afronding ondanks de (fysieke) hobbels die genomen moesten worden. Je deelde niet alleen wetenschappelijk inzicht, maar ook je visie op het aio-schap.

Suzanne, onder jou begeleiding tijdens mijn afstudeervak ontstond het idee om aio te worden. Bedankt voor de motiverende gesprekken.

Natuurlijk zijn ook leuke collega's onmisbaar voor een mooi proefschrift! Nam-Phuong, Yul en Dilek, ik heb genoten van de tijd die we samen in 306 doorbrachten. Naast aio-dingen konden we het ook hebben over de andere genoegens des levens: de nederlandse echtgenoot, chocola, ander lekker eten, familie, boeken, enz. Harry en Els, jullie waren onmisbaar voor alle praktische zaken! Elke, bedankt voor het delen van jou aio-afrondings-ervaring. Elisabete, Silvia, Jerome, Leonard, Gerben, jullie ook bedankt voor een fijne tijd op de afdeling. Jacob, Yvette, Christian, Tessa, Mirjam, Ning, Machteld, bedankt voor jullie bijdrage aan dit proefschrift, het was leuk om jullie te begeleiden! Christopher, leuk om met jou "beestjes" te kweken in mijn eerste jaar. Ook alle mensen uit het MicroNed-project 2B wil ik bedanken voor de fijne samenwerking.

Bob, bedankt voor de goede drukker-adviezen in spannende tijden.

Natuurlijk ben ik naast de direct betrokkenen bij dit proefschrift ook mensen dankbaar voor het meeleven en de onmisbare ontspanning naast het schrijven van een proefschrift. Magg, bedankt voor je vriendschap en de heerlijke lunches tussendoor. Eline, bedankt voor je vriendschap, en de mona-toetjes... Mieke, Ben, Mirjam, Sjoerd, Ruth, Gert-Jan, Silvia, Timon, Tamar, Rutgher, jullie zijn mooie vrienden, laten we die weekendjes erin houden!

Arend en Ruth, betere schoonouders had ik niet kunnen wensen, bedankt voor jullie betrokkenheid.

Pap, Remke, Mirte, Jorte en Chelle, het is goed om je geliefd te weten.

Jacob, bedankt voor je heerlijk relativerende houding. Op naar de volgende 5 jaar!



**Curriculum Vitae**

**Publications**

**Training activities**

## Curriculum Vitae

Ardy Kroes-Nijboer was born in Dronten, the Netherlands, on the 23<sup>rd</sup> of June 1983. She went to RSG de Borgen in Leek, where she received her VWO diploma in 2001. In the same year she started studying Food Technology at Wageningen University, specializing in product functionality. She concluded her Bachelor with a thesis about the water transport in crispy crunchy products at the department of Food Chemistry. During her Master study she became enthusiastic studying protein fibrils. Therefore she performed her Master thesis, about the optimization of the production of protein fibrils, at the department of Food Physics. She did her internship at DMV International in line with her Master study. With the completion of her internship she graduated in 2006. In that year she returned to the department of Food Physics to start a PhD project about the formation and properties of whey protein fibrils. Currently the author is proceeding her career as a visual artist.

## Publications

Kroes-Nijboer, A., Lubbersen, Y. S., Venema, P., van der Linden, E. (2009) Thioflavin T fluorescence assay for  $\beta$ -lg fibrils hindered by DAPH. *Journal of Structural Biology* (165) 140-145.

Kroes-Nijboer, A., Bouman, J., Venema, P., van der Linden, E. (2009) The critical aggregation concentration of  $\beta$ -lg based fibril formation. *Food Biophysics* (4) 59-63.

Kroes-Nijboer, A., Venema, P., Baptist, H., van der Linden, E. (2010) Fracture of protein fibrils as induced by elongational flow. *Langmuir* 26 (16) 13097-13101.

Kroes-Nijboer, A., Venema, P., Bouman, J., van der Linden, E. (2011) The influence of protein hydrolysis on the growth kinetics of  $\beta$ -lg fibrils. *Langmuir* 27 (10), 5753-5761.

Oboroceanu, D., Wang, L., Kroes-Nijboer, A., Brodkorb, A., Venema, P., Magner, E., Auty, M.A. (2011) The effect of high pressure microfluidization on the structure and length distribution of whey protein fibrils. *International Dairy Journal* (21) 823-830.

## Proceedings

Kroes-Nijboer, A., Venema, P., Bouman, J., van der Linden, E. (2009) The critical aggregation concentration of  $\beta$ -lactoglobulin based fibril formation. *Proceedings 5th International Symposium on Food Rheology and Structure (ISFRS)* 284-285.



## Training activities

### **Discipline specific activities**

#### *Courses*

Rheological Measurements (KU, Leuven, 2007)

Polysaccharides as Food Colloids and Biomaterials (VLAG, 2007)

Physical Chemistry (Han-sur-Lesse Winterschool, 2008 and 2009)

#### *Conferences and meetings*

MicroNed symposium (Deventer, 2006)

Mini-Symposium Food Structuring (Wageningen, 2007)

NWO-meeting Liquids and Interfaces (Lunteren, 2007 and 2009)

MicroNano Conference (Wageningen, 2007)

MicroNano Conference (Wageningen, 2008)

International Symposium on Food Rheology and Structure (Zurich, 2009)

Symposium Delivery of Functionality in Complex Food Systems (Wageningen, 2009)

Food Professional Day (Ede, 2010)

### **General courses**

VLAG PhD week (VLAG, 2007)

Philosophy and Ethics of Food Science and Technology (VLAG, 2008)

Organizing and supervising MSc and BSc thesis (WUR, 2008)

Techniques for writing and presenting a scientific paper (WUR, 2008)

Advanced course Guide to scientific artwork (WUR, 2008)

Teaching methodology and skills for PhD students (WUR, 2009)

Career Assessment (Meijer & Meijaard, 2010)

### **Optional courses and activities**

Workshop creative problem solving (Wildhaus, 2009)

Organizing PhD study tour to Japan (2010)

The research in this thesis was financially supported  
by the national consortium MicroNed.